Institute of Earth and Environmental Science

Coastal Floods in View of Sea Level Rise: Assessing Damage Costs and Adaptation Measures

Markus Böttle

A cumulative dissertation for the degree of *doctor rerum naturalium* (Dr. rer. nat.) in *Natural Hazards Research*
submitted to the Faculty of Mathematics and Natural Sciences at the University of Potsdam

Submitted: 22 September 2015
Defended: 27 April 2016

Referees:

Prof. Dr. Jürgen P. Kropp
University of Potsdam, Institute of Earth and Environmental Science
Potsdam Institute for Climate Impact Research (PIK)

Prof. Dr. Axel Bronstert
University of Potsdam, Institute of Earth and Environmental Science

Prof. Dr. Klaus Eisenack
Carl von Ossietzky University Oldenburg, Department of Economics

Published online at the
Institutional Repository of the University of Potsdam:
URN urn:nbn:de:kobv:517-opus4-91074
http://nbn-resolving.de/urn:nbn:de:kobv:517-opus4-91074

Abstract

The sea level rise induced intensification of coastal floods is a serious threat to many regions in proximity to the ocean. Although severe flood events are rare they can entail enormous damage costs, especially when built-up areas are inundated. Fortunately, the mean sea level advances slowly and there is enough time for society to adapt to the changing environment. Most commonly, this is achieved by the construction or reinforcement of flood defence measures such as dykes or sea walls but also land use and disaster management are widely discussed options. Overall, albeit the projection of sea level rise impacts and the elaboration of adequate response strategies is amongst the most prominent topics in climate impact research, global damage estimates are vague and mostly rely on the same assessment models. The thesis at hand contributes to this issue by presenting a distinctive approach which facilitates large scale assessments as well as the comparability of results across regions. Moreover, we aim to improve the general understanding of the interplay between mean sea level rise, adaptation, and coastal flood damage.

Our undertaking is based on two basic building blocks. Firstly, we make use of *macroscopic flood-damage functions*, i.e. damage functions that provide the total monetary damage within a delineated region (e.g. a city) caused by a flood of certain magnitude. After introducing a systematic methodology for the automatised derivation of such functions, we apply it to a total of 140 European cities and obtain a large set of damage curves utilisable for individual as well as comparative damage assessments. By scrutinising the resulting curves, we are further able to characterise the slope of the damage functions by means of a functional model. The proposed function has in general a sigmoidal shape but exhibits a power law increase for the relevant range of flood levels and we detect an average exponent of 3.4 for the considered cities. This finding represents an essential input for subsequent elaborations on the general interrelations of involved quantities.

The second basic element of this work is *extreme value theory* which is employed to characterise the occurrence of flood events and in conjunction with a damage function provides the probability distribution of the annual damage in the area under study. The resulting approach is highly flexible as it assumes non-stationarity in all relevant parameters and can be easily applied to arbitrary regions, sea level, and adaptation scenarios. For instance, we find a doubling of expected flood damage in the city of Copenhagen for a rise in mean sea levels of only 11 cm. By following more general considerations, we succeed in deducing surprisingly simple functional expressions to describe the damage behaviour in a given region for varying mean sea levels, changing storm intensities, and supposed protection levels. We are thus able to project future flood damage by means of a reduced set of parameters, namely the aforementioned damage function exponent and the extreme value parameters. Similar examinations are carried out to quantify the aleatory uncertainty involved in these projections. In this regard, a decrease of (relative) uncertainty with rising mean sea levels is detected. Beyond that, we demonstrate how potential adaptation

measures can be assessed in terms of a Cost-Benefit Analysis. This is exemplified by the Danish case study of Kalundborg, where amortisation times for a planned investment are estimated for several sea level scenarios and discount rates.

Zusammenfassung

Viele Regionen in Küstennähe sehen sich durch den Anstieg des mittleren Meeresspiegels einer erhöhten Hochwassergefahr ausgesetzt und die zunehmende Intensität extremer Flutereignisse stellt eine ernstzunehmende Bedrohung dar. Vor allem bei der Überschwemmung bebauter Gebiete können die resultierenden Schäden ein gewaltiges Ausmaß erreichen. Glücklicherweise steigt der mittlere Meeresspiegel langsam und es bleibt ausreichend Zeit sich an die verändernden Umweltbedingungen anzupassen. Dies geschieht üblicherweise durch den Bau oder die Verstärkung von Hochwasserschutzmaßnahmen wie z. B. Deichen oder Ufermauern aber auch angepasste Raumplanung und Katastrophenschutz sind vieldiskutierte Lösungsansätze. Obwohl die Folgenabschätzung des Meeresspiegelanstieges und die Entwicklung von entsprechenden Antwortstrategien zu den bedeutendsten Themen der Klimafolgenforschung gehören, bleiben globale Schadensschätzungen vage und stützen größtenteils auf den gleichen, wenigen Bewertungsmodellen. Diesem Umstand wollen wir mit der vorliegenden Arbeit Rechnung tragen und präsentieren einen eigenen Ansatz, der sowohl großskalige Abschätzungen als auch überregionale Vergleichbarkeit ermöglicht. Darüber hinaus leisten wir einen Beitrag zum allgemeinen Verständnis des Zusammenspiels zwischen dem mittleren Meeresspiegel, Anpassungsmaßnahmen und Flutschäden.

Unser Vorhaben basiert auf zwei Grundbausteinen. Zum einen sind das *makroskopische Flutschadensfunktionen*, d. h. Schadensfunktionen zur Bestimmung des gesamten monetären Schadens in einem vorgegebenen Gebiet (z. B. einer Stadt) der durch eine Flut gewissen Ausmaßes verursacht wird. Dazu stellen wir einen systematischen Ansatz zur automatisierten Ermittlung solcher Kurven vor und bestimmen damit die Schadensfunktionen für 140 europäische Städte. Diese können sowohl für individuelle Schadensabschätzungen als auch für vergleichende, überregionale Studien herangezogen werden. Darüber hinaus ermöglicht die große Anzahl an Kurven eine grundlegende Charakterisierung des Anstieges der Schadensfunktion mit Hilfe eines funktionalen Modells. Das vorgeschlagene Modell ist im Allgemeinen s-förmig, weist jedoch für die relevanten Fluthöhen einen potenzgesetzartigen Anstieg auf und wir erhalten für die untersuchten Städte einen durchschnittlichen Exponenten von $3,4$. Zur späteren Beschreibung der allgemeinen Zusammenhänge aller beteiligten Größen ist dieses Ergebnis von entscheidender Bedeutung.

Der zweite grundlegende Baustein dieser Arbeit ist die *Extremwerttheorie* mittels derer wir das Auftreten von Flutereignissen schätzen und die in Verbindung mit einer Schadensfunktion die Wahrscheinlichkeitsverteilung der auftretenden Schäden im untersuchten Gebiet liefert. Da alle relevanten Parameter als variabel angenommen werden, bietet der beschriebene Ansatz größtmögliche Flexibilität und lässt sich auf beliebige Regionen anwenden. In Kopenhagen, beispielsweise, stellen wir bei einem Anstieg des mittleren Meeresspiegels von lediglich $11\,\mathrm{cm}$ bereits eine Verdopplung des jährlichen, zu erwarteten Schadens fest. Des Weiteren gelingt es uns, allgemeingültige funktionale Beziehungen zwischen den erwarteten Flutschäden und dem mittle-

ren Meeresspiegel, sich verändernden Sturmbedingungen, sowie vorhandenen Schutzhöhen abzuleiten. Damit sind wir in der Lage, zukünftige Flutschäden auf Grundlage nur weniger Parameter zu schätzen: dem bereits erwähnten Exponenten der Schadensfuntion sowie den Extremwertparametern. Ähnliche Untersuchungen stellen wir zur Quantifizierung der aleatorischen Unsicherheit dieser Schätzungen an, wobei wir unter anderem einen Rückgang der Unsicherheit mit steigendem Meeresspiegel feststellen. Schlussendlich zeigen wir wie potenzielle Anpassungsmaßnahmen mit Hilfe einer Kosten-Nutzen-Analyse bewertet werden können. Dies wird anhand der dänischen Fallstudie Kalundborg veranschaulicht, für die wir die Amortisierungszeiten einer geplanten Investition für verschiedene Meeresspiegelszenarien und Diskontierungsraten untersuchen.

Acknowledgments

I would like to thank everyone who supported me throughout the different stages of my dissertation and thus greatly contributed to the successful completion of this work. In particular, I am very thankful to the following people:

- Jürgen Kropp, for offering me the possibility to work in his group and for his valuable advice and feedback during the preparation of this dissertation.
- Axel Bronstert and Klaus Eisenack, for taking time to read and review my thesis.
- Annegret Thieken, for taking over the chair of my doctoral defense, as well as Bruno Merz and Anders Levermann, for agreeing to be members of the examination committee.
- Diego, for supervising all parts of my work and for the continuous support and exchange during the last years. I think our our collaboration was a 'complete success'.
- Boris, Diego, Jürgen, and Prajal, for reading major parts of this work and their critical comments and the discussions that significantly improved the manuscript.
- Steven, for sacrificing parts of his holiday to make linguistic corrections and improvements in my overarching chapters (all present errors have been introduced by myself afterwards).
- Anne, Bin, Bobby, Boris, Carsten, Diego, Linda, Luís, Prajal, Tabea, and many others, for all kind of help and advice as well as the enjoyable time spent during and after working hours.

I really enjoyed being part of the NSP/CCD group, and I am very grateful to all people who made it such a pleasant time. Thanks for all the cakes and sweets in the kitchen, Mensa-conversations, Pappel-grillings, Fohrde-retreats, and kicker matches (particularly the memorable after hour battles together with Bobby against Boris and Carsten).

Contents

List of Figures

List of Tables

Acronyms

CBA	Cost-Benefit Analysis
CCA	City Cluster Algorithm
CLC	Corine Land Cover
DEM	Digital Elevation Model
DIVA	Dynamical Interactive Vulnerability Assessment
DTM	Digital Terrain Model
DVR90	Danish Vertical Reference 1990
FLEMO	Flood Loss Estimation MOdel
FUND	Climate Framework for Uncertainty, Negotiation and Distribution
GEV	Generalised Extreme Value
GDP	Gross Domestic Product
GPD	Generalised Pareto Distribution
IPCC	Intergovernmental Panel on Climate Change
JRC	Joint Research Centre
LUCAS	Land Use/Cover Area frame Statistical Survey
PIK	Potsdam Institute for Climate Impact Research
POT	Peak Over Threshold
PP	Point Process
REMIND	Regional Model of Investments and Development
RQ	Research Question
SRES	Special Report on Emissions Scenarios
SREX	Special Report on Managing the Risks of Extreme Events and Disasters to Advance Climate Change Adaptation
UNFCCC	United Nations Framework Convention on Climate Change

I

Introduction

1.1 Sea Level Rise and its Impacts

The estimation of future sea levels is one of the most prominent topics in climate research. While in the long run, global mean sea levels are expected to rise by more than an unimaginable ten metres even if global warming is limited to 2 °C (Levermann et al., 2013), projections for the near future lie in the range of 28–98 cm by 2100 (Church et al., 2013). The interpretation of the latter range is crucial. As it provides 'likely' limits in terms of a 66–100 % probability, it implicitly allows for a 34 % chance of deviating from it. This poses a major challenge to coastal risk management and especially to risk-averse decision making, which aims at also being prepared for less likely, pessimistic scenarios. As a consequence, the estimation of more certain upper limits (so called *high-end scenarios*) have become a matter of scientific interest (e.g. Ibáñez et al., 2014; Katsman et al., 2011; Vellinga et al., 2009) and their inclusion into future Assessment Reports of the Intergovernmental Panel on Climate Change (IPCC) is demanded (Hinkel et al., 2015; Nicholls et al., 2014). However, the current IPCC methodology for deriving 'likely' intervals from multi-model ensemble outcomes is not adequate to provide such high probability ranges and it remains unclear how they should be attained (Hinkel et al., 2015). Two such attempts have been published recently by Jevrejeva et al. (2014a) and Horton et al. (2014), who estimate upper boundaries for global mean sea level rise by 2100 (with an exceedance probability of 5 %) of 180 cm and 150 cm, respectively.

A glance at the past shows that the rates of sea level change have always been subject to heavy variations (Fleming et al., 1998). For instance, while maximum increase rates of up to 70 $mm\,yr^{-1}$ after the last glacial maximum have been found by Liu and Milliman (2004), the average rate during the 20th century is estimated to be only 2 $mm\,yr^{-1}$ (Jevrejeva et al., 2014b). Supposing the latter rate to persist would imply very moderate sea level projections. However, due to an acceleration of sea level rise within recent decades, available projections are much higher (see above) and the rates of this acceleration as well as the link to global temperatures are a matter of ongoing research (Hay et al., 2015; Haigh et al., 2014; Houston and Dean, 2011; Rahmstorf and Vermeer, 2011; Vermeer and Rahmstorf, 2009). Needless to say that an acceleration entails higher rates of sea level rise and thus amplifies the forthcoming threats of flooding (Kriebel et al., 2015). An additional effect that has to be taken into account when projecting future flood risks is the *local* variation of mean sea levels (Cazenave and Le Cozannet, 2013). This can be due to meteo-oceanographic factors or vertical land movements and can induce regional sea level changes that superimpose global estimates significantly (Nicholls et al., 2014; Carbognin et al., 2010).

The reasons for the strong interest in sea level rise are clearly the potential adverse effects for human systems on large parts of coastal regions (e.g. Nicholls and Cazenave, 2010). Increasing flood damage, dry- and wetland loss,

saltwater intrusion, rising water tables and impeded drainage have been recently stated as major impacts by the IPCC (Gattuso et al., 2014). It should be emphasised that most of these impacts do not result from the permanently increased sea level itself but from temporary flooding due to extreme sea levels. Such extreme events have gained additional attention in the climate change community since the IPCC devoted its Special Report on Managing the Risks of Extreme Events and Disasters to Advance Climate Change Adaptation (SREX) to the threats of natural disasters and how expected changes in the frequency of occurrence and intensity of severe weather patterns can be managed (IPCC, 2012). In the case of coastal floods, extreme events are regional phenomena, typically caused by storm surges, which are in turn determined by several constituents, namely tides, winds, and waves (Menéndez and Woodworth, 2010). Due to the fact that the coincidental occurrence of flood causing factors can only be predicted, if at all, in the short term, floods are commonly considered to occur stochastically and are characterised by their exceedance probabilities. Nevertheless, the mean sea level is of particular importance as it constitutes the base quantity on which surge effects are superimposed (Hunter, 2010; Orlić and Pasarić, 2013). It thus represents the most relevant driver for future sea level extremes (Abeysirigunawardena and Walker, 2008; Lowe et al., 2010).

Coastal regions are centres of attraction for population as well as economic activity (McGranahan et al., 2007; Sachs et al., 2001). Hence, there is no doubt that the societal impacts from sea level rise are most striking in light of their economic relevance as they represent threats to commerce, business, and livelihoods (Fernando et al., 2014; Dossou and Glehouenou-Dossou, 2007). Hinkel et al. (2014) recently estimated that the annual losses due to coastal floods in 2100 could reach up to 9.3 % of the global Gross Domestic Product (GDP), underlying worst case assumptions about socio-economic as well as sea level pathways. But even in the most optimistic scenario they project a 0.3 % loss of global GDP, which still represents an increase by a factor of more than four compared to the year 2013[1]. As a matter of fact, high economic damages mostly occur in built-up (i.e. urban) areas and hence coastal cities require special attention when flood damages shall be assessed (Jongman et al., 2012; Hunt and Watkiss, 2011). Consequently, the ability to estimate upcoming flood risks in urban regions is vital in order to minimise adverse economic impacts from sea level rise.

Considering the potential risks emerging from sea level rise, the question of possible response strategies arises naturally – particularly in view of increasing rates of sea level rise (Obeysekera and Park, 2013). Whereas in the general climate change context, the reduction of greenhouse gas emissions (mitigation) is the most discussed solution, its effectiveness with regard to sea level rise is impaired (at least in the short and medium term) owing to the long response time of the ocean as well as the cryosphere to the global temperature (Jevrejeva et al., 2012; Solomon et al., 2009). That is to say, even without further warming, the global mean sea level will continue to rise in the forthcoming decades due to an inexorable melting of land ice and the thermal expansion of the oceans. Society is therefore bound to face the consequences and adaptation is urgently needed as a complement to greenhouse gas mitigation (Nicholls, 2007). Commonly discussed and implemented adaptation measures comprise

1 Based on damage and GDP data from Munich Re (2014) and World Bank (2014), respectively.

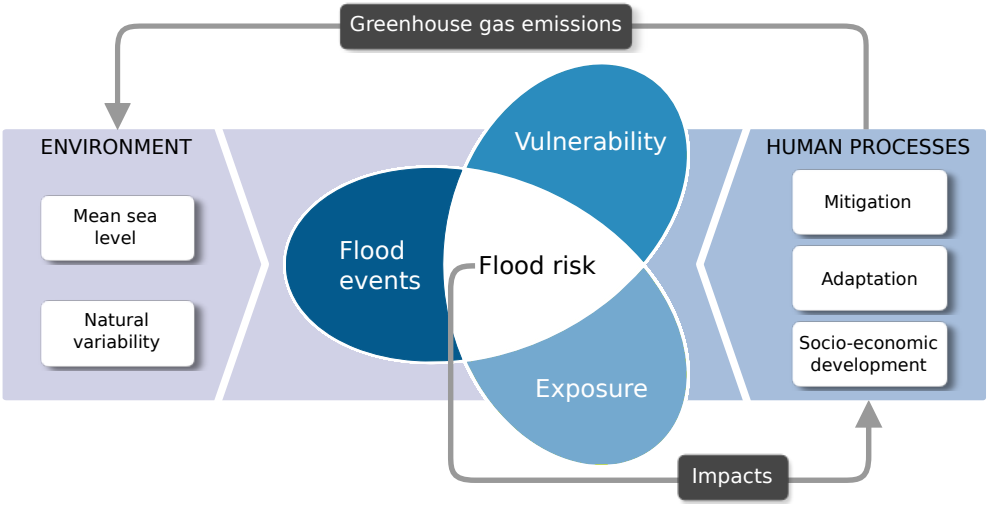

Figure 1.1: Illustration of environmental and human processes relevant for the assessment of sea level rise impacts. Adapted from IPCC (2014).

the construction or reinforcement of hard protection (i.e. engineered constructions such as dykes or sea walls), soft protection (e.g. beach nourishment or wetland creation), as well as land-use and urban planning (Delcan Corporation, 2012; Hurlimann et al., 2014). From an economic point of view, such measures can entail enormous costs. The World Bank, for instance, estimates the costs for dyke construction/upgrade and beach nourishment by the 2040s to be in the range of 26–89 billion US$ per year (Nicholls et al., 2010). Even so, the benefits are expected to exceed these expenses (Gattuso et al., 2014).

The development of coastal flood threats in the future is to a large extent driven by human action. Figure 1.1 illustrates the fundamental interactions in this context. A change in the mean sea level or the natural variability of sea levels can influence the occurrence of *flood events*, which, in turn, affects the *flood risk* and eventually results in a climate change impact. The flood risk, often interpreted monetarily and describing the expected (annual) damage (as e.g. in Elmer et al., 2012; Dawson et al., 2011), is further dependent on the existence of exposed assets (*exposure*) as well as the degree of damage they suffer from a specific flood (*vulnerability*). The anthropogenic side, at the same time, can alter the exposure and the vulnerability towards coastal flooding by means of adaptation and disaster management measures, or, less directly, through the socio-economic development. Furthermore, human behaviour can influence the global climate via the emission of greenhouse gases and can thus affect the occurrence of flood events. Understanding these interactions is the key challenge in order to explain the consequences of human action and to moderate the adverse impacts of sea level rise (IPCC, 2014).

1.2 Approaches and Challenges

Knowing the threats of sea level rise is crucial when it comes to the development of adequate adaptation strategies. As the title of this thesis suggests, we contribute to this issue by studying the (direct monetary) damage from coastal floods, including the effect of sea level rise as well as adaptation thereto. At this point, we want to highlight once more the fundamental distinction between

mean sea levels and *extreme sea levels*. When talking about sea level rise impacts, we actually mean the intensification of impacts from temporary flooding due to extreme sea levels (whose occurrence is determined, among others, by the mean sea level). Since there exists a variety of ongoing research in this field, we provide a brief review of state-of-the-art approaches available in literature and pinpoint the most urgent challenges.

Contrary to existing standards on coastal protection (see, e.g. CPSL, 2010, and references therein), a methodological standard on the assessment of the potential impacts from sea level rise is missing. In general, as addressed in the previous section, adequate impact assessments require the consideration of environmental as well as anthropogenic aspects and thus involve contributions from diverse research fields. Initially, all manner of climate impact studies are driven by results from *earth system/climate science*. In our context, projections of mean sea levels and their dependence on greenhouse gas emissions represent the indispensable basis for meaningful investigations of sea level rise impacts (e.g. Milne et al., 2005; Church and White, 2011; Levermann et al., 2013). *Hydrology*, on the other hand, covers broadly speaking the characterisation of surge events mostly on a regional scale. In particular, statistical methods and hydrodynamic modelling are employed in order to estimate the frequency of flood events (e.g. Mudersbach and Jensen, 2010; Bender et al., 2014) and their propagation on land (e.g Hunter et al., 2008; Horritt and Bates, 2002). The consequences of the resulting inundations are then studied in *natural hazard research*, where an abundance of studies on damage functions (Merz et al., 2010b, and references therein), exposure (e.g. Hanson et al., 2011), vulnerability (e.g. Balica et al., 2012), as well as the resulting flood risk (e.g. Grünthal et al., 2006) can be found. These approaches mostly investigate the consequences of a presupposed hazard, i.e. they are based on 'what if?' considerations without analysing the occurrence of floods.

None of the mentioned research fields is capable of explaining the impacts of sea level rise by itself. Their contributions, however, are essential in the field of *climate impact research*, where the subject of this thesis can be located. The elaboration of a comprehensive approach suitable to investigate sea level rise as well as adaptation effects therefore requires a holistic view on the system illustrated in Fig. 1.1. Because of the multi-disciplinarity of aspects to be considered, this poses a big scientific challenge which is difficult to meet in its entirety. Depending on the scope of consideration, certain simplifications are therefore unavoidable and not all aspects can be fully represented in an assessment.

The number of existing approaches for the assessment of sea level rise impacts on larger than regional scales is fairly limited. This becomes particularly apparent when looking at the most prominent reports – e.g. by the IPCC (Gattuso et al., 2014), the UNFCCC (Nicholls, 2007) or the World Bank (Nicholls et al., 2010) – which all refer exclusively to the same two assessment models, namely DIVA and FUND. While the Dynamical Interactive Vulnerability Assessment (DIVA) model is based on the consideration of coastal segments of similar characteristics and assesses multiple sea level rise impacts and protection measures (Hinkel and Klein, 2009), the Climate Framework for Uncertainty, Negotiation and Distribution (FUND) is a more general, economic model. FUND is actually designed to estimate the social cost of atmospheric carbon in the context of climate change (Tol, 2002b) but comprises a coastal

module to calculate the damages caused by sea level rise (Anthoff et al., 2010). Beyond this, there are plenty of research articles based on the outcomes of these models (e.g. Hinkel et al., 2014, 2013; Anthoff and Tol, 2013; Costa et al., 2009). These, however, merely represent an interpretation of existing results and do not add methodological concepts. Another assessment model that needs to be mentioned here for the sake of completeness is SimCLIM[2]. This software tool simulates the general impacts of climatic variations on agriculture, health, water, and the coast. In particular, coastal impacts from sea level rise as well as adaptation can be assessed on several scales (Mcleod et al., 2010; Warrick, 2009). Nevertheless, it has not become prevalent in the scientific context, presumably not least because of its commercial licensing.

Although the aforementioned models take all relevant aspects discussed above into account, they hardly allow to build upon the employed methodologies, which is mainly due to their complexity and to some extent a lack of transparency. But the major shortcoming from our perspective is that they do not contribute to the general understanding of interrelations. For instance, will an acceleration of sea level rise lead to a similar increase in damages or do non-linearities take effect? Even though these models produce a vast amount of numbers, the investigation of such aspects is hindered as they only consider a predefined set of sea level and protection pathways. Besides, calling to mind the relevance of high-end sea level scenarios, it must be observed that projections for such scenarios are not available and a simple inclusion is not possible.

Further approaches for the assessment of sea level rise impacts can be found in a variety of individual studies. For instance, Hallegatte et al. (2013) estimate expected flood losses in the 136 largest coastal cities worldwide under current and future conditions. Their analysis is based on the flood exposure (estimated by means of population numbers and national GDP) and the occurrence probabilities of certain flood events (extracted from the DIVA database, Hinkel and Klein, 2009). A similar methodology for the assessment of exposed assets in port cities was followed by Hanson et al. (2011) who ultimately refrain from estimating the resulting flood damages. In contrast, there are studies assessing sea level rise impacts without accounting for extreme events (e.g. Dasgupta et al., 2008; Michael, 2007). In our view, such approaches fall short of the mark and are not adequate to build upon. A very comprehensive approach based on storm surge simulations has been recently presented by Aerts et al. (2014), who estimate the expected annual flood losses for the City of New York. Still, due to the high level of detail, it does not allow for transferable conclusions or a generalisation.

Most of the mentioned studies also investigate the effect of specific adaptation strategies in the considered region. For this purpose, the expected damages from flooding are typically estimated for different adaptation scenarios and compared subsequently. Having available also the costs for implementing and maintaining the options, all costs and benefits can be calculated and the economic efficiency of each adaptation option can be evaluated by means of a Cost-Benefit Analysis (CBA). In any case, when different protection strategies shall be compared, a set of options to be investigated must be chosen in the first place. Although this preselection is arguably of high relevance for policy

2 http://www.climsystems.com/simclim/

making, surprisingly little attention is paid to it in the literature. While on the local scale well elaborated strategies can be found (e.g. Aerts et al., 2014), the suggested protection measures on larger scales are often very vague and not always well chosen. The DIVA model, for example, supposes dyke constructions of a given protection height along the entire considered coastline, independent from the prevailing land use and sometimes ignoring existing river courses (Hinkel and Klein, 2009). Accordingly, we note a large potential for more meaningful assessments of protection needs on the large scale.

As stated by the IPCC with regard to global sea level rise impacts, the 'uncertainties are largely unknown and the need for further research is great' (Gattuso et al., 2014). Indeed, none of the available studies provides an analysis of uncertainties. As identified by Apel et al. (2004), such can stem from several sources in the flood process chain: the estimation of events (i.e. the extreme value statistics), the flood routing (i.e. the hydrodynamic model), the modelling of protection measures as well as the employed damage functions. Several studies have been conducted to quantify these uncertainties individually, albeit without setting them in the context of damage projections (El Adlouni et al., 2007; de Moel et al., 2012; Bubeck et al., 2011; Apel et al., 2008; Merz et al., 2002). An additional uncertainty, that is commonly disregarded entirely, emerges from the stochastic occurrence of extreme sea levels. E.g. the 100-year event occurs *on average* once in 100 years but in fact, we cannot predict its occurrence in a given time window.

The most common way of treating uncertainties for the estimation of forthcoming flood damages we have found is the consideration of different socioeconomic scenarios (from which in particular a sea level pathway is derived). From our perspective, however, this merely indicates how different scenario assumptions evolve through the damage assessment without considering any uncertainties from the actual damage estimation. It thus provides rather a sensitivity analysis of the damage assessment and not a measure of uncertainty as such. In any case, there is a scientific consensus that the consideration of uncertainties is essential for optimal decision making and therefore a high demand for uncertainty estimations exists (Adler and Hirsch Hadorn, 2014; Gattuso et al., 2014).

Overall, despite a great volume of available literature, there is no comprehensive approach that describes the interrelations of sea level rise, adaptation, and flood damages. Such a framework, which in particular needs to allow for a generalisation in the sense that it should not rely on individual case studies, would be of great importance for gaining a better understanding of the investigated system (Fig. 1.1). Further, the comparison of impacts across different regions represents a major challenge. Only a systematic approach of straightforward applicability can ensure transferability and lead to comparable results that facilitate the identification of the most exposed regions. Finally, an ideal framework should be flexible enough to be applicable to arbitrary sea level and protection scenarios. In this way, impacts from high-end sea level scenarios can also be assessed and optimal adaptation strategies can be identified.

1.3 Research Questions

The previous sections introduced the thematic setting of this thesis and outlined current research approaches in the field of sea level rise impact and adaptation assessment. The provided overview illustrates the complexity of the subject and, at the same time, posed some overarching challenges that we aim to meet in the following chapters. This is, in the first place, to better understand the interrelations between a rising mean sea level, adaptation, and coastal flood damages. Furthermore, we want to pave the way for a systematic assessment of sea level rise impacts as well as an evaluation of flood protection measures, particularly in urban areas.

The presented work will be guided by four Research Questions (RQ), which on the one hand shall structure the document and on the other serve as a yardstick for our achievements. Beside making progress in solving these issues, it is the central goal of this thesis to gain general insights into the system introduced beforehand (Fig. 1.1).

When studying sea level rise impacts by means of coastal flood damage, it is indispensable, in the first place, to know the damage associated with single flood events. For this purpose, so called *(stage-)damage functions* are typically used in order to relate a flood height with the resulting monetary damage (Merz et al., 2010b). Damage functions can be found on different scales – from *microscopic*, i.e. for individual buildings or assets (Smith, 1994; Apel et al., 2009), to *macroscopic*, i.e. for entire cities or regions (e.g. Hallegatte et al., 2011, 2013). While the elaboration of microscopic damage functions is often based on historical damage records (e.g. the FLEMO or Hazus-MH model, Thieken et al., 2008; FEMA, 2006), adequate data for the macroscopic scale is de facto not available. This poses an additional challenge since it impedes a calibration and/or validation of a derived macroscopic damage function.

So far, little attention has been paid to the elaboration of macroscopic damage functions and – in sharp contrast to *microscopic damage functions* – only very few curves are available. While the influencing factors, such as the distribution and the values of assets, their elevation and connectivity to the coast as well as their susceptibility to damage, seem to be evident, it remains unclear to what extent they take effect on the resulting damage curve. This knowledge, however, could prove very valuable as it provides a starting point for an improvement of available curves. Further, the typical shape of macroscopic damage functions is largely unknown, i.e. how steep is the increase of damages with increasing flood heights? A priori, flood damages could exhibit any behaviour: from sub-linear to an increase of higher-order. As there is only very little historical data on macroscopic damages, knowledge about the functional shape of such curves could considerably improve their estimation, especially in data-scarce cases. This gives rise to our first Research Question:

RQ 1: What are the major determinants of macroscopic flood damage functions and what is their typical shape?

Decision making about appropriate adaptation measures with regard to sea level rise is a common issue in practice that is often discussed on a monetary basis. Knowledge about the economic efficiency of an investment is there-

fore vitally needed. In other words, one wants to know whether the averted damages justify the investment and maintenance costs of a measure. Referring again to Fig. 1.1, macroscopic damage functions (discussed in RQ 1) comprise information about the *exposure* and the *vulnerability* but not about the occurrence of *flood events* in the considered region. Studying sea level rise impacts on the flood risk as well as the evaluation of potential adaptation measures therefore require a characterisation of extreme sea levels. Moreover, in order to perform meaningful analyses, the employed methodology necessitates a flexibility that allows for an easy application to different regions as well as any kind of sea level and adaptation scenarios. This is the subject of the second Research Question:

RQ 2: How can the assessment of sea level rise impacts and the economic efficiency of adaptation measures be designed in a systematic and flexible way?

Being able to estimate the damage for specific regions, with or without a presupposed flood defence, is of utmost importance to local planning authorities who need to decide on strategies to cope with rising mean sea levels. From a broader, scientific perspective, however, it is desirable to gain more fundamental insights, such as a general description of interrelations between the considered quantities. For instance, does a doubling of sea level rise rates in general also imply a doubling of additional expected damage or will the effect be amplified by the system? To our knowledge, there is no general understanding of the interactions between mean sea levels, protection levels and flood damage. Still, such information could be of great relevance to integrated assessment models in the context of climate change, which aim to relate a climate change stimulus (or sea level rise in particular) with its economic impacts. Based on the two previous Research Questions RQ 1 and RQ 2, we therefore ask for more universal insights:

RQ 3: What are the functional relationships of the mean sea level and the implemented protection height with coastal flood damage?

The estimation of flood damage unavoidably involves a number of uncertainties. In fact, every single step in the analysis introduces further inaccuracies. While *epistemic* uncertainties, resulting from incomplete knowledge (e.g. due to a simplified flood modelling or uncertain sea level projections), can generally be reduced by improving the data basis or the applied methodologies, *aleatory* uncertainties are inherent in the system and are thus unavoidable (Apel et al., 2004). The attribution to these two categories is often ambiguous and depends on the specifications of the employed assessment technique (by increasing the level of detail, every aleatory uncertainty can be ultimately considered as epistemic). In our context, the major source of aleatory uncertainty is the stochastic characterisation of flood occurrences (Merz and Thieken, 2004). This makes it impossible to *predict* flood damage and requires the use of, for instance, expectation values as damage estimates. Accordingly, regarding a single year, the actual damage may deviate significantly from the expected damage. It is noteworthy, that this uncertainty is inherent in *any* stochastic model and hence practically unavoidable. Nevertheless, its quantification can be of

high relevance for planning issues, where relying on the expected values alone can lead to significant misplanning. Our last Research Question complements the assessment of sea level rise impacts (RQ 2) and is directed towards this issue:

RQ 4: How large is the aleatory uncertainty in flood damage estimations?

These four Research Questions will provide a content-related frame for the subsequent chapters and are eventually revisited in the conclusive Chapter VII.

1.4 Methods and Structure of the Thesis

The general structure of the document is depicted in Fig. 1.2. While the introductory Chapter I represents an overarching part of this work, the subsequent Chapters II–V are stand-alone research articles, which all include an individual introduction and a discussion.

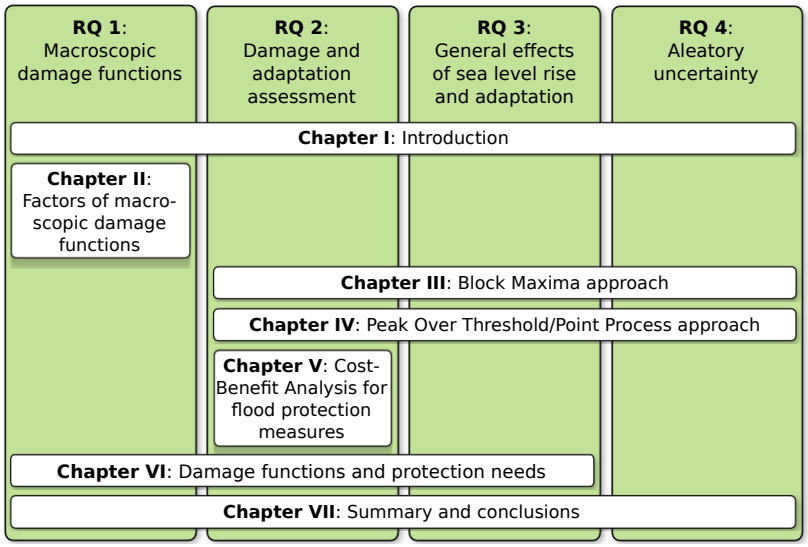

Figure 1.2: Structure of the thesis and coverage of Research Questions by chapters.

The first article (Chapter II) elaborates on flood damages in a case study region in Denmark. Based on a bottom-up approach, several modes of deriving a macroscopic damage function are applied. Varying the underlying elevation data quality, the presupposed *microscopic* damage functions as well as the use of different modes of inundation modelling lead to a total of 42 damage curves. These macroscopic damage functions are then subject to further analyses with a focus on a comparison of their magnitudes. In this way, the most relevant factors of the damage function are identified and we thus contribute to answer RQ 1.

The subsequent Chapters III and IV each introduce a stochastic framework for the estimation of coastal flood damages. Both approaches follow the basic idea of combining (non-stationary) extreme value statistics with the concept of damage functions in order to obtain a probabilistic description of the annual flood damage in a considered region. By employing two different methodologies from extreme value theory – namely a Block Maxima and a Peak Over

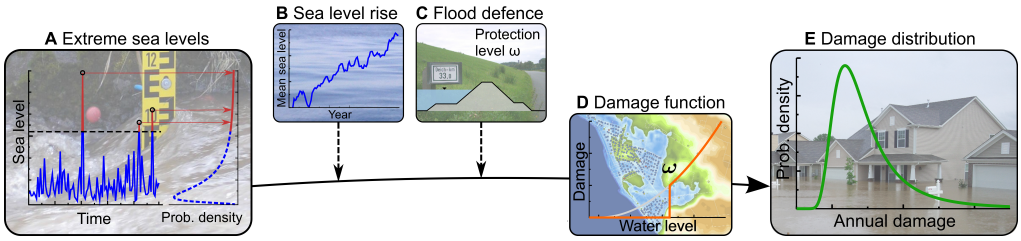

Figure 1.3: From extreme sea levels to damage. (**A**) The analysis of extreme sea levels provides parameter estimations for the *generalised Pareto distribution*. (**B**) The distribution of sea levels is influenced by mean sea level rise. (**C**) Flood defence measures, such as dikes, set the threshold below which any damage is prevented. (**D**) The distribution of extreme sea levels is combined with the corresponding damage via a damage function, providing the total damage in the region under study at a certain maximum flood level. (**E**) From the resulting distribution of total annual damage the expected annual damage and its standard deviation can be derived. (Photographs: 'Ilmpegel Ilmenau' by Michael Sander (2006), 'Sea' by Dedda71 (2008), 'Kilometermarkierung Deich' by Georg HH (2006), and 'Nashville Flood' by Eric Hamiter (2010) from Wikimedia Commons – CC:BY-SA.)

Threshold (POT)/Point Process (PP) approach – the two chapters nicely complement each other and provide a full view on the stochastic assessment of flood damages. Their general methodology is illustrated in Fig. 1.3: Starting with extreme value statistics and adding the effect of mean sea level rise, a macroscopic damage function is used to calculate the probability distribution of the annual damage in the considered area. The effect of potential flood protection measures is integrated by modifying the available damage function accordingly. Within this framework it is possible to estimate the flood damage in a specific region but also in a generalised setting. That is, the development of flood damage is examined for varying parameters without being restricted to a specific case study. In this way, simple analytic expressions for the approximation of the damage are derived based on asymptotic considerations. Overall, the presented framework contributes substantially to RQ 2 and RQ 3. Moreover, the stochastic nature of the approaches enables the assessment of the aleatory uncertainty involved in the estimations and hence provides essential insights for answering RQ 4.

The applicability of the framework is demonstrated in Chapter V, where it is used to evaluate the proposed construction of a flood protection measure in the previously mentioned case study region. Based on several sea level rise scenarios and presupposed discount rates, the expected cumulative damage in the case study is estimated and amortisation times for the investment are projected. In this way, the article makes further contribution to RQ 2.

Additional advances with regard to RQ 1 through RQ 3 are presented in Chapter VI, which is part of ongoing work and is therefore unpublished so far. We derive macroscopic damage functions for 140 coastal cities in Europe and estimate their flood protection needs for various protection levels. A particular focus is laid on a systematic methodology in order to facilitate the comparability of results across different cities. We thus contribute a crucial prerequisite for meaningful assessments of sea level rise and adaptation impacts on a large scale, which can be nicely fed into the introduced frameworks from Chap-

ters III and IV. Eventually, we gain fundamental knowledge about the typical shape of macroscopic damage functions by analysing the derived curves and propose a unifying functional form.

The conclusive Chapter VII is again an overarching part and consists of a synthesis as well as a critical discussion of the achievements in this work – in particular with regard to the Research Questions.

II

About the Influence of Elevation Model Quality and Small-scale Damage Functions on Flood Damage Estimation

Markus Böttle, Jürgen P. Kropp, Lena Reiber, Olivia Roithmeier, Diego Rybski, and Carsten Walther

Potsdam Institute for Climate Impact Research (PIK), Potsdam, Germany

Abstract. The assessment of coastal flood risks in a particular region requires the estimation of typical damages caused by storm surges of certain characteristics and annualities. Although the damage depends on a multitude of factors, including flow velocity, duration of flood, precaution, etc., the relationship between flood events and the corresponding average damages is usually described by a stage-damage function, which considers the maximum water level as the only damage influencing factor. Starting with different (microscale) building damage functions we elaborate a macroscopic damage function for the entire case study area Kalundborg (Denmark) on the basis of multiple coarse-graining methods and assumptions of the hydrological connectivity. We find that for small events, the macroscopic damage function mostly depends on the properties of the elevation model, while for large events it strongly depends on the assumed building damage function. In general, the damage in the case study increases exponentially up to a certain level and then less steep.

This chapter is published as:
Boettle, M., Kropp, J. P., Reiber, L., Roithmeier, O., Rybski, D., and Walther, C. (2011). About the influence of elevation model quality and small-scale damage functions on flood damage estimation, *Nat. Hazards Earth Syst. Sci.*, 11(12):3327–3334, doi:10.5194/nhess-11-3327-2011.

II.1 Introduction

In order to estimate the damage costs of future storm surges one can apply the concept of stage-damage functions (see e.g. Smith, 1994) which provide for a flood of certain water level a corresponding direct monetary damage. Combined with extreme value statistics, the risk can be calculated. Both components, extreme value statistics and damage functions, involve uncertainties (Merz and Thieken, 2004; Merz et al., 2004) and crucially influence the outcome (Merz et al., 2002; Apel et al., 2009).

A *macroscopic stage-damage function* (i.e. a function that represents the total damage in the entire considered area) can be obtained by summing up all damages of a lower scale (e.g. building scale) or by an indirect approach (Steinhäuser et al., 2015). Here we follow the former approach to assess the macroscopic damage function of a case study area in Denmark. For this purpose it is necessary to determine the inundation height of each asset (e.g. building) for certain flood events in order to calculate the corresponding damage. Since hydrodynamic modelling requires more effort and computational power, many studies use a simple flood fill algorithm, i.e. they determine the intersection between the plane of the raised water level and the Digital Elevation Model (DEM), and treat the entire connected area between sea and intersection as inundated (Dasgupta et al., 2008; Mazria and Kershner, 2007; Rowley et al., 2007). This procedure overestimates the flooded area since it corresponds to an asymptotic filling of all land that would be flooded at a certain permanent sea level.

Obviously the quality of the underlying DEM plays an important role in this process. DEM of various horizontal resolutions are employed in flood risk case studies and horizontal resolutions ranging from $1\,\mathrm{m}\times1\,\mathrm{m}$ to $90\,\mathrm{m}\times90\,\mathrm{m}$ can be found (Büchele et al., 2006; Merz and Thieken, 2009; Hallegatte et al., 2011). The influence of the quality of such elevation data (regarding horizontal resolution and vertical accuracy) on the identification of inundated areas has been addressed by Poulter and Halpin (2008) and Gesch (2009). We want to broaden the view and look at the effect on the resulting damages. Therefore, we estimate the direct monetary damage to buildings (without inventory) and study the influence of different modes of this approach on the macroscopic damage function. We consider a case study in Denmark (south of the city of Kalundborg) and estimate the damage function based on 14 variations of the inundation procedure which differ in: (i) Determining the inundation area via the 4 nearest neighbours of the DEM cells or via the 8 nearest neighbours (this represents different assumptions about the hydrological connectivity according to Poulter and Halpin, 2008). (ii) Coarse-graining (aggregating) the DEM in 2 by 2 cells or 3 by 3 cells (or no coarse-graining). (iii) Using the minimum, mean, or maximum within the coarse-grained cells. Furthermore, we base our calculations on linear, square root, or quadratic *building damage functions*.

We find that all macroscopic damage functions can be characterised by three regimes: a zero level for moderate water levels followed by an exponential and a less steep increase for high water levels. Moreover, we show that the inundation mode is the most dominant factor for the damage estimation of small events, whereas the choice of the building damage function is dominating for heavy floodings.

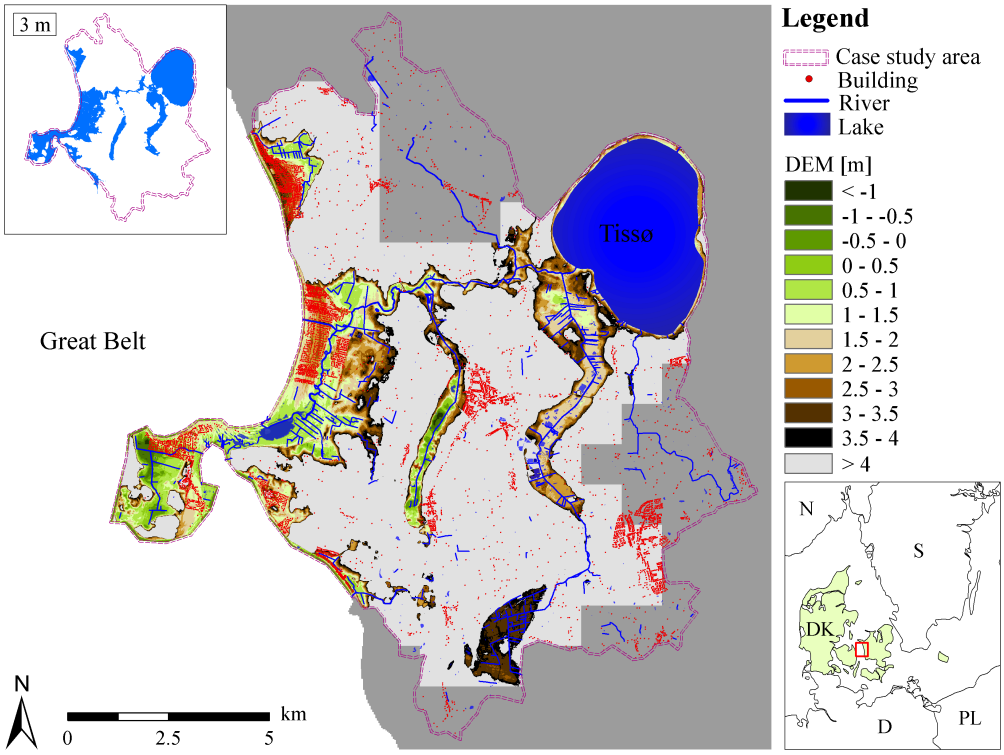

Figure II.1: Map of the case study area and location within Northern Europe. The elevation according to the available DEM is colour coded (light grey represents elevations above 4 m) and buildings are indicated by red dots. The dark grey area delineates land for which no elevation data is available and the white area in the east is the sea. The inset in the upper left corner indicates the inundated area for a 3 m sea level referred to DVR90 (no aggregation, 4 nearest neighbours). The inset in the lower right shows the country contours and the cut-out represents the major map. DEM owned by BlomInfo A/S, Denmark.

In Sec. II.2 we provide information about the case study and the data used. The performed analysis is described in Sec. II.3 and the obtained results are presented in Sec. II.4. We summarise and draw conclusions in Sec. II.5.

II.2 Case Study Area

The case study area (displayed in Fig. II.1) is situated in the south of the city of Kalundborg in Denmark. The considered area belongs to the municipality of Kalundborg which itself is located on the west coast of the island of Zealand. To the west, the case study area borders at the Jammerland Bay, the Musholm Bay, and the Great Belt which connects the Baltic Sea with the marine area Kattegat. There are a few small rivers and the fourth-largest lake of Denmark, Lake Tissø, in the area.

The case study area has a size of approx. 143 km^2. The available DEM covers 115 km^2 which corresponds to the low-elevation area. The DEM – obtained from the Kalundborg municipality (DEM owned by BlomInfo A/S, Denmark) – is based on a LIDAR dataset from 2007 and relates to the reference system DVR90 (Danish Vertical Reference 1990). It does not take account of any artificial elevations, such as buildings (therefore it is sometimes referred to as a

Digital Terrain Model, DTM). Currently, there exist no flood defence measures apart from natural protecting elevations that need to be considered. The cell size of the DEM is 1.6 m×1.6 m, with a vertical resolution of 10 cm. The region is predominantly rather flat with a range in elevation of almost 55 m. However, some areas lie below sea level (approx. 0.9 km^2).

The case study area contains more than 6000 properties with almost 17,000 structures concentrated in a few settlements with approx. 200 to 4500 inhabitants. The cadastral dataset contains information about the building position, type of the building, property value and land value but not about the size and shape of the structures. This implies, that the flood flow procedure cannot consider the buildings as barriers, which is only a minor limitation, since most buildings stand separately and are not adjacent. Property and land value were obtained from the calculation basis for property taxes and were provided by the municipality. Their difference leads to the building value, which was used to estimate building damages in combination with relative stage-damage functions.

The buildings are grouped into six main types: garages, carports etc. (42 %); year-round residential (25 %); recreational purposes (18 %); agriculture, industry etc. (13 %); trade, transport etc. (1 %); (social) institutions (1 %). Accordingly, the case study area is characterised by small localities, a low population density, many summer cottages, agriculture, and minor industry.

11.3 Analysis

In the performed analysis, we focus on a hypothetical storm surge event of certain level E (referred to DVR90) and assume that the sea water completely inundates the terrain at this considered water level. Thus, we disregard the dynamics and study an asymptotic static inundation scenario; it does not take into account any decline in flood level and volume with increasing distance from the coast. Accordingly, the inundated area is defined as the connected area between the sea and the intersection of the raised water level and the elevation model.

In order to identify the inundated area, we start from a cell that is clearly located in the sea. Then we check if the neighbouring cells have an elevation below the chosen sea level (this is true for cells belonging to the sea). If this is the case, we mark it as inundated and proceed with its neighbouring cells. This procedure is continued until all adjacent cells below the chosen level are identified. Please note, that low lying areas that are not connected are not included.

In the next step, we determine which of the properties are within the inundated area and calculate how deep each building is flooded. Since the available dataset locates each building to a grid cell in the DEM, representing the centre of the building, the corresponding elevation is assigned to the structure. The buildings have no cellar and a typical foundation base of 20 cm above which we estimate the damage for individual buildings as a fraction of their value.

A wide range of functional forms, such as logarithmic, square-root, linear and quadratic (see Nascimento et al., 2007; Dutta et al., 2003; Büchele et al., 2006; Apel et al., 2009, and references therein) have been used as building

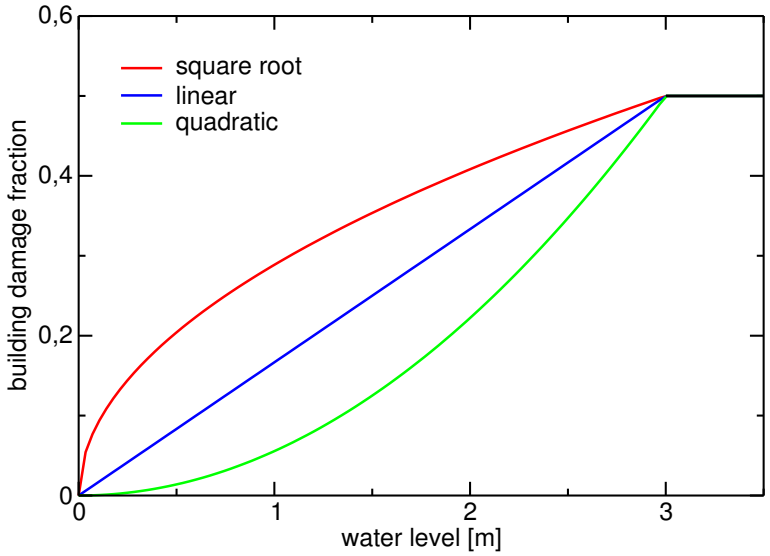

Figure II.2: Assumed building damage functions according to Eqs. (II.1), (II.3), and (II.4). The fraction of building damage (without inventory) is plotted against the water level from the lower edge of the building. The parameters of the linear, square root, and quadratic building damage function are determined by two anchor points, i.e. no damage for no inundation and 50 % damage at 3 m inundation.

damage functions in previous studies. To exemplify our approach, we choose a linear function

$$d_{lin}(e) = \begin{cases} 0 & \text{for } e < 0\,m \\ \frac{e}{3\,m}\,0.5 & \text{for } 0\,m \leqslant e \leqslant 3\,m \\ 0.5 & \text{for } e > 3\,m \end{cases} , \tag{II.1}$$

where e denotes the water level relative to the foundation base of the building (see Fig. II.2).

This is done for all affected buildings and the total damage for the considered sea level E is calculated as

$$D_{lin}(E) = \sum_i d_{lin}(e_i)\,V_i \ , \tag{II.2}$$

where e_i is the flood height at building i and V_i its value. We consider $D(E)$ as an estimate of the total monetary damage (without inventory) caused by a certain flood of level E to the buildings in the entire case study area. By varying the sea level E in steps of 10 cm between 0 m and 3 m we obtain a macroscopic damage function. Based on sea level records, provided by the municipality of Kalundborg, a 3 m storm surge corresponds approx. to a 800-year event (the upper left inset of Fig. II.1 depicts a 3 m flood).

We want to elaborate how sensitive this summary function is to assumptions, technical details, and data quality. Therefore, we test variations which differ in the following details (see Tab. II.1):

1. Inundation via 4 or 8 adjacent cells
   In the above described procedure the inundated area is identified by

rank	neighbours	coarse graining	aggregation mode	first considerable damage
1.	8	3×3	min	60 cm
2.	4	3×3	min	110 cm
3.	8	2×2	min	110 cm
4.	4	2×2	min	110 cm
5.	8	3×3	mean	120 cm
6.	4	3×3	mean	120 cm
7.	8	2×2	mean	130 cm
8.	4	2×2	mean	130 cm
9.	8	-	-	140 cm
10.	4	-	-	140 cm
11.	8	2×2	max	140 cm
12.	4	2×2	max	140 cm
13.	8	3×3	max	140 cm
14.	4	3×3	max	150 cm

Table II.1: Overview of the explored inundation determination modes sorted by the estimated damage (high damage from top) along with the lowest water level, for which a considerable damage (over 1 million DKK) is found (last column). The options differ in the number of nearest neighbours considered (2nd column), the coarse-graining (3rd column), and the value associated to the coarse-grained cells (4th column), see Sec. II.3.

checking whether neighbouring cells have an elevation below a certain threshold. Since the inundation might not only propagate to the east, north, west, and south, but also in diagonal direction, we test these two options. As illustrated in Fig. II.3 either the 4 or 8 nearest cells are considered as adjacent. This means in the latter case also the second nearest neighbours are included.

2. Resolution of the elevation model (no coarse-graining, 2×2, or 3×3 cells)
   Since each DEM has a limited horizontal resolution, we test by coarse-graining (i.e. aggregation) how sensitive the result responds to the resolution of the data. The available DEM can be considered as a coarse-grained DEM from an even higher resolution. In many areas only low resolution DEM are available.

3. Minimum, mean, or maximum coarse-graining
   When coarse-graining, we elaborate three options of associating an elevation value to the new aggregated cells, as illustrated in Fig. II.4. These options specify, whether we assume that the flood is strong enough to overtop or break through higher elevated areas. In a sense, these options correspond to worst and best case scenarios.

4. Linear, square root, or quadratic building damage function
   As mentioned above, many different building damage functions are pro-

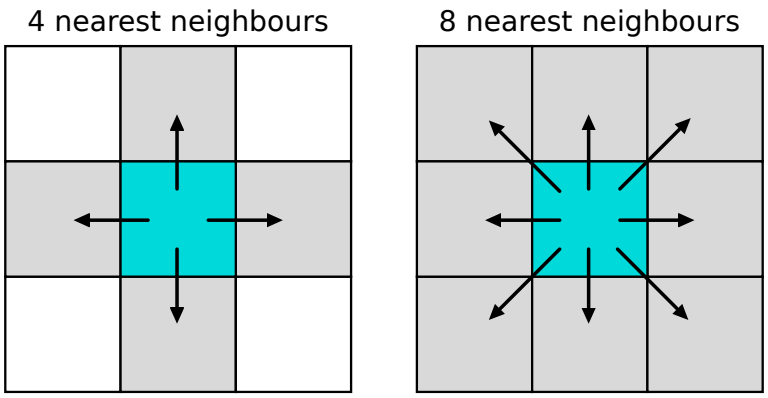

Figure II.3: Illustration of inundation via 4 nearest (left) or 8 nearest (right) neighbours. The former uses only nearest neighbours, i.e. at cell distance 1, the latter also includes second nearest neighbours, i.e. at cell distance $\sqrt{2}$.

posed and used in the literature. We study the influence of a linear, Eq. (II.1), a square root,

$$d_{\text{sqrt}}(e) = \begin{cases} 0 & \text{for } e < 0\,\text{m} \\ \left(\frac{e}{3\,\text{m}}\right)^{1/2} 0.5 & \text{for } 0\,\text{m} \leqslant e \leqslant 3\,\text{m} \\ 0.5 & \text{for } e > 3\,\text{m} \end{cases}, \tag{II.3}$$

and a quadratic,

$$d_{\text{quad}}(e) = \begin{cases} 0 & \text{for } e < 0\,\text{m} \\ \left(\frac{e}{3\,\text{m}}\right)^{2} 0.5 & \text{for } 0\,\text{m} \leqslant e \leqslant 3\,\text{m} \\ 0.5 & \text{for } e > 3\,\text{m} \end{cases}, \tag{II.4}$$

functional form on the final macroscopic damage function. As can be confirmed with Fig. II.2, the parameters have been chosen so that there is no damage if the building is not flooded and a maximum damage of 50 % when the building is flooded by 3 m or more. Of course these two points influence the final results but our major findings are independent of their actual values.

We end up with 14 combinations (modes) of determining the inundated area and building inundation for each of the three damage functions.

II.4 Results

Beginning with the linear building damage function, Eq. (II.1), we obtain a variety of different macroscopic damage functions which are displayed in Fig. II.5. Different things can be observed:

1. The minimum level for which a damage is expected depends strongly on the mode of inundation determination.
2. At low sea levels around 1–1.5 m the damage increases abruptly from zero to the order of 10 million Danish Krones (DKK).

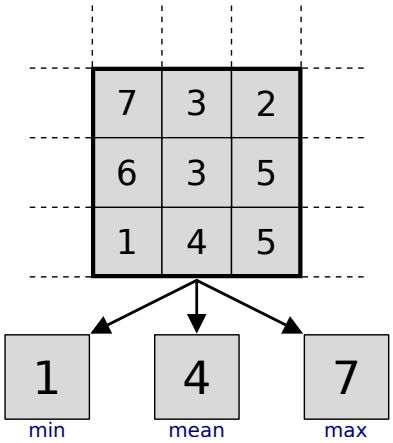

Figure II.4: Illustration of coarse-graining modes of the elevation model employing minimum, mean, and maximum. For an aggregation of 3×3 grid cells in the DEM (top) an example of the different resulting cell values (bottom) is displayed (with exemplary numbers).

3. The damage increases exponentially up to 2–2.5 m above which it follows a less steep function.

4. The damages for all inundation modes at intermediate and high sea levels range approx. 10 %.

The abrupt increase in the macroscopic damage is a natural effect to be expected. Once the sea level exceeds natural or artificial barriers in the DEM, the entire area behind is considered as inundated. In this context, a barrier is a set of grid cells, that is higher elevated than the water level and that is located in a way, such that the water cannot flow around. However, at which sea level such a step occurs depends on the applied inundated mode. Already at 60 cm a damage of approx. 6 million DKK is found in the case of 3×3, minimum, 8 neighbours. In the best case, the first considerable damage (over 1 million DKK) occurs at 1.5 m with approx. 29 million DKK (3×3, maximum, 4 neighbours). The water levels, at which this jump occurs in each inundation mode are listed in Tab. II.1.

In addition, Tab. II.1 ranks all combinations according to their damage. It is apparent, that taking the minimum in the coarse-graining leads always to larger damages and taking the maximum leads to smaller damages. This is clear, because possible barriers as well as buildings are lowered or raised. In addition, this effect is more pronounced for coarse-graining in 3×3 than in 2×2 cells.

We would like to note that in practice coarse-graining taking the mean value is the relevant mode. If we compare the damage functions from the coarse grained and non-coarse-grained DEM, we find that the damage range for high water levels is approximately constant, which implies that the relative difference becomes insignificant. For the damage determination of severe events the resolution of the DEM is therefore of minor importance. This can be explained by the fact that for high water levels the buildings are flooded more deeply and the error caused by coarse-graining therefore becomes less important. However, for low flood levels, the abrupt jumps in the functions can lead to large differences for singular levels, usually with larger damage in the coarse-grained

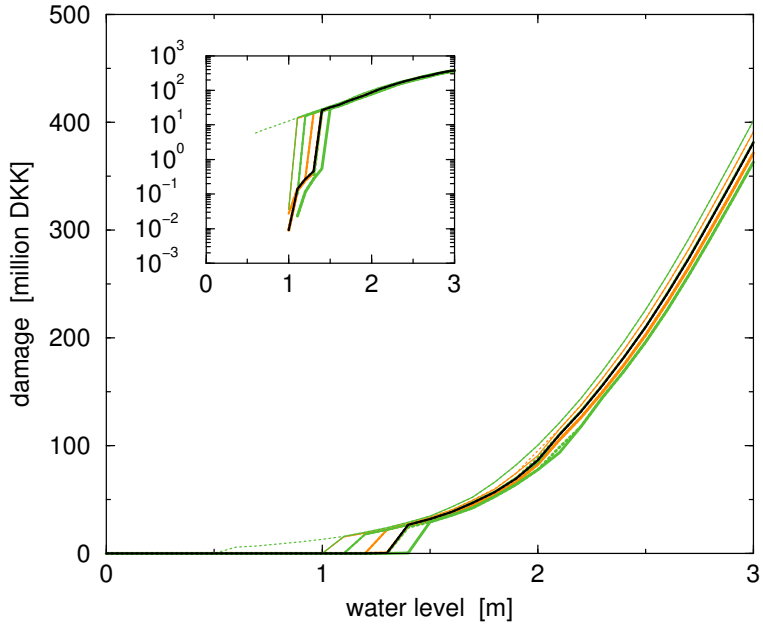

Figure II.5: Macroscopic damage function for different modes of inundation determination. The estimated direct monetary damage is plotted against the water level for the following variations as detailed in Tab. II.1 (top to bottom). (i) Considering 4 or 8 nearest neighbours is represented by a solid or dotted line. (ii) Coarse-graining in 2×2 cells or 3×3 cells is represented by orange or green (no coarse-graining: black). (iii) The width of the lines represents the value associated to the coarse grained cells: minimum - thin, mean - medium, maximum - thick. A linear building damage function according to Eq. (II.1) has been used, see Fig. II.2. The inset shows the same curves but in semi-logarithmic scale.

cases. Hence, the quality of the DEM is decisive for the damage determination of small events. Although the impact of such water levels is rather low, this can play an important role in the estimation of risk due to their frequent occurrence.

Further, in each combination the 8 nearest neighbours mode imply larger damage than the 4 nearest neighbours mode. This is due to the fact that including the diagonal path more area can be reached.

The exponential form after the rapid increase that can be detected in Fig. II.5 must originate from the orography and the locations of the buildings, since there is no function of such a form involved in the process. Whether this finding can be generalised is not clear.

Next we study the influence of different building damage functions. In Fig. II.6 we also show the damage functions for square root and quadratic building damage functions. For a better visibility we only show the range emerging from all 14 modes and the non-aggregated mode (4 nearest neighbours). On the one hand, we find that for high sea levels, the largest damage is obtained assuming a square root damage function while the lowest damage is obtained assuming a quadratic damage function, which is already expected from Fig. II.2. However, the 3 m damage for linear and quadratic damage functions differs by a factor of 2 and for square root and linear by a factor of 1.5. In particular, we find that the range due to the 14 modes of inundation covers a much smaller interval than the one due to the 3 different building damage

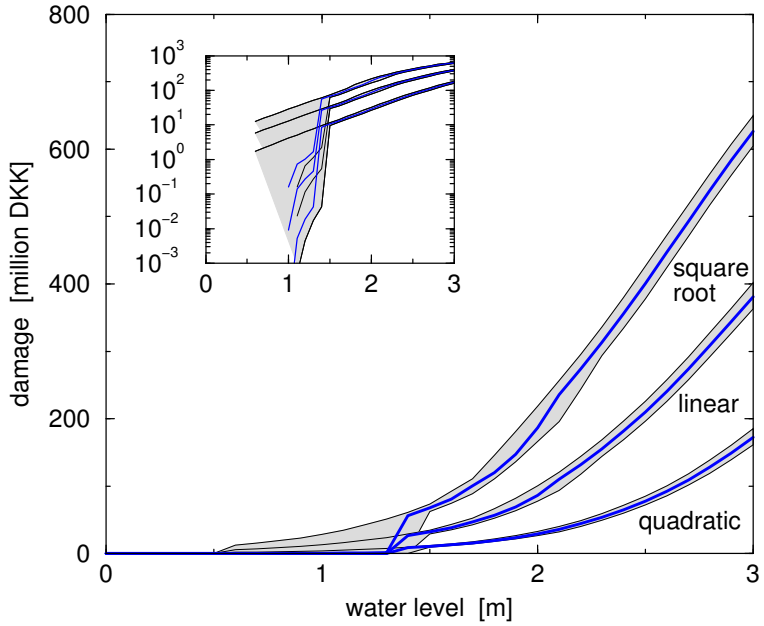

Figure II.6: Macroscopic damage functions assuming different building damage functions. The estimated direct monetary damage is plotted against the water level, whereas the central blue line corresponds to the non-coarse-grained case (using 4 nearest neighbours). The grey bands represent the range between highest and lowest of all 14 combinations. We assume square root, linear, or quadratic building damage functions (from top), Eqs. (II.1), (II.3), and (II.4), see Fig. II.2. The result for the linear building damage functions is the same as in Fig. II.5. The inset shows the curves in semi-logarithmic scale.

functions. Hence, in particular for high water levels, the choice of the building damage is much more important than the quality of the elevation model.

On the other hand, for small sea levels we see in the semi-logarithmic inset of Fig. II.6 that the stepwise character of the macroscopic damage functions due to the inundation modes span a range of approx. 3 orders of magnitude which is much larger than the range due to the building damage functions (one order of magnitude). This confirms the importance of the DEM for small events and we can conclude that depending on the range of considered sea levels, either the inundation technique or the building damage functions dominates the estimated damage.

In Fig. II.6 one can also see that the cross-over from the exponential to a less steep increase depends on the chosen building damage function. While for the quadratic one, there is almost no change, for the square root one, it appears already around 2 m and the remaining 2–3 m increase approximately linearly.

Finally, we elaborate the inundated area and the damage density as a function of the water level for the simplest mode with no coarse-graining, considering only the 4 nearest neighbours. The results are illustrated in Fig. II.7. We find that the area increases approximately quadratically (i.e. a power-law with exponent 2) with the water level up to almost 3 m. Obviously, this strongly depends on the orography in the considered case study area. In contrary, the damage densities, defined as damage per unit of inundated area, show a sharp increase at around 1.4 m – which is consistent with the jumps in the damage functions (Fig. II.6). Upon closer examination, one can also detect a slight jump

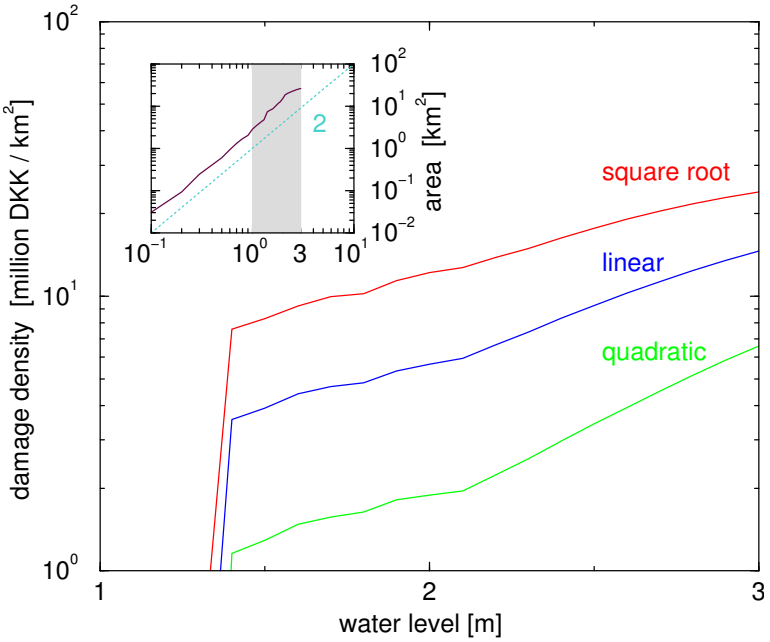

Figure II.7: Damage density and inundated area vs. water level. The damage density, defined as damage per area, is plotted as a function of the water level for the non-coarse-grained mode with 4 nearest neighbours. We assume square root, linear, or quadratic building damage functions (from top), Eqs. (II.1), (II.3), and (II.4), see Fig. II.2. The inset shows the inundated area as a function of the water level. The dotted line is a guide to the eye and follows a power-law with exponent 2. The grey area indicates the range of water levels shown in the main panel.

of the inundated area in this region, which is less steep and visible due to the logarithmic scale of the ordinate. However, this implies that for moderate water levels up to 1.4 m, the inundated area increases more or less steadily but does not comprise any assets. This is expected since such elevations are frequently flooded and therefore undeveloped. In general, it is very desirable to avoid damages from such frequent floodings. Therefore, a similar behaviour along with a sudden jump in the damage function can be expected elsewhere.

In the range above 2 m, all three curves in Fig. II.7 exhibit a smooth increase, which indicates, that the number of flooded buildings saturates and no sudden increase of affected buildings happens. In particular, in the case of the quadratic building damage function the density increases approximately exponentially between 2.2 and 3 m, which can be attributed to the corresponding damage function (Fig. II.6, lower set of curves).

II.5 Conclusions

We find that after a sudden jump, in any case the macroscopic damage functions increase exponentially up to a certain water level above which they change to a less steep increase, whereas the cross-over level depends on the assumed building damage function. Moreover, the range covered by the final damage functions obtained from the various modes of inundation determination differ by an approximately constant factor. In particular, we show that for large events the assumed building damage function dominates the final damage,

while for small events the mode of coarse-graining has a dominating influence on the estimated damage.

Additional inundation methods could be obtained by varying the way elevation heights are assigned to the buildings. As mentioned in Sec. II.3, we defined the elevation of a building as the height of the building's centre. Other Choices could be the minimum, maximum or average elevation of the terrain covered by the building. Since the available building information is a point dataset, these methods could not be applied. However, we expect only an insignificant effect on the macroscopic damage, since the terrain in the case study area is rather flat and the buildings are small.

While the overall shape of the macroscopic damage function likely depends on the local conditions of the considered area, it is plausible that the DEM and the building damage function should have a similar effect for moderate and heavy flood events, respectively, at other sites.

In general, we conclude that different regimes of a damage function have to be considered. With regard to low and moderate sea levels an accurate DEM is indispensable, since it provides information about whether low-lying properties are flooded or not. This can affect the total flood risk decisively because of the high frequency of such water levels. On the other hand, at higher flood levels, the building damage function becomes more dominant than the quality of the DEM and although such events are very rare, the corresponding damages need careful estimations due to their catastrophic consequences.

Accordingly, our results suggest that depending on the flood height the DEM or the building damage function is more important.

Finally, it needs to be mentioned that climate change and sea level rise in many regions most likely lead to an increased frequency and magnitude of high water levels (Nicholls, 2004; Nicholls et al., 2007, and references therein). According to our results, this might enter the regime where the building damage functions become more important. This suggests that more research is needed to better estimate and determine building damage.

Acknowledgements. We would like to thank Jacob Arpe and the municipality of Kalundborg for the provision of data and Luís Costa for fruitful discussions and comments. We appreciate financial support by the BaltCICA Project (part-financed by the EU Baltic Sea Region Programme 2007-2013).

III

How Changing Sea Level Extremes and Protection Measures Alter Coastal Flood Damages

*Markus Böttle**, *Diego Rybski**, *and Jürgen P. Kropp**,†

*Potsdam Institute for Climate Impact Research (PIK), Potsdam, Germany
†University of Potsdam, Institute of Earth and Environmental Science, Potsdam, Germany

Abstract. While sea level rise is one of the most likely consequences of climate change, the provoked costs remain highly uncertain. Based on a Block Maxima approach, we provide a stochastic framework to estimate the increase of expected damages with sea level rise as well as with meteorological changes and demonstrate the application to two case studies. In addition, the uncertainty of the damage estimations due to the stochastic nature of extreme events is studied. Starting with the probability distribution of extreme flood levels, we calculate the distribution of implied damages in a specific region employing stage-damage functions. Universal relations of the expected damages and their standard deviation, which demonstrate the importance of the shape of the damage function, are provided. We also calculate how flood protection reduces the damages leading to a more complex picture, where the extreme value behaviour plays a fundamental role.

This chapter is published as:
Boettle, M., Rybski, D., and Kropp, J. P. (2013). How changing sea level extremes and protection measures alter coastal flood damages. *Water Resour. Res.*, 49(3):1199–1210, doi:10.1002/wrcr.20108.

III.1 Introduction

In the debate about climate change induced sea level rise, land loss is a commonly mentioned consequence (Nicholls et al., 2010; Devoy, 2008). Under a closer look, however, it turns out that land loss itself is often a result of extreme events, such as storm surges, which either erode the coastline (Stive et al., 2002) or inundate the considered area so frequently that a repeated restoration might be inefficient and the land is abandoned.

Considering sea levels, one can observe that the mean sea level is superposed by fluctuations, whose magnitudes significantly surpass the expected mean sea-level rise. Accordingly, if one wants to investigate consequences of sea level rise, these fluctuations need to be taken into account. Tides and winds are the main influencing factors of these fluctuations (Woodworth et al., 2011) and together with the mean sea level they determine the magnitude of an extreme event. Thus, extreme floods are influenced by climate change in two ways: via sea level rise and via meteorological changes. We study the consequences of these two effects as well as the impact of potential flood protection measures on the expected flood damages, where damages describe the monetary losses in a specific area. Furthermore, the variability of the damages is examined.

We employ extreme value theory for the characterisation of flood events (Katz, 2010), and damage functions (Merz et al., 2010b), in order to obtain the associated damages. Accordingly, the distribution of extreme sea levels is translated via the damage function into the distribution of damages, i.e. the probability that a damage higher than a certain value occurs is related to the probability that the annual maximum flood exceeds a certain level. In particular, sea level rise, which is the main driver for changing extreme value behaviour (Menéndez and Woodworth, 2010), leads to modified damages. Additionally, climate change could alter meteorological patterns, which induces a change of variability of extreme events (McInnes et al., 2013; Woth et al., 2006) and in turn affects the damage distribution.

We elaborate this setting in a general sense and analytically derive relations for the expectation value of the damages and the standard deviation as a function of the mean sea level and as a function of the variability of annual maximum sea levels. The resulting expressions describe the asymptotic behaviour and highlight the importance of the damage function. We complement the results with an analysis of the effect of a protection measure in the form of a dyke or a sea wall protecting the area from floods up to a specific maximum sea level. Again, we derive analytical expressions and find that in this case the expressions depend sensitively on the extreme value behaviour of sea levels.

All general results are supported by numerical calculations for the city of Copenhagen and a case study area in Kalundborg (Denmark).

The manuscript is organised as follows. In Sec. III.2 our approach connecting extreme sea levels and damage functions is introduced. Information on the two case studies is provided in Sec. III.3. Changes in the extremes are presented in Sec. III.4 and the influence of protection in Sec. III.5. In Sec. III.6 we draw conclusions and discuss limitations of our findings. Detailed derivations are provided in the Appendix Sec. III.A.

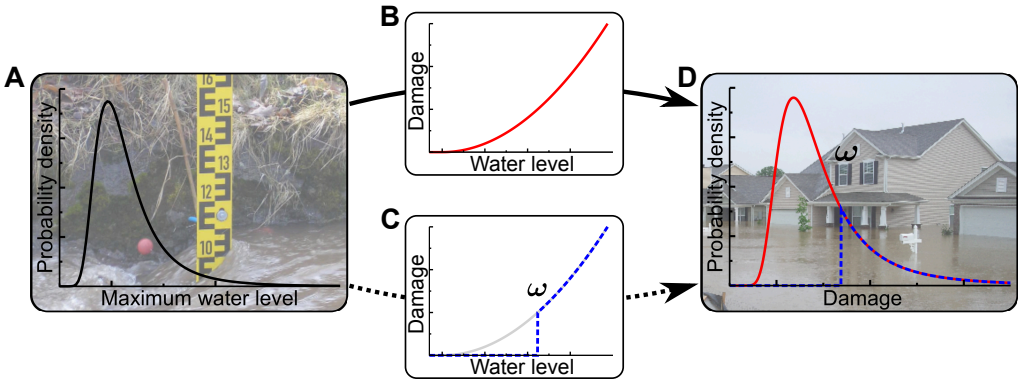

Figure III.1: Illustration of the damage model. (**A**) The distribution of annual maximum water levels transforms via (**B**), the damage function, into (**D**), the probability density of damages. (**C**) An implemented protection measure filters moderate events up to a threshold ω and leads to a modified damage function. In this case, the damage distribution (**D**) (dashed, blue line) consists of an additional discrete part in 0, which cannot be depicted. (Photographs 'Ilmpegel Ilmenau' by Michael Sander (2006) and 'Flooding in Nashville, Tennessee' by Eric Hamiter (2010) used under a Creative Commons Attribution-ShareAlike license: `http://creativecommons.org/licenses/by-sa/3.0/`).

III.2 Methodological Approach

We want to estimate the annual, monetary damages caused by coastal floods, For this purpose, we assume there is one extreme flood per year in the considered region and obtain the corresponding damage costs from a macroscopic damage function, providing the typical damage of a coastal flood of specific magnitude (other contributing factors such as inundation duration or flow velocity, see e.g. Wind et al., 1999; Thieken et al., 2005; Middelmann-Fernandes, 2010, are not taken into account).

Thus, we consider the distribution of annual maximum sea levels and derive the distribution of annual damages by using the damage function. Naturally, if the distribution of maxima changes, also the distribution of damages is altered. This is the starting point of our approach. Once the distribution of damages is known, the expectation value and the standard deviation can be calculated. Moreover, protection measures modify the damage function, e.g. sea walls determine the flood level below which no damage occurs.

The approach is sketched in Fig. III.1. The distribution of maximum sea levels is illustrated in Fig. III.1A, the damage function in Fig. III.1B, and the distribution of damages in Fig. III.1D. An alternative damage function supposing a protection measure is displayed in Fig. III.1C leading to a different damage distribution (Fig. III.1D).

III.2.1 *Extreme Value Statistics*

The reason why we base our analysis on extreme value statistics is that in general the distribution of sea levels is unknown. Considering a certain case study, one can analyse the gauge sea level values (if available in high resolution and with sufficient statistics), make assumptions about its functional form,

and generate a histogram in order to estimate the distribution. Next, one can impose a sea level rise and move the distribution in order to estimate the increase of damages. The problem, however, is that the sea level distributions differ from gauge to gauge and the assumption about the functional form is not transferable. Therefore, such an approach is hardly feasible in practice and typically extreme value theory (which is well established in flood frequency analysis and mathematically substantiated) is employed. We follow a widely spread extreme value method – namely the Block Maxima approach.

The maxima in blocks of asymptotic length follow the *Generalised Extreme Value (GEV)* distribution (Coles, 2001; Leadbetter et al., 1983; Embrechts et al., 1997), characterised by three parameters: μ (location), σ (scale), and ξ (shape). It combines the Gumbel ($\xi = 0$), Fréchet ($\xi > 0$) and Weibull ($\xi < 0$) families and has the following cumulative distribution function:

$$P_{\xi,\sigma,\mu}(x) = \begin{cases} \exp[-(1+\xi\frac{x-\mu}{\sigma})^{-1/\xi}] & \text{if } \xi \neq 0 \\ \exp[-\exp(-\frac{x-\mu}{\sigma})] & \text{if } \xi = 0 \end{cases}, \tag{III.1}$$

where the corresponding probability density function is denoted by $p_{\xi,\sigma,\mu}$. In practice, this distribution is used to approximate the distribution of maximum annual water levels (Hawkes et al., 2008), which is in general unknown.

III.2.2 *Damage Functions*

Most commonly, a damage function describes the damage to an asset, given a certain inundation depth, either as a percentage damage rate (relative) or as monetary value (absolute). Several damage models have been proposed in literature, which are typically associated to certain asset types and exhibit different functional forms (Merz et al., 2010b).

When one wants to calculate the total damage from a certain flood event, the inundation heights at each asset in the affected region need to be determined (e.g. by hydrodynamic modelling) and the single damages (obtained by small scale damage functions) are aggregated. We call such a damage function, providing the total damage in a case study region as a function of the sea level, *macroscopic*. The availability of macroscopic damage functions in literature is very scarce and their general form unknown. Two functions are provided by Hallegatte et al. (2011) and Boettle et al. (2011), which can be well approximated by power laws, i.e.

$$F(x) \sim x^{\gamma}, \tag{III.2}$$

with a damage function exponent $\gamma > 0$ (in order to ensure the existence of the standard deviation of damages, we further need to assume $\gamma < 0.5/\xi$ in the case $\xi > 0$). While in most literature, (stage-) damage functions refer to individual buildings or assets (e.g. Büchele et al., 2006; Merz and Thieken, 2009; Dutta et al., 2003), here they refer to an entire region under consideration. This macroscopic damage function provides an aggregate of the building damages as obtained from microscopic damage functions (Boettle et al., 2011). I.e. it gives an estimate of the total monetary damage if case study YZ is affected by a coastal flood of maximum flood level x.

III.2.3 *Computational Calculations*

Combining the damage function F with the probability density function $p_{\xi,\sigma,\mu}$ of the GEV distribution, for the expected annual damage holds

$$E_D := \int_{-\infty}^{\infty} F(x) p_{\xi,\sigma,\mu}(x) dx$$

and for its standard deviation

$$STD_D := \left(\int_{-\infty}^{\infty} \left(E_D - F(x)\right)^2 p_{\xi,\sigma,\mu}(x) dx \right)^{1/2}.$$

For the numerical calculations, the integrals need to be discretised and the range of integration to be bounded. Here, the interval $[x_{min}, x_{max}]$ was partitioned by equidistant steps of width Δx, where x_{min} is the highest water level, for which no damage occurs and x_{max} represents the 100,000-year event (or the highest possible sea level in the Weibull case) at the current conditions. For varying protection heights, x_{max} was adjusted correspondingly. Naturally, due to computational limitations a trade-off between increment size and the highest considered annuality has to be made. We found that taking into account return levels of up to 100,000 years, both sources of error could be kept negligible. The equidistant spacing of the interval $[x_{min}, x_{max}]$ with midpoints $x_1, \ldots, x_N$ yields the discrete approximations

$$E_D \approx \Delta x \sum_{i=1}^{N} F(x_i) p_{\xi,\sigma,\mu}(x_i) \quad \text{and} \tag{III.3}$$

$$STD_D \approx \left(E_D^2 P_{\xi,\sigma,\mu}(x_{min}) + \Delta x \sum_{i=1}^{N} \left(E_D - F(x_i)\right)^2 p_{\xi,\sigma,\mu}(x_i) \right)^{1/2}. \tag{III.4}$$

Using these equations, the expected annual damage and its variability are calculated for changing parameters in Sec. III.4 and III.5.

III.3 Case Studies

In order to support our theoretical findings, we consider two case studies in Denmark: Copenhagen and Kalundborg. While Copenhagen, the capital, has more than 500,000 inhabitants, Kalundborg is much smaller and the case study refers to a threatened small population area in the south of the city of Kalundborg. For both regions, a macroscopic damage function is available. In the Copenhagen case, Hallegatte et al. (2011) elaborated a curve, which provides the direct losses to buildings and their contents in several sectors as well as infrastructural damages in absence of protection as a function of the flood level. The objective of this study was to assess the economic impacts of climate change and possible benefits of adaptation. For Kalundborg, Boettle et al. (2011) derived a damage function, comprising monetary damages to residential buildings in the area and investigated the macroscopic damage function for different Digital Elevation Model (DEM) qualities and small scale damage functions.

The case studies have been chosen because two essentials are available: (i) a record of annual maximum sea levels and (ii) a macroscopic damage function. Any other case study providing both would be equally applicable.

III.3.1 *GEV Parameter Estimation*

In order to obtain an estimation of the extreme value parameters for the Copenhagen gauge, a time series of maximum water levels at the gauge in the harbour of Copenhagen between 1890 and 2007 was analysed. The dataset consists of 95 values, which represent the maximum water levels within a hydrological year (October-September). The estimation of extreme value parameters requires the assumption of constant parameters. Although this is not given in practice, removing the mean sea level trend should legitimate the assumption of a stationary location parameter. After adding a linear trend of 0.45 mm per year (derived from mean sea level data, available at `http://www.psmsl.org`), the GEV parameters $\mu \approx 87.50$, $\sigma \approx 18.98$, and $\xi \approx -0.19$ were obtained as maximum likelihood estimators for censored sample data (Phien and Fang, 1989). This implies a Weibull distribution of annual peak values (in agreement with Hallegatte et al., 2011) with a maximum water level of approximately 187 cm.

The analogous analysis of 32 maximum water levels at the gauge in Kalundborg between 1971 and 2006 combined with mean sea level data from the Korsør gauge close to Kalundborg provided estimates for the GEV parameters, again using a maximum likelihood estimation for censored sample data (Phien and Fang, 1989). The values $\mu \approx 91.30$ (location), $\sigma \approx 16.96$ (scale) and $\xi \approx 0.00$ (shape) were obtained, implying a Gumbel distribution, which is unbounded on both sides. Due to the small sample size, these estimates cannot be considered as reliable. Nevertheless, we will proceed with these estimates since more extensive data were not available and the exact parameters are not crucial for our purposes.

III.3.2 *Extrapolation of Damage Functions*

The damage functions of both case studies are macroscopic damage functions providing monetary damages for flood levels of variable magnitude. In case of strongly altered GEV parameters, future flood heights might exceed the maximum level covered by the damage functions. Accordingly, in order to evaluate our results, we need to extend the damage functions to higher levels. The shape of such a continuation is in general unknown. Although a saturation of damages for sea levels above a certain magnitude seems plausible, at which point this saturation is reached is not clear and even an increased steepness cannot be ruled out, in case further areas become affected by extreme sea levels. Therefore, we extrapolate the curves with the same behaviour as they expose for lower sea levels – namely by a power law (see below).

The damage function for the city of Copenhagen was published in Hallegatte et al. (2011) and was obtained from Stéphane Hallegatte. It provides the direct losses for water levels between 0 and 4 m above current mean sea level. Figure III.2 depicts the curve and the extrapolation as power function.

In Boettle et al. (2011) the Kalundborg case study was treated in detail including the elaboration of a macroscopic damage function for water levels between 0 and 4 m (Fig. III.3). As in the Copenhagen case study the following extrapolation technique was used.

The given damage functions were extrapolated by fitting the power law, Eq. (III.2), with an additional proportionality constant to the available curve.

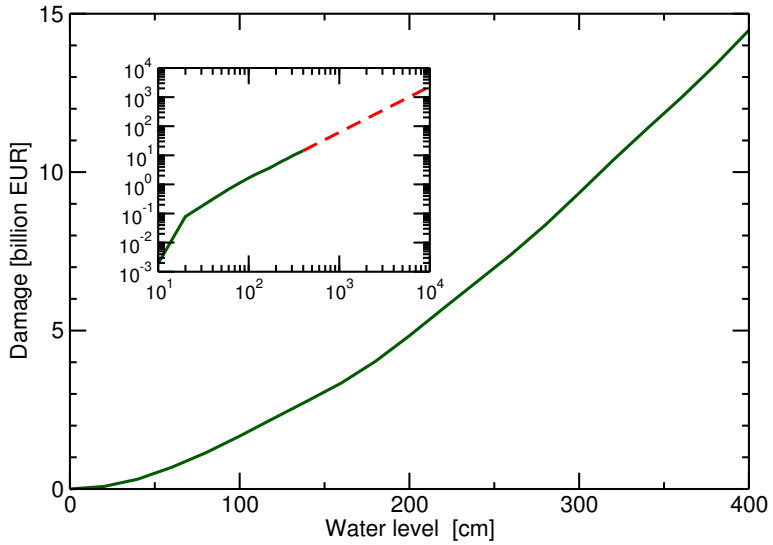

Figure III.2: Damage function (green) for the case study Copenhagen obtained from Hallegatte et al. (2011). The inset additionally shows the extrapolation as a power law with exponent $\gamma \approx 1.57$ (dashed red) in double logarithmic scale.

Only water levels for which the curve shows power law behaviour, i.e. above a certain threshold, were used for the fitting. The thresholds were 20 cm in Copenhagen and 140 cm in Kalundborg. Minimising the mean squared error, the exponents $\gamma \approx 1.57$ (with 95 % confidence interval $[1.56, 1.59]$) and $\gamma \approx 4.06$ (with 95 % confidence interval $[4.00, 4.12]$) were estimated for Copenhagen and Kalundborg, respectively.

III.4 Changes in the Extremes

We investigate how damages are influenced by changes in the water level extremes. Considering sea level rise, we assume that it is solely reflected in an increasing location parameter μ of the flood level GEV distribution (Kauker and Langenberg, 2000), which corresponds to a shift of all flood levels by the corresponding sea level rise. In contrast, an alteration of the scale parameter σ could be attributed to altering meteorological conditions.

We derive the distribution of damages as caused by the distribution of block maxima via a general damage function of the form of Eq. (III.2) and determine the expectation value E_D and the standard deviation STD_D of the damages. Finally, we provide the dependencies of E_D and STD_D on μ and σ.

III.4.1 *Influence of the Location Parameter*

First, we investigate a systematic alteration of the location parameter μ. This describes a simple shift of today's extreme events towards higher water levels. As derived analytically in the Appendix Sec. III.A, we find that the expected annual damage, Eq. (III.3), increases asymptotically for high values of μ with the damage function exponent γ, i.e.

$$E_D(\mu) \sim \mu^\gamma \quad . \tag{III.5}$$

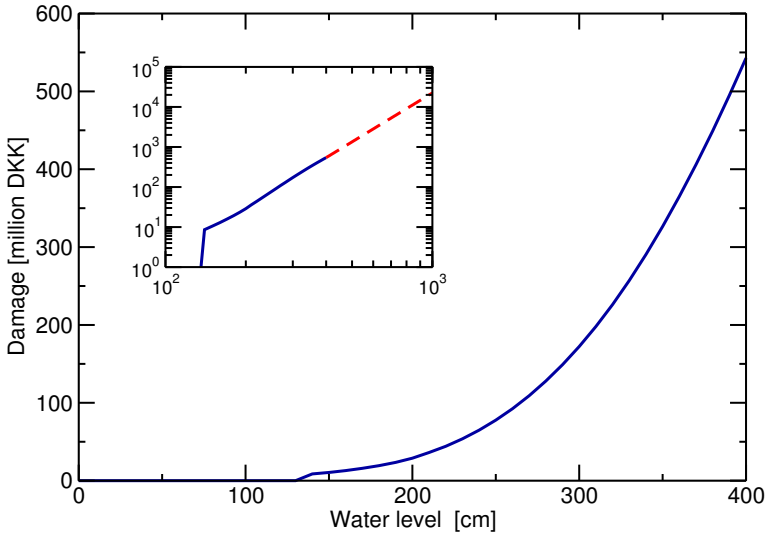

Figure III.3: Damage function (blue) for the case study Kalundborg using quadratic building damage functions and a flood fill algorithm via 4 nearest neighbours (Boettle et al., 2011). The inset additionally shows the extrapolation as a power law with exponent $\gamma \approx 4.1$ (dashed red) in double logarithmic scale.

Since damage functions are typically steeper than linear (e.g. Hallegatte et al., 2011; Boettle et al., 2011), the damage increases faster than the sea level. Presuming a certain case study where the damage increases cubically with the flood level (i.e. $\gamma = 3$, which is between the values of both case studies) and assuming that the sea level rises quadratically over time at the corresponding coast (as suggested by Rahmstorf et al., 2012), Eq. (III.5) implies that the expected annual damages increase with exponent $3 \times 2 = 6$ over time.

The damage variability, which emerges from the stochasticity of extreme events, can be characterised by the standard deviation STD_D as a measure of uncertainty. For large μ, we obtain asymptotically

$$\mathrm{STD}_D(\mu) \sim \mu^{\gamma-1} \ , \tag{III.6}$$

as derived in the Appendix Sec. III.A. This expression comprises only the aleatory uncertainty, i.e. the inherent variability due to the stochasticity. Further (epistemic) uncertainties (Thieken et al., 2005), for instance caused by the vague stage-damage relation, are not considered in this context. A quantification of these uncertainties would require very detailed additional information about the building damage functions and the entire inundation process (e.g. possible flow velocities, contaminations, etc.). Including these uncertainties, significantly higher values for the standard deviations could be expected (Merz et al., 2004).

In case of rising sea levels at a specific site with $\gamma > 1$ (which in general can be presumed) both, the expected damages and their standard deviation, increase. However, the standard deviation grows less steep, which leads to decreasing relative errors of our estimates $\mathrm{STD}_D/\mathrm{E}_D$. This reduced relative variability of annual damages can be perceived as a better predictability of flood damages, since the relative deviation of the real damages from our estimates becomes smaller. We would like to note that both relations are independent of the extreme value type, i.e. independent of ξ.

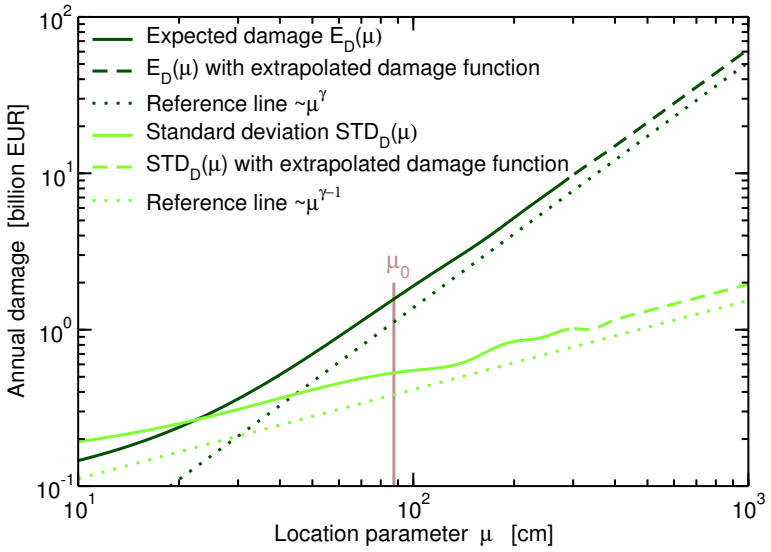

Figure III.4: Expected annual damage (dark green) and standard deviation (light green) in Copenhagen as a function of the location parameter μ of the GEV distribution. The solid lines were numerically calculated with the available damage function using Eqs. (III.3) and (III.4), the dashed continuations used an extrapolation of the damage function as a power law with exponent $\gamma \approx 1.57$ (see Fig. III.2). The dotted lines show the asymptotic relations Eqs. (III.5) and (III.6). The current value of the location parameter $\mu_0 \approx 88\,\mathrm{cm}$ is displayed as brown vertical line.

These general asymptotic findings shall be compared with calculations from the case studies. Using the Copenhagen damage function with a power law extrapolation for water levels above 4 m and the determined GEV parameters, Fig. III.4 exhibits the numerically calculated expectation values and standard deviations of damages as a function of the location parameter. It can be seen that a rising sea level and the corresponding shift of μ leads to an increase of damages, approaching the asymptotic relation expressed by Eq. (III.5). The same holds for the standard deviation and Eq. (III.6).

At this point, we are also interested on how the expected damages evolve in time. From the Dynamical Interactive Vulnerability Assessment (DIVA) tool (Hinkel and Klein, 2003; Vafeidis et al., 2008) mean sea level projections for the city of Copenhagen have been extracted for several socio-economic scenarios (IPCC, 2000). Assuming that changes in mean sea levels take place in the form of a shift of extreme events, we add sea level changes to the location parameter μ of the GEV distribution. Sea level projections are shown in Fig. III.5A for two socio-economic scenarios: (i) the ecologically friendly and globally homogeneous scenario B1 supposing medium climate sensitivity and (ii) a rapid economically growing world A1B with with a balanced emphasis on all energy sources, supposing high climate sensitivity. As can be seen in Fig. III.5B, the corresponding expected damages are steeper than the rise itself. Finally, an increase of flood risk by the factors 1.48 (B1 medium) and 2.37 (A1B high) for a mean sea level rise of 28 cm (B1) and 74 cm (A1B) by 2100 was found.

Figure III.6 is the analogue of Fig. III.4 for the Kalundborg case study. The expected damages and standard deviations for varying parameters μ show good agreement with the asymptotic results already for moderate parameter

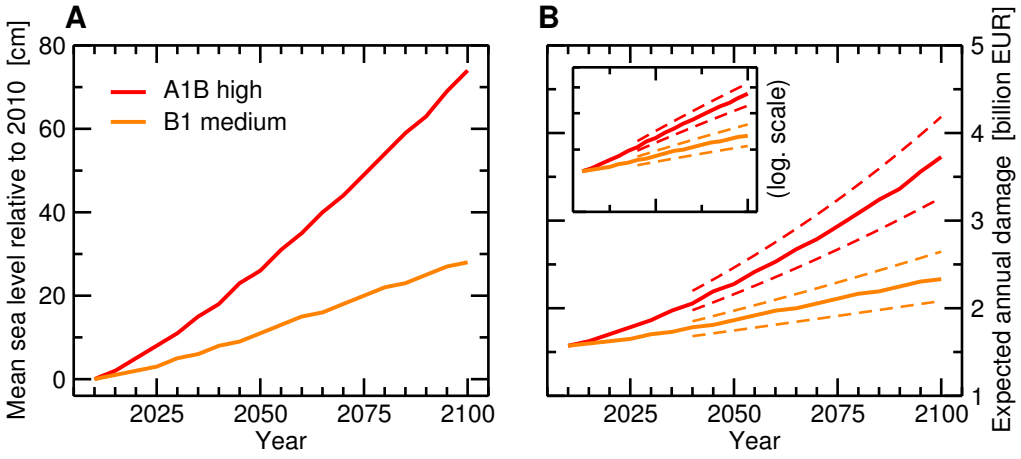

Figure III.5: (**A**) Mean sea level projections for Copenhagen provided by the DIVA tool (Hinkel and Klein, 2003; Vafeidis et al., 2008) for the SRES scenarios A1B (high) and B1 (medium). (**B**) The expected annual damage as a function of time, based on the two scenarios. The dashed lines are reference curves according to $f(\text{year}) = (\text{year} - k)^\tau$ with $k = 1650$ and $\tau = 4.5, 3.5, 2.5, 1.5$ (from top to bottom). The inset shows the same curves in a semi-logarithmic scale.

values. The asymptotic behaviours in Eqs. (III.5) and (III.6) therefore provide good estimations.

III.4.2 *Influence of the Scale Parameter*

Climate change can also affect the scale parameter σ of the water level distribution (Mudersbach and Jensen, 2010), which reflects changes in the variability, e.g. through evolving meteorological patterns. For varying σ, we obtain asymptotically (again, independent of ξ):

$$E_D(\sigma) \sim \sigma^\gamma \quad \text{and} \quad STD_D(\sigma) \sim \sigma^\gamma \ , \tag{III.7}$$

as analytically derived in the Appendix Sec. III.A. Accordingly, the expected annual damage increases with the width of the distribution of maximum sea levels following the same degree as the damage function. Contrary to Eq. (III.6), this holds also for the standard deviation. Hence, the relative uncertainty STD_D/E_D is (asymptotically) constant being basically unaffected by changes in the width of the extreme value distribution.

For the Copenhagen case study, the asymptotic predictions from Eq. (III.7) for a varying shape parameter σ are confirmed in Fig. III.7. However, a less steep increase for σ close to the present value σ_0 is found. The analogous results for Kalundborg are shown in Fig. III.8. In this case, the curves show good agreement with the asymptotic results already for parameter values around the current value σ_0. In summary, the asymptotics show the same sensitivity of damages for a changing variability as for changing sea levels. However, both case studies suggest a less steep increase in the near future.

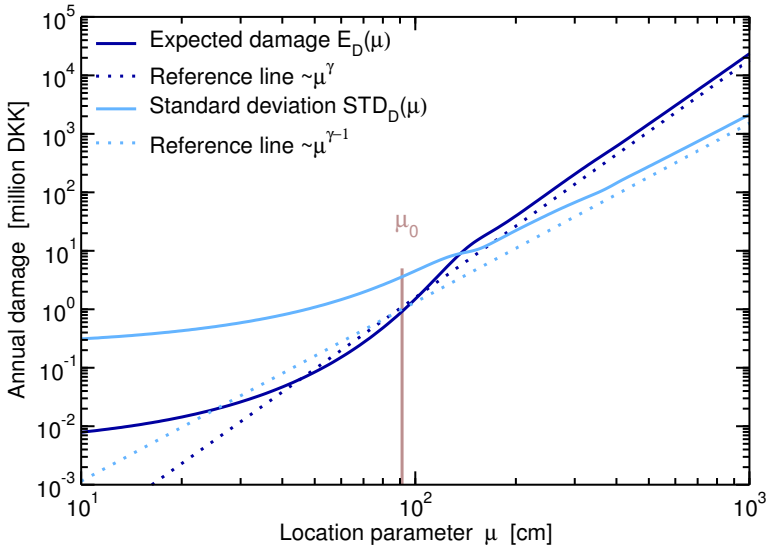

Figure III.6: Expected annual damage (dark blue) and standard deviation (light blue) in the case study area Kalundborg, as a function of the location parameter μ of the GEV distribution (analogous to Fig. III.4). The solid lines were calculated with the available damage function and its extrapolation as a power law with exponent $\gamma \approx 4.1$. The dotted line represents the asymptotic relations Eqs. (III.5) and (III.6). The current value of the location parameter $\mu_0 \approx 91.3\,\mathrm{cm}$ is displayed as brown vertical line.

III.5 Influence of Protection Measures

Finally, we investigate how the expected damage and the uncertainty depend on the height of hypothetical protection measures. For this purpose, we follow the same approach as in Sec. III.4 but take protection measures, such as a dyke or a sea wall, into account by censoring small floods, i.e. setting the damage function to zero below the corresponding threshold value ω. Please note that our model excludes protection failures such as dyke breaches. The parameters μ and σ are kept constant. Then, we study the damage distribution and extract the expectation value and the standard deviation of the damages as functions of the protection height ω.

In contrast to the previous results, the expected damages as a function of the protection height depend fundamentally on the GEV type. The asymptotic relations are analytically derived in the Appendix Sec. III.A.

1. *Gumbel case*
   We find in the Gumbel case ($\xi = 0$) the asymptotic relationship

   $$E_D(\omega) \sim \omega^{\gamma} e^{-\omega/\sigma} \ , \tag{III.8}$$

   for large ω. The decay is independent from μ and dominated by an exponential component. It is noteworthy, that the range of ω, for which the expression in Eq. (III.8) increases, is not relevant for the asymptotic behaviour.

2. *Fréchet case*
   For large ω, we find a power law decay in the Fréchet case ($\xi > 0$):

   $$E_D(\omega) \sim \omega^{\gamma - 1/\xi} \ , \tag{III.9}$$

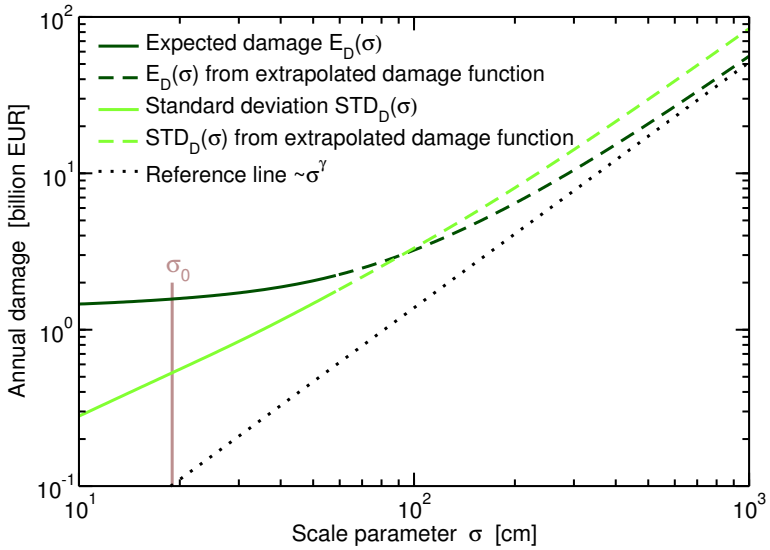

Figure III.7: Expected annual damage (dark green) and standard deviation (light green) in Copenhagen as a function of the scale parameter σ of the GEV distribution. The dotted line shows the theoretical asymptotic results from Eqs. (III.7). The current value of the scale parameter $\sigma_0 \approx 19\,\mathrm{cm}$ is displayed as brown vertical line.

which is independent from the scale parameter σ.

3. *Weibull case*
   In the Weibull case ($\xi < 0$), the possible water levels are bounded from above, which means that the water level cannot exceed a certain maximum value x_{max}. Hence, within our model, a protection height of x_{max} guarantees full flood safety and the expected damage becomes 0. Therefore, we investigate the behaviour for a protection height ω approaching the maximum water level x_{max} from below and obtain

$$E_D(\omega) \sim (x_{max} - \omega)^{-1/\xi} \quad . \tag{III.10}$$

   Remarkably, this expression is independent from the power of the damage function γ – in contrast to the other cases. Still, due to its range of validity, this result is rather of theoretical interest.

The corresponding standard deviations are given in Tab. III.1. They differ by a factor 0.5 in the exponents from the expressions for the expectation value. For the Gumbel case we find an exponential and for the Fréchet case a power law decay. Therefore, in the latter case the damages decrease much slower with enhanced flood defence. However, in both cases there is always a residual risk, which vanishes in the Weibull case for large enough ω. Accordingly, although protection suggests safety, it cannot avoid very extreme events in the Gumbel and Fréchet cases. This is also reflected in the increasing relative uncertainty, STD_D/E_D, which indicates a higher contribution of 'low-probability high-impact' events to the total damage (Merz et al., 2009).

The expressions were calculated for the case studies and are displayed in Figs. III.9 and III.10. Since the extreme values of the Copenhagen case follow the Weibull distribution, we use Eq. (III.10) and find good agreement between the numerically calculated damages and the predictions for protection levels

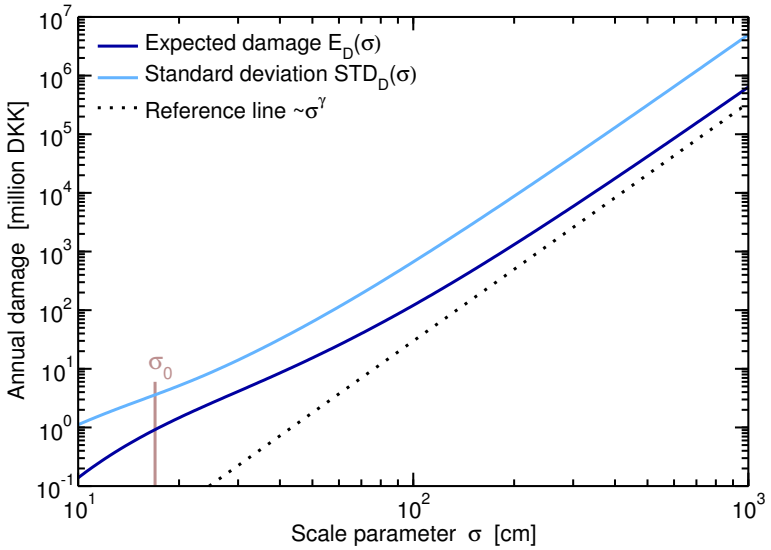

Figure III.8: Expected annual damage (dark blue) and standard deviation (light blue) in the case study area Kalundborg as a function of the scale parameter σ of the GEV distribution (analogous to Fig. III.7). The dotted lines represent the theoretical asymptotic results from Eqs. (III.7). The current value of the scale parameter $\sigma_0 \approx 17\,\mathrm{cm}$ is displayed as brown vertical line.

above 100 cm. Also for Kalundborg (Gumbel distribution) a good approximation of the numerical calculation by Eq. (III.8) is found for protection heights above 140 cm. For lower protection levels, there is no visible effect on the damages, which implies that the maximum annual sea level exceeds the height in most years and makes the protection measure dispensable.

Performing a cost-benefit analysis, these results can be used to derive an optimal protection height, for which the total costs, comprising implementation costs and residual damages, are minimised.

III.6 Conclusions

We have derived expressions for the expected damage from coastal floods and its standard deviation for a general case study region as a function of varying location and scale parameters. The findings are complemented with the corresponding expressions as a function of the protection height, i.e. the value below which any damage is suppressed.

The relations are summarised in Tab. III.1. In particular, we find that while the expectation value increases as a power law with the location parameter involving the damage function exponent γ, the standard deviation comprises an exponent $\gamma - 1$. Hence, the relative uncertainty, i.e. the ratio of both quantities decreases as μ^{-1} with the consequence that, from a relative perspective, the damages become more certain. For instance, the relative error of our estimation for Copenhagen, STD_D/E_D, which currently amounts to 34 % would decrease to approximately 26 %, supposing 20 cm of sea level rise. This also indicates, that the expected damages are increasingly determined by more common floods and that the contribution of 'low-probability high-impact' events to the expected damages declines with rising sea levels.

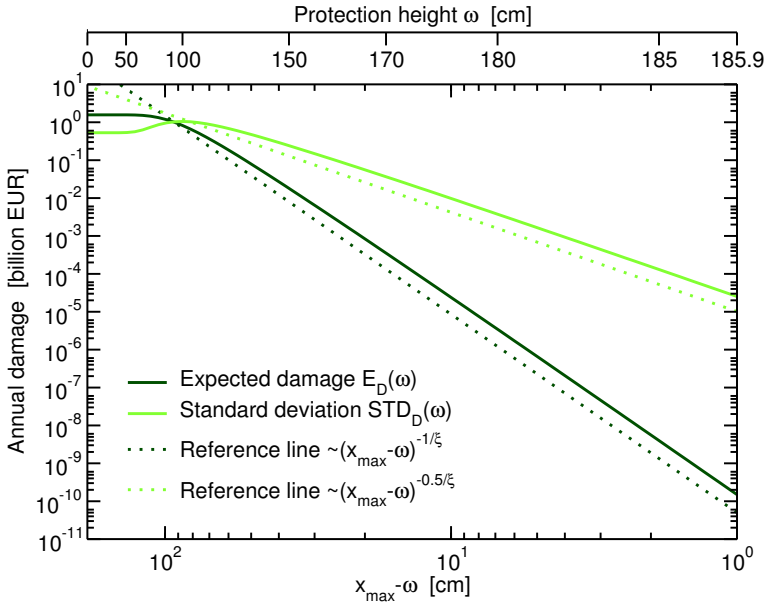

Figure III.9: Expected annual damage (dark green) and standard deviation (light green) in Copenhagen as a function of the difference between the protection level ω and the maximum possible water level $x_{max} \approx 186.9\,\mathrm{cm}$. The dotted lines follow a power law with exponent $-1/\xi$ (dark green) and $-0.5/\xi$ (light green) as expressed by Eq. (III.10) and Eq. (III.12), respectively, where $\xi \approx -0.19$. Please note that the abscissa has been inverted in order to illustrate that the quantities decrease with increasing protection level ω (on top, corresponding protection heights are displayed).

This does not hold for the quantities as a function of the scale parameter. Here, the expectation value and the standard deviation increase with the same exponent and the relative uncertainty is constant. In fact, all relations are power laws with exponent γ, except the standard deviation as a function of μ which goes with a by 1 reduced exponent.

Surprisingly, the expressions are *universal*, i.e. the expectation value and the standard deviation as a function of location and scale parameter are all independent of the shape parameter ξ of the extreme value distribution. This makes the results easy applicable to arbitrary regions, since no information about the extreme value behaviour is necessary. Overall, the damage function exponent γ, that appears in all relations, is the most decisive factor for the estimation of future damages. If $\gamma > 1$ – as in both case studies – the expected damages rise super-linearly with the sea level.

Investigating the influence of protection measures, we find different expressions for the different GEV types (see last column of Tab. III.1). While the Gumbel case involves the scale parameter and the damage function exponent, the Fréchet case involves the shape parameter and the damage function exponent, and the Weibull case involves the shape parameter and surprisingly not the damage function exponent. Interestingly, in all cases, the expectation value and the standard deviation differ only by a factor 0.5 in the exponent. Accordingly, the relative uncertainty increases and the damages become more uncertain the higher the protection level is.

Since, in general, sea level records follow an unknown distribution, we applied a Block Maxima approach, which allows to describe the highest water

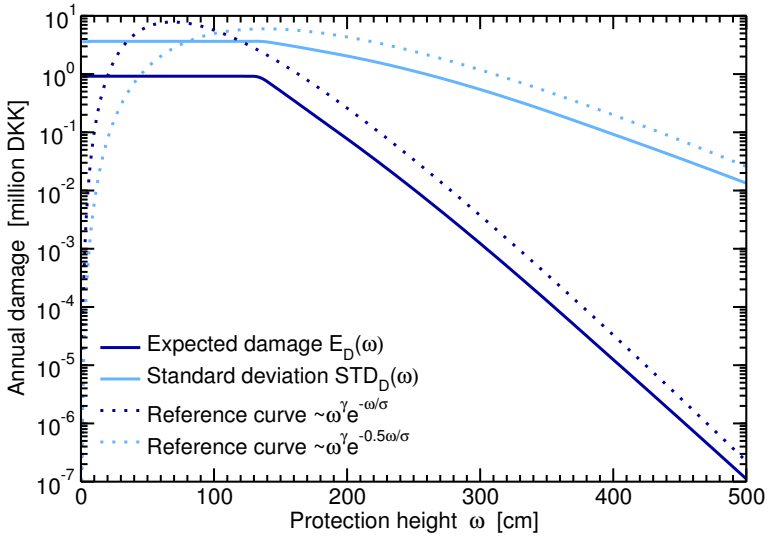

Figure III.10: Expected annual damage (dark blue) and standard deviation (light blue) in the case study area Kalundborg as a function of the protection level ω. The dotted lines follow $\omega^{\gamma}e^{-\omega/\sigma}$ and $\omega^{\gamma}e^{-0.5\omega/\sigma}$ as expressed by Eq. (III.8) and Eq. (III.14).

level per year by one of three limiting distributions. These GEV distributions, in turn, can be fully examined. However, the drawback are inherent limitations. Since our Block Maxima approach considers only the largest flood event per year and neglects possible further floods. At the current conditions, this is only a minor shortcoming, since coastal floodings are per se rare in most areas, which is expected to change with rising mean sea levels. However, the integration of additional flood events (e.g. the second largest per year) in the framework would cause further inaccuracies, since several events in quick succession would not lead to independent damages.

In Summary, based on a set of assumptions, simple analytic expressions have been found for all dependencies. Although these results are derived for the asymptotic case, they showed good agreements with the numerical calculations from the two case studies. Therefore, the results provide a reasonable estimation for the development of future damages and could be employed in

Table III.1: Summary of the asymptotic behaviour of expected damage and the standard deviation as a function of involved parameters μ, σ, and ω. The asymptotics hold for $\omega \to x_{max}$ in the case $\xi < 0$ and for large parameter values otherwise.

	location μ	scale σ	protection height ω	
E_D	$\sim \mu^{\gamma}$	$\sim \sigma^{\gamma}$	$\sim \omega^{\gamma} e^{-\omega/\sigma}$	if $\xi = 0$
			$\sim (x_{max} - \omega)^{-1/\xi}$	if $\xi < 0$
			$\sim \omega^{\gamma - 1/\xi}$	if $\xi > 0$
STD_D	$\sim \mu^{\gamma-1}$	$\sim \sigma^{\gamma}$	$\sim \omega^{\gamma} e^{-0.5\omega/\sigma}$	if $\xi = 0$
			$\sim (x_{max} - \omega)^{-0.5/\xi}$	if $\xi < 0$
			$\sim \omega^{\gamma - 0.5/\xi}$	if $\xi > 0$

integrated assessment models in the context of climate impact research (e.g. Tol, 2002b).

Appendix

III.A Asymptotic relations

The asymptotic relations in Eqs. (III.5) – (III.10) are proven analytically in Theorems 1 – 5. Additionally, relations for the standard deviation of annual damages with respect to the protection height are provided. Some of the results (Theorems 3 – 5) are shown only for power damage functions with integer exponents, their general validity could still be confirmed by numerical calculations following Eqs. (III.3) and (III.4). For all considerations with regard to Fréchet-distributed water levels, the assumption $\gamma < 1/\xi$ has to be made (Katz et al., 2002) in order to ensure the existence of the expected damage. An even stricter limitation of $\gamma < 0.5/\xi$ is necessary for the examination of the corresponding standard deviations. All following integrals without integration limits are meant to integrate over the largest possible interval, typically over the support of the corresponding probability distribution.

We start with some general lemmata to arrange the subsequent theorems more clearly.

Lemma 1. *Given a probability density* p *with existing* r*-th moment* $m_r := \int x^r p(x)dx$ *and* $r, a, b \in \mathbb{R}^+$*, for the integral*

$$I_{a,b} := \int (a + bx)^r p(x)dx$$

holds

$$\lim_{a\to\infty} I_{a,b}/a^r = 1 \quad \text{and} \quad \lim_{b\to\infty} I_{a,b}/b^r = m_r \ .$$

Proof. The integral can be written as

$$I_{a,b} = a^r \int (1 + \frac{b}{a}x)^r p(x)dx = b^r \int (\frac{a}{b} + x)^r p(x)dx$$

and the uniform convergence of the integrands for $a \to \infty$ and $b \to \infty$, respectively, allows the swapping of the integral and the limit. It follows

$$\begin{aligned} \lim_{a\to\infty} I_{a,b}/a^r &= \int \lim_{a\to\infty} (1 + \frac{b}{a}x)^r p(x)dx \\ &= \int p(x)dx \\ &= 1 \end{aligned}$$

and

$$\begin{aligned} \lim_{b\to\infty} I_{a,b}/b^r &= \int \lim_{b\to\infty} (\frac{a}{b} + x)^r p(x)dx \\ &= \int x^r p(x)dx \\ &= m_r \ . \end{aligned}$$

□

Lemma 2. *Given a probability density* p *with existing* $2r$*-th moment* $m_{2r} := \int x^{2r} p(x)\mathrm{d}x$ *and* $r, b \in \mathbb{R}^+$*, for the integral*

$$I_a := \int (a+bx)^{2r} p(x)\mathrm{d}x - \left(\int (a+bx)^r p(x)\mathrm{d}x\right)^2$$

holds

$$\lim_{a\to\infty} I_a / a^{2r-2} = \text{const.} \neq 0 \ .$$

Proof. We start with the Taylor expansion of $(a+bx)^r$ around $x = 0$:

$$\begin{aligned}(a+bx)^r &= \sum_{i=0}^{\infty} \binom{r}{i} a^{r-i} b^i x^i \\ &= a^r + r a^{r-1} bx + \frac{r(r-1)}{2} a^{r-2} b^2 x^2 + \mathcal{O}(a^{r-3}),\end{aligned}$$

where $\binom{r}{i}$ denotes the generalised binomial coefficient $\binom{r}{n} = r(r-1)\cdot\ldots\cdot(r-n+1)/n!$. Applying this also to the term $(a+bx)^{2r}$, it follows

$$\begin{aligned}I_a &= \int \left[a^{2r} + 2ra^{2r-1}bx + \frac{2r(2r-1)}{2} a^{2r-2} b^2 x^2 + \mathcal{O}(a^{2r-3})\right] p(x)\mathrm{d}x \\ &\quad - \left(\int \left[a^r + ra^{r-1}bx + \frac{r(r-1)}{2} a^{r-2} b^2 x^2 + \mathcal{O}(a^{r-3})\right] p(x)\mathrm{d}x\right)^2 \\ &= \frac{2r(2r-1)}{2} a^{2r-2} b^2 m_2 - r^2 a^{2r-2} b^2 m_1^2 - r(r-1) a^{2r-2} b^2 m_2 \\ &\quad + \int \mathcal{O}(a^{2r-3}) p(x)\mathrm{d}x \\ &= (m_2 - m_1^2) r^2 b^2 a^{2r-2} + \int \mathcal{O}(a^{2r-3}) p(x)\mathrm{d}x \ .\end{aligned}$$

Since the integrand is uniform convergent again, swapping the integral and the limit leads to

$$\begin{aligned}\lim_{a\to\infty} I_a / a^{2r-2} &= \lim_{a\to\infty} (m_2 - m_1^2) r^2 b^2 + \lim_{a\to\infty} \int \underbrace{\mathcal{O}(a^{-1})}_{\to 0} p(x)\mathrm{d}x \\ &= (m_2 - m_1^2) r^2 b^2 \ ,\end{aligned}$$

which is constant and in general non-zero. In the special case of $r \in \mathbb{N}$, the Taylor expansions are finite and the result can be obtained more easily. □

Lemma 3. *Given a probability density* p *with existing* $2r$*-th moment* $m_{2r} = \int x^{2r} p(x)\mathrm{d}x$ *and* $r, a, b \in \mathbb{R}^+$*, for the integral*

$$I_b := \int (a+bx)^{2r} p(x)\mathrm{d}x - \left(\int (a+bx)^r p(x)\mathrm{d}x\right)^2$$

holds

$$\lim_{b\to\infty} I_b / b^{2r} = \text{const.} \neq 0 \ .$$

Proof. Using the uniform convergence of the integrands, it holds

$$\begin{aligned}\lim_{b\to\infty} I_b/b^r &= \int \lim_{b\to\infty} (\frac{a}{b}+x)^{2r} p(x)dx - \left(\int \lim_{b\to\infty} (\frac{a}{b}+x)^r p(x)dx\right)^2 \\ &= \int x^{2r} p(x)dx - \left(\int x^r p(x)dx\right)^2 ,\end{aligned}$$

which is $m_{2r} - m_r^2$ and in general a non-zero constant. □

Now we can proof the statements from the main text more easily, starting with the expected damage as functions of of the location μ and the scale σ.

Theorem 1. *Assuming GEV-distributed maximum water levels* $X \sim \mathrm{GEV}_{\xi,\sigma,\mu}$ *and a power damage function* $F(x) = x^\gamma$ *($0 < \gamma < 1/\xi$), for the expected annual damage* E_D *holds asymptotically (for large* μ *and* σ*, respectively)*

$$E_D(\mu) \sim \mu^\gamma \quad \text{and} \quad E_D(\sigma) \sim \sigma^\gamma.$$

Proof. It holds

$$\begin{aligned}E_D &= \int F(x)\mathrm{GEV}_{\xi,\sigma,\mu}(x)dx \\ &= \int (\mu+\sigma x)^\gamma \underbrace{\mathrm{GEV}_{\xi,1,0}(x)}_{=:p(x)} dx.\end{aligned}$$

Lemma 1 now provides $E_D(\mu)/\mu^\gamma \overset{\mu\to\infty}{\longrightarrow} 1$ and $E_D(\sigma)/\sigma^\gamma \overset{\sigma\to\infty}{\longrightarrow} m_\gamma$, where m_γ denotes the γ-th moment of the GEV-distributed water levels X. Since $\gamma < 1/\xi$ is presumed, $m_\gamma \neq 0$ exists, which proves the lemma. □

Theorem 2. *Assuming GEV-distributed maximum water levels* $X \sim \mathrm{GEV}_{\xi,\sigma,\mu}$ *and a power damage function* $F(x) = x^\gamma$ *($0 < \gamma < 0.5/\xi$), for the standard deviation* STD_D *of the annual damage holds asymptotically (for large* μ *and* σ*, respectively)*

$$\mathrm{STD}_D(\mu) \sim \mu^{\gamma-1} \quad \text{and} \quad \mathrm{STD}_D(\sigma) \sim \sigma^\gamma.$$

Proof. For the variance holds

$$\mathrm{Var} = \int (\mu+\sigma x)^{2\gamma} \underbrace{\mathrm{GEV}_{\xi,1,0}(x)}_{=:p(x)} dx - \left(\int (\mu+\sigma x)^\gamma \underbrace{\mathrm{GEV}_{\xi,1,0}(x)}_{=:p(x)} dx\right)^2 .$$

Lemmas 2 and 3 provide $\mathrm{Var}(\mu)/\mu^{2\gamma-2} \overset{\mu\to\infty}{\longrightarrow}$ const. $\neq 0$ and $\mathrm{Var}(\sigma)/\sigma^{2\gamma} \overset{\sigma\to\infty}{\longrightarrow}$ const. $\neq 0$, respectively. Consequently, the same holds for $\mathrm{STD}_D = \mathrm{Var}^{1/2}$. □

Now, we provide results to proof the relations for the dependencies on the the protection height ω.

Lemma 4. *Considering the probability density function* $\mathrm{GEV}_{\xi,\sigma,\mu}$ *of a Fréchet distribution (i.e.* $\xi > 0$*) and* $n \in \mathbb{N}$ *($n < 1/\xi$), it holds asymptotically (for large* ω*)*

$$I_n := \int_\omega^\infty x^n \mathrm{GEV}_{\xi,\sigma,\mu}(x)dx \sim \omega^{n-1/\xi}.$$

Proof. We start with the integral

$$I_n = \frac{1}{\sigma}\int_\omega^\infty x^n \left(1+\xi\frac{x-\mu}{\sigma}\right)^{-1/\xi-1} \exp\left(-\left(1+\xi\frac{x-\mu}{\sigma}\right)^{-1/\xi}\right)dx$$

and substitute $z := \left(1+\xi\frac{x-\mu}{\sigma}\right)^{-1/\xi}$:

$$\begin{aligned}
I_n &= \int_0^{\left(1+\xi\frac{\omega-\mu}{\sigma}\right)^{-1/\xi}} \left(\frac{\sigma}{\xi}z^{-\xi} - \frac{\sigma}{\xi} + \mu\right)^n e^{-z}dz \\
&= \sum_{i=0}^{n} \underbrace{\binom{n}{i}\left(\mu-\frac{\sigma}{\xi}\right)^{n-i}\left(\frac{\sigma}{\xi}\right)^i}_{=:K_{n,i}} \underbrace{\int_0^{\left(1+\xi\frac{\omega-\mu}{\sigma}\right)^{-1/\xi}} z^{-i\xi}e^{-z}dz}_{=\text{lower incomplete Gamma function } \gamma} \\
&= \sum_{i=0}^{n} K_{n,i}\gamma\left(1-i\xi, \left(1+\xi\frac{\omega-\mu}{\sigma}\right)^{-1/\xi}\right) \\
&= \sum_{i=0}^{n} \underbrace{K_{n,i}}_{\text{const.}} \underbrace{\left(1+\xi\frac{\omega-\mu}{\sigma}\right)^{i-1/\xi}}_{\to\omega^{i-1/\xi}} \underbrace{\exp\left(-\left(1+\xi\frac{\omega-\mu}{\sigma}\right)^{-1/\xi}\right)}_{\to 1} \\
&\quad \cdot \underbrace{\sum_{k=0}^{\infty} \frac{\left(1+\xi\frac{\omega-\mu}{\sigma}\right)^{-k/\xi}}{(1-i\xi)(2-i\xi)\cdot\ldots\cdot(1+k-i\xi)}}_{\to\text{const.}} \\
&\sim \omega^{n-1/\xi},
\end{aligned} \tag{III.11}$$

for large ω. The properties of the incomplete Gamma function can be found in Arfken and Weber (2005). □

Theorem 3 (ω-relation, Fréchet)**.** *Given Fréchet-distributed maximum water levels $X \sim GEV_{\xi,\sigma,\mu}$ ($\xi > 0$), a power damage function $F(x) = x^\gamma$ ($\gamma \in \mathbb{N}, \gamma < 0.5/\xi$) and an implemented protection measure of height ω, for the annual damage holds asymptotically (for large ω)*

$$E_D(\omega) \sim \omega^{\gamma-1/\xi} \quad \text{and} \quad STD_D(\omega) \sim \omega^{\gamma-0.5/\xi}.$$

Proof. Lemma 4 gives the relation for the expectation value E_D (setting $n = \gamma$) and $Var - E_D^2 \sim \omega^{2\gamma-1/\xi}$ (setting $n = 2\gamma$). The expression for the standard deviation follows immediately. □

Please note, that the case $\gamma \notin \mathbb{N}$ is not included in the theorem. Nevertheless, its validity could be confirmed by numerical calculations.

Lemma 5. *Considering the probability density function $GEV_{\xi,\sigma,\mu}$ of a (reversed) Weibull distribution (i.e. $\xi < 0$) and $n \in \mathbb{N}$, for ω close to the maximum value $x_{max} := \mu - \sigma/\xi$ of $X \sim GEV_{\xi,\sigma,\mu}$ holds*

$$I_n := \int_\omega^R x^n GEV_{\xi,\sigma,\mu}(x)dx \sim (x_{max}-\omega)^{-1/\xi}.$$

Proof. We obtain Eq. (III.11) similar as in the proof above. For ω close to x_{max} follows

$$\begin{aligned} I_n &= (\text{III.11}) \\ &= \sum_{i=0}^{n} \underbrace{K_{n,i}}_{\text{const.}} \underbrace{\left(1+\xi\frac{\omega-\mu}{\sigma}\right)^{i-1/\xi}}_{\to (x_{max}-\omega)^{i-1/\xi}} \underbrace{\exp\left(-\left(1+\xi\frac{\omega-\mu}{\sigma}\right)^{-1/\xi}\right)}_{\to 1} \\ &\quad \cdot \underbrace{\sum_{k=0}^{\infty} \frac{1}{(1-i\xi)(2-i\xi)\cdot\ldots\cdot(1+k-i\xi)}}_{\text{const.}} \\ &\sim (x_{max}-\omega)^{-1/\xi} \quad . \end{aligned}$$

□

Theorem 4 (ω-relation, Weibull)**.** *Given Weibull-distributed maximum water levels* $X \sim GEV_{\xi,\sigma,\mu}$ *(*$\xi < 0$*), a power damage function* $F(x) = x^\gamma$ *(*$\gamma \in \mathbb{N}, \gamma < 0.5/\xi$*) and an implemented protection measure of height* ω *close to the maximum value of* X*,* $x_{max} := \mu - \sigma/\xi$*, for the annual damage holds*

$$E_D(\omega) \sim (x_{max}-\omega)^{-1/\xi}$$

and

$$STD_D(\omega) \sim (x_{max}-\omega)^{-0.5/\xi}. \tag{III.12}$$

Proof. Lemma 5 gives the relation for the expectation value E_D (setting $n = \gamma$) and $Var - E_D^2 \sim \omega^{2\gamma-1/\xi}$ (setting $n = 2\gamma$). The expression for the standard deviation follows immediately. □

As before, please note that the case $\gamma \notin \mathbb{N}$ is not included in the theorem. Nevertheless, its validity could be confirmed by numerical calculations.

Lemma 6. *Considering the probability density function* $GEV_{0,\sigma,\mu}$ *of a Gumbel distribution and* $n \in \mathbb{N}$*, it holds asymptotically (for large* ω*)*

$$I_n := \int_\omega^\infty x^n GEV_{\xi,\sigma,\mu}(x)dx \sim \omega^n e^{-\omega/\sigma}.$$

Proof. Starting with the substitution $z := \frac{x-\mu}{\sigma}$ we obtain

$$\begin{aligned} \frac{I_n}{\omega^n e^{-\omega/\sigma}} &= \frac{\sigma^n}{\omega^n e^{-\omega/\sigma}} \int_{\frac{\omega-\mu}{\sigma}}^\infty \left(\sum_{i=0}^{n} \binom{n}{i} \left(\frac{\mu}{\sigma}\right)^{n-i} z^i\right) \\ &\qquad \cdot \exp(-z) \underbrace{\exp(-\exp(-z))}_{\leqslant 1} dz \\ &\leqslant \frac{\sigma^n}{\omega^n e^{-\omega/\sigma}} \int_{\frac{\omega-\mu}{\sigma}}^\infty \left(\sum_{i=0}^{n} \underbrace{\binom{n}{i} \left(\frac{\mu}{\sigma}\right)^{n-i}}_{\leqslant \text{const.}} z^i\right) \cdot \exp(-z)dz \\ &\leqslant \text{const.} \cdot \frac{1}{\omega^n e^{-\omega/\sigma}} \sum_{i=0}^{n} \int_{\frac{\omega-\mu}{\sigma}}^\infty z^i \exp(-z)dz \\ &= \text{const.} \cdot \frac{1}{\omega^n e^{-\omega/\sigma}} \sum_{i=0}^{n} \Gamma(i+1, \frac{\omega-\mu}{\sigma}), \end{aligned} \tag{III.13}$$

which is constant for $\omega \to \infty$ with the upper incomplete Gamma function Γ. Equation (III.13) can also be bounded from below:

$$\begin{aligned}(\text{III.13}) &\geqslant \text{const.} \cdot \frac{1}{\omega^n e^{-\omega/\sigma}} \sum_{i=0}^{n} \int_{\frac{\omega-\mu}{\sigma}}^{\infty} z^n \exp(-z) dz \\ &= \text{const.} \cdot \frac{1}{\omega^n e^{-\omega/\sigma}} \sum_{i=0}^{n} \Gamma(i+1, \frac{\omega-\mu}{\sigma}),\end{aligned}$$

which is again constant for $\omega \to \infty$ and finishes the proof. □

Theorem 5 (ω-relation, Gumbel)**.** *Given Gumbel-distributed maximum water levels* $X \sim \text{GEV}_{0,\sigma,\mu}$*, a power damage function* $F(x) = x^\gamma$ *($\gamma > 0$) and an implemented protection measure of height* ω*, for the annual damage* E_D *holds asymptotically (for large* ω*)*

$$E_D(\omega) \sim \omega^\gamma e^{-\omega/\sigma} \quad \text{and} \quad \text{STD}_D(\omega) \sim \omega^\gamma e^{-\omega/(2\sigma)}. \tag{III.14}$$

Proof. The theorem follows immediately with Lemma 6. □

Acknowledgements. We would like to thank Stéphane Hallegatte, Jacob Arpe, and Carlo S. Sørensen for the provision of data and Boris F. Prahl, Luís Costa, and Dominik E. Reusser for fruitful discussions and comments. We appreciate financial support by the BaltCICA Project (part-financed by the EU Baltic Sea Region Programme 2007-2013).

IV

Quantifying the Effect of Sea Level Rise and Flood Defence – A Point Process Perspective on Coastal Flood Damage

*Markus Böttle**, *Diego Rybski**, *and Jürgen P. Kropp**,†

*Potsdam Institute for Climate Impact Research (PIK), Potsdam, Germany
†University of Potsdam, Institute of Earth and Environmental Science, Potsdam, Germany

Abstract. In contrast to recent advances in projecting sea levels, estimations about the economic impact of sea level rise are vague. Nonetheless, they are of great importance for policy making with regard to adaptation and greenhouse-gas mitigation. Since the damage is mainly caused by extreme events, we propose a stochastic framework to estimate the monetary losses from coastal floods in a confined region. For this purpose, we follow a Peak Over Threshold approach employing a Poisson Point Process and the Generalised Pareto Distribution. By considering the effect of sea level rise as well as potential adaptation scenarios on the involved parameters, we are able to study the development of the annual damage. An application to the city of Copenhagen shows that a doubling of losses can be expected from a mean sea level increase of only 11 cm. In general, we find that for varying parameters the expected losses can be well approximated by one of three analytical expressions depending on the extreme value parameters. These findings reveal the complex interplay of the involved parameters and allow conclusions of fundamental relevance. For instance, we show that the damage typically increases faster than the sea level rise itself. This in turn can be of great importance for the assessment of sea level rise impacts on the global scale. Our results are accompanied by an assessment of uncertainty, which reflects the stochastic nature of extreme events. While the absolute value of uncertainty about the flood damage increases with rising mean sea levels, we find that it decreases in relation to the expected damage.

This chapter is published as:
Boettle, M., Rybski, D., and Kropp, J. P. (2016). Quantifying the effect of sea level rise and flood defence – a point process perspective on coastal flood damage, *Nat. Hazards Earth Syst. Sci.*, 16(2):559–576, doi:10.5194/nhess-16-559-2016.

IV.1 Introduction

Considering current CO_2 emission pathways, severe climate change impacts need to be anticipated (IPCC, 2007; Nicholls and Cazenave, 2010). As one of the most perceivable effects of global warming, sea level rise will amplify the magnitude as well as the frequency of coastal floods (Rahmstorf and Coumou, 2011; Seneviratne et al., 2012) and is likely to have significant economic impacts (Hinkel et al., 2014; Nicholls and Tol, 2006). Even in the case of temperature stabilisation, sea levels will continue to rise for many decades (Meehl et al., 2012). Accordingly, greenhouse-gas mitigation alone will not be sufficient, and additional preventive measures need to be considered to cope with the consequences (Petherick, 2012). The most common method to assess the efficiency of such measures is Cost–Benefit Analysis (Tol, 2002a), in which the benefits in terms of averted damage are compared to the investment costs. For this purpose, a concise assessment of potential economic consequences is indispensable.

Adverse effects from sea level rise are particularly expected from storm surges, presupposing the coincidence of extreme tidal and storm conditions (Woodworth et al., 2011). Accordingly, not the mean sea level itself but rather its effect on the tail of the sea level distribution needs to be studied. Since the actual distribution of sea levels is in general unknown, extreme value theory is commonly employed in order to characterise extreme events by a unifying tail distribution (Hawkes et al., 2008).

For estimating the *annual flood damage* at a specific site (that is the sum of all damages caused within a year), information on the occurrence of flood events, their magnitude as well as the corresponding damage is required. Due to the stochastic nature of extreme events, the annual damage cannot be predicted for a specific year and is characterised by its average value over a longer time period. In reality, the actual damage fluctuates around this expected annual damage with a certain variability. For instance, there are years without any damage and others where a very unlikely flood event (e.g. a 100- or 1000-year event) occurs. This variability can be measured by several means such as the skewness of the distribution or specific quantile values. We will use the standard deviation for this purpose as it can be straightforwardly derived and further provides an intuitive way to quantify the uncertainty of our damage estimations. Since environmental as well as climatic changes alter the statistics of extreme events, we assume non-stationarity and investigate the development of damage for specific parameter scenarios.

Considering sea level rise, we find analytic relations describing the damage for asymptotic parameter values (i.e. for very large changes) and show that they represent good approximations for the behaviour of damage under current conditions. Furthermore, studying the mitigation effects due to coastal protection measures in an analogous way, we provide three potential decays of residual damage, depending on the shape of the sea level distribution. In general, our analytical relations are capable of describing the development of damage for all parameter variations.

The paper is organised as follows. Section IV.2 provides the methodologies for the estimation of annual flood damage via a Point Process. The effect of sea level rise is investigated in Sec. IV.3, where we provide analytical expressions

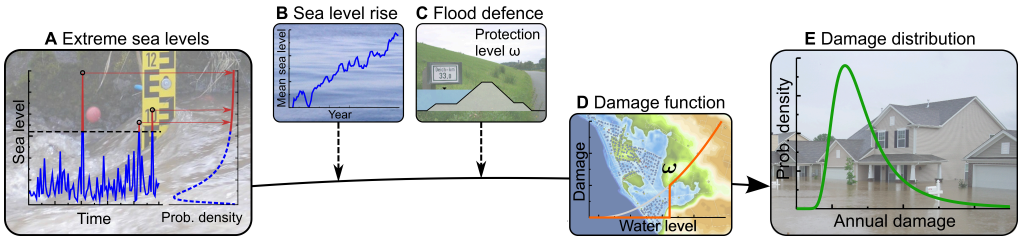

Figure IV.1: From extreme sea levels to damage. (**A**) The analysis of extreme sea levels provides parameter estimations for the *generalised Pareto distribution*. (**B**) The distribution of sea levels is influenced by mean sea level rise. (**C**) Flood defence measures, such as dikes, set the threshold below which any damage is prevented. (**D**) The distribution of extreme sea levels is combined with the corresponding damage via a damage function, providing the total damage in the region under study at a certain maximum flood level. (**E**) From the resulting distribution of total annual damage the expected annual damage and its standard deviation can be derived. (Photographs: 'Ilmpegel Ilmenau' by Michael Sander (2006), 'Sea' by Dedda71 (2008), 'Kilometermarkierung Deich' by Georg HH (2006), and 'Nashville Flood' by Eric Hamiter (2010) from Wikimedia Commons – CC:BY-SA.)

describing the asymptotic behaviour in a general setting. The generic form of these results allows their application to arbitrary regions, which is exemplified by two case studies in Denmark (Sec. IV.4). Section IV.5 investigates the effect of coastal protection in a similar manner. A complementary block maxima approach using the Generalised Extreme Value (GEV) distribution was followed previously (Boettle et al., 2013b), in which exactly one – namely the most severe – flood event per year is taken into account. A comparison of the two methods is presented in Sec. IV.6. Finally, our findings are discussed in Sec. IV.7. Further results and the derivation of our analytic results are provided in the Appendix.

IV.2 Methodology

Our proposed methodology (illustrated by Fig. IV.1) is based on the combination of extreme value theory (Secs. IV.2.1, IV.2.2 and IV.2.3) and the concept of (stage-)damage functions (Sec. IV.2.4). Thus, we are able to calculate the expected annual damage (Secs. IV.2.5 and IV.2.6) within a considered region for different parameter scenarios. All employed symbols and their meanings are summarised in Table IV.1.

IV.2.1 *Peak Over Threshold Approach*

Extreme events are commonly characterised by employing extreme value theory (Coles, 2001; Hawkes et al., 2008). Besides the block maxima method, Peak Over Threshold (POT) is a widely used approach (Coles, 2001), where the distribution of water levels, given that they exceed a certain threshold u, is estimated. Supposing the threshold u to be high enough and assuming the independence of flood events, the excess water levels follow approximately a Generalised Pareto Distribution (GPD). In addition to u, the GPD is determined by

Table IV.1: Overview of employed symbols, their meanings, and section in which they are introduced.

Symbol	Meaning	Section
ξ	Shape parameter of the extreme value distribution	IV.2.1
σ	Scale parameter of the extreme value distribution	IV.2.1
u	Considered threshold of the extreme value distribution	IV.2.1
μ	1-year event; i.e. sea level that is exceeded on average once a year	IV.2.2
Λ	Intensity of the Poisson process; i.e. average number of sea level exceedances per year above u	IV.2.2
γ	Exponent of the damage function	IV.2.4
ω	Presumed protection level; i.e. maximum sea level against which the considered region is protected	IV.5

a shape parameter ξ and a scale parameter σ. Its cumulative distribution is of the following form:

$$H_{u,\xi,\sigma}(x) = \begin{cases} 1 - \exp(-\frac{x-u}{\sigma}) & \text{if } \xi = 0 \\ 1 - \left(1 + \xi\frac{x-u}{\sigma}\right)^{-1/\xi} & \text{if } \xi \neq 0, \end{cases} \tag{IV.1}$$

with $x > u$. In the case $\xi < 0$, the water level is bounded from above by a maximum possible water level $x_{max} := u - \sigma/\xi$ and we set $H_{u,\xi,\sigma}(x) = 1$ for $x \geqslant x_{max}$ accordingly.

In our context, u is the critical water level above which damage occurs or corresponds to the given protection height at the site. However, bearing in mind that $H_{u,\xi,\sigma}$ describes the limiting distribution of exceedances for an asymptotically increasing threshold, u needs to be large enough to obtain a good approximation of the true distribution. In particular, if no protection is given and u is freely chosen, a compromise between the adequacy of the statistical model (the larger u, the better the approximation) and the omission of smaller events ($x < u$) needs to be found.

IV.2.2 *Point Process*

Section IV.2.1 provided the distribution of water levels given that the threshold u is exceeded. However, an estimation of annual damage requires additional information on how often the sea level exceeds u. Therefore, we define a flood event as such an exceedance and use a point process to model the incidence of these events (Coles, 2001; Embrechts et al., 1997). By employing a Poisson process (Reiss and Thomas, 2007), the number of flood events N within a specific year is Poisson-distributed with a certain mean value Λ, i.e.

$$N \sim \text{Poi}(\Lambda). \tag{IV.2}$$

Consequently, Λ is the average number of flood events and $P(N = k) = \frac{\Lambda^k}{k!}e^{-\Lambda}$ the probability of k events within 1 year. The Poisson property Eq. (IV.2) is

a strong assumption, which is strictly valid for independent water levels and is commonly assumed in practice (e.g. Mudersbach and Jensen, 2010; Hawkes et al., 2008). The parameter Λ can be estimated by counting the number of observed events divided by the corresponding time period. Furthermore, Λ can be directly related to the GPD parameters: denoting μ as the *1-year event*, i.e. the water level that is exceeded on average once per year, it holds (Coles, 2001) that

$$\Lambda = \begin{cases} \exp\left(-\frac{u-\mu}{\sigma}\right) & \text{if } \xi = 0 \\ \left(1+\xi\frac{u-\mu}{\sigma-\xi(u-\mu)}\right)^{-1/\xi} & \text{if } \xi \neq 0 \end{cases}. \tag{IV.3}$$

IV.2.3 *Parameter Effects*

We want to study the impact of sea level rise as well as potential protection measures on the flood damage. As illustrated in Fig. IV.2, two general effects can be observed within our framework. On the one hand, the frequency of flood events, i.e. the number of annual floods N_i, is expected to change. On the other hand, the intensities of occurring flood events can change, which would be represented in a change of the probability distribution of exceedances.

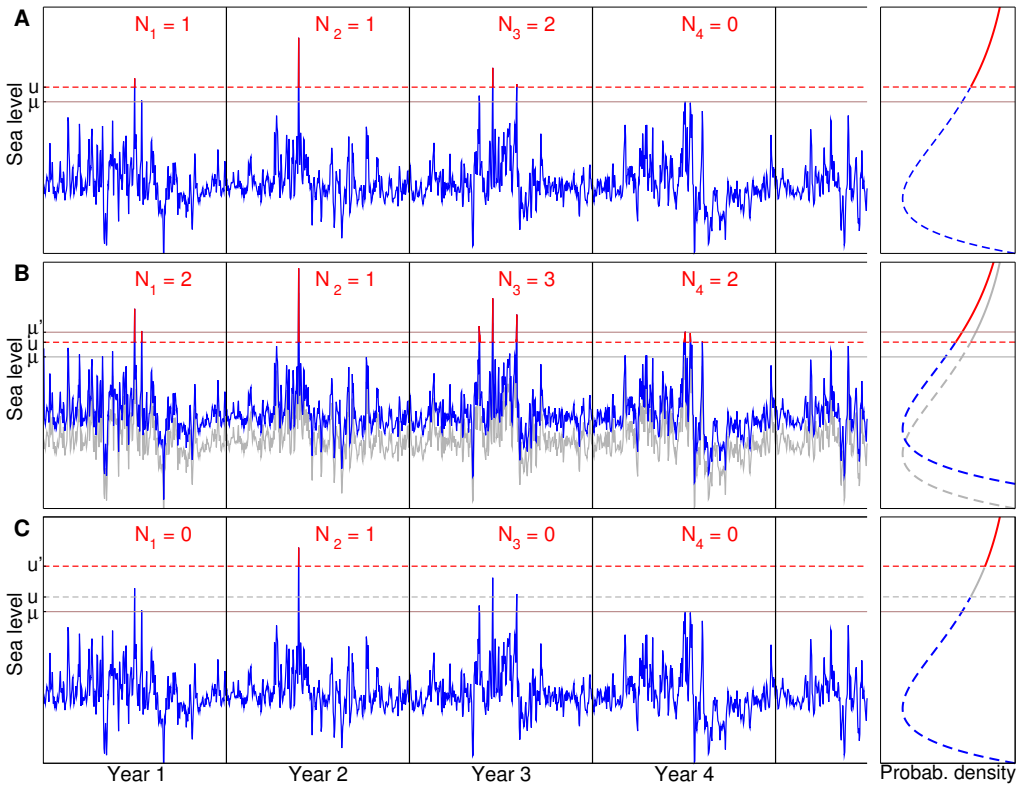

Figure IV.2: Illustrative time series of sea levels and their probability density function for several scenarios. **(A)** Current conditions with a threshold u and the 1-year event μ. **(B)** Increased mean sea level with a corresponding shift of the time series and thus the 1-year event from μ to μ'. **(C)** Supposing a protection height of u' implying an adjustment of the threshold from u to u'. The values $N_1, N_2, \ldots$ represent in all cases the number of exceedances within the corresponding year. The average value of the N_i provides an estimator for occurrence rate Λ.

IV.2.3.1 *Sea Level Rise*

We assume that a rise in mean sea levels results in a shift of today's sea level distribution towards higher water levels without deformation of the distribution (Kauker and Langenberg, 2000; Mudersbach et al., 2013). Other possible effects, e.g. a changing tide behaviour, can be modelled by a varying scale parameter σ (see Appendix IV.A). This scenario is illustrated in Fig. IV.2B where the time series is shifted by the mean sea level rise leading to increased numbers of flood events N_i (which in turn change the parameter $\Lambda = \sum_{i=1}^{l} N_i/l$) and a modified probability distribution of exceedances. Accordingly, we adjust our model in such a way that every event of certain annuality in a particular year is increased by the corresponding sea level rise (McInnes et al., 2013). This is achieved by a simple modification of the parameters. Firstly, the frequency of exceedances will increase. Using the 1-year event μ as variable parameter, we consider a shift from μ to μ' (i.e. a sea level rise of $(\mu' - \mu)$ cm) and use Eq. (IV.3) to derive the altered occurrence rate. Prior to this, also the scale parameter σ of the exceedance distribution needs to be adjusted (Coles, 2001):

$$\sigma' = \sigma + \xi(\mu - \mu'), \tag{IV.4}$$

which implies an altered width of the distribution in the case $\xi \neq 0$. These modifications result in a shift of each event with certain annuality by the magnitude of mean sea level rise.

IV.2.3.2 *Protection Measures*

The implementation of a coastal protection measure will be considered in such a way that any damage from flood levels up to a specific protection height ω is avoided (as suggested by Hallegatte et al., 2013). Hence, we choose a new threshold $u' = \omega$ representing the implemented protection height. Figure IV.2C illustrates this approach and it can be seen that the number of flood events N_i as well as the probability distribution of exceedances changes if we raise the threshold from u to u'.

Given the GPD parameters with respect to a threshold u, the GPD distribution with respect to u' has the same shape parameter ξ but a modified scale parameter σ' (see e.g. Katz et al., 2005):

$$\sigma' = \sigma + \xi(u' - u). \tag{IV.5}$$

Again, this also enters the derivation of a change in flood frequency using Eq. (IV.3).

IV.2.4 *Damage Functions*

After having information about the occurrence of flood events, the resulting damage is obtained by means of a (stage-)damage function (Smith, 1994; Merz et al., 2010b), which describes the correlations between the flood height and the corresponding damage (Fig. IV.1D).

Most commonly, damage functions are applied on the building scale (see e.g. Merz et al., 2010b, and references therein). In our context, we use *macroscopic* damage functions (Boettle et al., 2011; Prahl et al., 2016), which provide the

total damage within a spatially delineated region as a function of the maximum flood level. We assume that the form of such damage functions follows a power law (as suggested in Hallegatte et al., 2011; Boettle et al., 2011), i.e. for the damage caused by a flood of maximum height x holds the proportionality

$$F(x) \sim x^{\gamma} . \tag{IV.6}$$

See Boettle et al. (2013b) for more details. In general the *damage function exponent* γ is unknown, but values of 1.6 and 4.1 have been found for our case studies (Boettle et al., 2013b).

IV.2.5 *Expected Annual Damage & Uncertainty*

The combination of the methodologies above provides the probability distribution of the annual flood damage in a specific region (Fig. IV.1E). However, we restrict our investigations to the *expectation value* and the *standard deviation* of the annual damage. The annual damage D is calculated as the sum of all single event damages D_i, i.e. $D = D_1 + \cdots + D_N$, where $N \sim \mathrm{Poi}(\Lambda)$ is the number of flood events in the considered year. The Poisson property of N implies for the expected number of flood events $E_N = \Lambda$ and for its variance $\mathrm{Var}_N = \Lambda$. Using Wald's identities (Beichelt, 2006), the expected annual damage E_D and the standard deviation STD_D are

$$E_D = \Lambda E_{D_i} \quad \text{and} \tag{IV.7}$$

$$\mathrm{STD}_D = (\mathrm{Var}_D)^{1/2} = \left(\Lambda \left(\mathrm{Var}_{D_i} + E_{D_i}^2\right)\right)^{1/2}, \tag{IV.8}$$

where E_{D_i} and Var_{D_i} describe the expected damage of a single flood event and its variance, respectively. Please note that all event magnitudes D_i within 1 year are assumed to be independent and identically distributed (Coles, 2001).

IV.2.6 *Computational Calculations*

Given the extreme value parameters u, ξ, σ, Λ, and a damage function F, we calculate the expected annual damage E_D and the standard deviation STD_D by virtue of Eqs. (IV.7) and (IV.8). For this purpose, the required information on the single events D_i is obtained via $E_{D_i} = \int_u^\infty F(x) h_{u,\xi,\sigma}(x)\,dx$ and $\mathrm{STD}_{D_i}^2 = \int_u^\infty (E_{D_i} - F(x))^2\, h_{u,\xi,\sigma}(x)\,dx$, where $h_{u,\xi,\sigma}(x) = \frac{d}{dx} H_{u,\xi,\sigma}(x)$ is the probability density function of exceedances. From the computational perspective, the mentioned integrals need to be discretised and the upper limit replaced by a finite value x_{max}. In the case $\xi < 0$, the limit x_{max} represents the maximal possible water level as described in Sec. IV.2.1, otherwise it is set to such a high value that the resulting error becomes negligible. Partitioning the range of integration $[u, x_{max}]$ by equidistant steps Δx with n midpoints $x_1, \ldots, x_n$, the following approximations are used:

$$E_{D_i} \approx \Delta x \sum_{j=1}^{n} F(x_j) h_{u,\xi,\sigma}(x_j) \quad \text{and} \tag{IV.9}$$

$$\mathrm{STD}_{D_i}^2 \approx \Delta x \sum_{j=1}^{n} \left(E_{D_i} - F(x_j)\right)^2 h_{u,\xi,\sigma}(x_j). \tag{IV.10}$$

IV.3 Sea Level Rise Impacts

We start in a general setting where the GPD parameters ξ, σ, u, as well as the damage function exponent γ are given and investigate the behaviour of damage for rising sea levels.

All other parameters are kept constant in the following. As described in Sec. IV.2.3.1, we parametrise the mean sea level by the 1-year event μ. The following results are derived analytically (see Appendix IV.B for details) and hold in an asymptotic sense. More precisely, the expected damage E_D divided by the provided expression, Eqs. (IV.11)–(IV.13), converges to a non-zero constant number for $\mu \to \infty$ (or, if it is bounded, by a value μ_{max}, for $\mu \to \mu_{max}$). Hence, the following relations represent limit behaviours. Their practical use as approximations of the actual behaviour is examined in Sec. IV.4.

We find an increase of the annual damage by means of two separate effects (as described in Sec. IV.2.3.1): (i) higher frequency of events or (ii) higher severity of the events. Depending on the shape parameter ξ, three possible behaviours need to be distinguished:

(i) In the case $\xi = 0$ (indicating an exponential tail in the sea level distribution), sea level rise leads to an exponentially increasing number of flood events while the alterations of single floods are negligible, overall implying an exponential dependence of the expected annual damage on the sea level:

$$E_D(\mu) \sim e^{\mu/\sigma}. \tag{IV.11}$$

(ii) In contrast, we find a less steep relation if the water levels are bounded tailed (i.e. $\xi < 0$):

$$E_D(\mu) \sim \mu^{\gamma - 1/\xi}. \tag{IV.12}$$

Here, the two effects are superposed: the average damage of an event increases with exponent γ and the number of events with exponent $-1/\xi$.

(iii) For the heavy-tailed case ($\xi > 0$), the damage can be characterised by a power law:

$$E_D(\mu) \sim (\mu_{max} - \mu)^{-1/\xi}, \tag{IV.13}$$

which holds for μ close to the maximum possible value μ_{max}. Approaching this value, the number of flood occurrences becomes very large and ends in a permanent flooding of the area under study for $\mu = \mu_{max}$. As for $\xi = 0$, this behaviour is solely caused by more frequent inundations and not by a changing severity of flood events.

It can be seen that each of the three possible relations involves a different set of parameters. Surprisingly, the damage function exponent γ is not involved (in the case $\xi \geqslant 0$) or plays only a minor role (for $\xi < 0$, the term $-1/\xi$ in Eq. (IV.12) is predominant for typical parameter values). This implies that the functional behaviour of $E_D(\mu)$ is mostly independent of the determining factors of the damage function, such as the orography and the location of values in the case

study area. In general, considering that $|\xi|$ typically takes small values, the expected damage increases super-linearly in all cases.

The expected annual damage only represents average values, and the actually occurring losses fluctuate considerably. Therefore, we also examine the uncertainty of our estimations by means of the standard deviation of the damage, STD_D, and find expressions similar to the average value but with an additional factor of 0.5 in the exponents (see Appendix IV.B for their derivations):

$$\mathrm{STD}_D(\mu) \sim \begin{cases} e^{0.5\mu/\sigma} & \text{if } \xi = 0 \text{ (for large } \mu) \\ \mu^{\gamma - 0.5/\xi} & \text{if } \xi < 0 \text{ (for large } \mu) \\ (\mu_{max} - \mu)^{-0.5/\xi} & \text{if } \xi > 0 \text{ (for } \mu \text{ close to } \mu_{max}) \end{cases} . \quad \text{(IV.14)}$$

This uncertainty measure represents just a lower bound since it includes only the aleatory uncertainty from the fact that one does not know *when* the extremes occur and does not take into account additional epistemic uncertainties due to a lack of knowledge, e.g. stemming from the stage–damage relation (Merz et al., 2004) or the estimation of extreme value parameters (Hosking and Wallis, 1987). However, the relations imply that although the variability increases in all cases, the relative error of the estimate, STD_D/E_D, *decreases* with rising sea levels. Surprisingly, this implies that, in a sense, flood damage becomes more foreseeable.

Besides sea level rise, which is regarded as the main driver for higher and more frequent extremes (Menéndez and Woodworth, 2010), meteorological changes can play an important role. Evolving wind patterns, for instance, can lead to a modified distribution of water levels (Haigh et al., 2010), which in turn alters the damage distribution. Although this effect is not understood (Mudersbach and Jensen, 2010), the influence of a hypothetically changing scale parameter σ on the damage is studied in Appendix IV.B.

IV.4 Application

We would like to illustrate how the respective variables behave in real examples and compare our analytic derivations from the previous section with numerical calculations (as described in Sec. IV.2.6) for two Danish case studies – namely the city of Copenhagen and the municipality of Kalundborg. The two locations were chosen due to the availability of damage functions as well as sea level records. Details on the case studies can be found in Hallegatte et al. (2011) and Boettle et al. (2011), respectively.

For the estimation of extreme value parameters in the two case studies, extreme sea level records from closely located gauges were preprocessed by subtracting a linear trend of 0.45 cm (Copenhagen) and 0.16 cm (Kalundborg) per year (derived from mean sea level data, available at `http://www.psmsl.org`). Next, a threshold u, above which the behaviour of water levels is modelled, needs to be chosen where a trade-off between bias (low u) and variance (high u) is required. One necessary condition for an appropriate threshold u is the linear dependence between the mean excesses and the thresholds close to u (Coles, 2001). As can be seen in the *mean excess plots* in Fig. IV.3, this holds for thresholds around 100 cm (Copenhagen) and above 80 cm (Kalundborg),

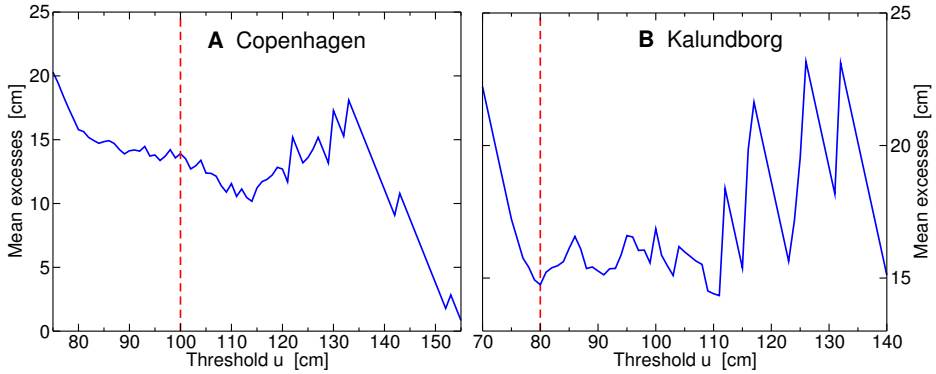

Figure IV.3: Average magnitudes of excesses over the threshold u from available sea level records for varying thresholds in **(A)** Copenhagen and **(B)** Kalundborg. The dashed red lines represent the thresholds $u = 100\,\text{cm}$ (Copenhagen) and $u = 80\,\text{cm}$ (Kalundborg), which were used for our analysis.

respectively. Bearing also in mind that a sufficient number of sea levels above the threshold is needed for the determination of parameters, the GPD parameters were estimated on the basis of the remaining 69 (Copenhagen) and 106 (Kalundborg) extreme sea levels. Using a maximum likelihood estimation (Embrechts et al., 1997), the parameters $\xi = -0.14$ and $\sigma = 15.79\,\text{cm}$ for Copenhagen and $\xi = 0.08$, $\sigma = 13.65\,\text{cm}$ for Kalundborg were obtained. Since the damage function of Kalundborg shows only a negligible damage for sea levels below 140 cm, the threshold was raised to $u = 135\,\text{cm}$, which entails a modified scale parameter of $\sigma = 17.78\,\text{cm}$ according to Eq. (IV.5). Please note that this adjustment does not affect the stochastic accuracy and just avoids the consideration of negligible flood events. As the shape parameter ξ is negative for Copenhagen, the possible sea levels are bounded and a maximum possible sea level of $x_{max} \approx 215\,\text{cm}$ is deduced. These parameters deviate from the previously performed estimation of GEV parameters based on annual maximum sea level records (Boettle et al., 2013b). The occurrence rates Λ for the description of the Poisson process were estimated by the average number of observed exceedances per year. These are $\Lambda = 0.585$ (Copenhagen) and $\Lambda = 0.083$ (Kalundborg). Finally, the 1-year events $\mu = 91.21\,\text{cm}$ (Copenhagen) and $\mu = 95.35\,\text{cm}$ (Kalundborg) were calculated by using Eq. (IV.3).

The available damage functions support our presumption from Sec. IV.2.4 and follow roughly power laws with exponents $\gamma = 1.6$ (Copenhagen) and $\gamma = 4.1$ (Kalundborg). Further details on the damage functions can be found in Boettle et al. (2013b). The exponent γ is used for two purposes: (i) the parametrisation of the damage function needed for the functional description of sea level rise effects (Sec. IV.3) and (ii) for an extrapolation of the damage function beyond the provided range which in some cases is required for numerical calculations (namely, if $x_{max} > 10\,\text{m}$, Sec. IV.2.6).

Once having this information, the annual damage can be calculated numerically (as described in Sec. IV.2.6) for varying mean sea levels parametrised by the 1-year event μ. Figure IV.4 shows this annual mean damage and its standard deviation as a function of μ and compares it with the asymptotic results. Since $\xi > 0$ holds in the Kalundborg case, the parameter μ is bounded from above by a value μ_{max} and we parametrise the damage by the difference $\mu_{max} - \mu$. For μ approaching $\mu_{max} \approx 332\,\text{cm}$, the number of flood events

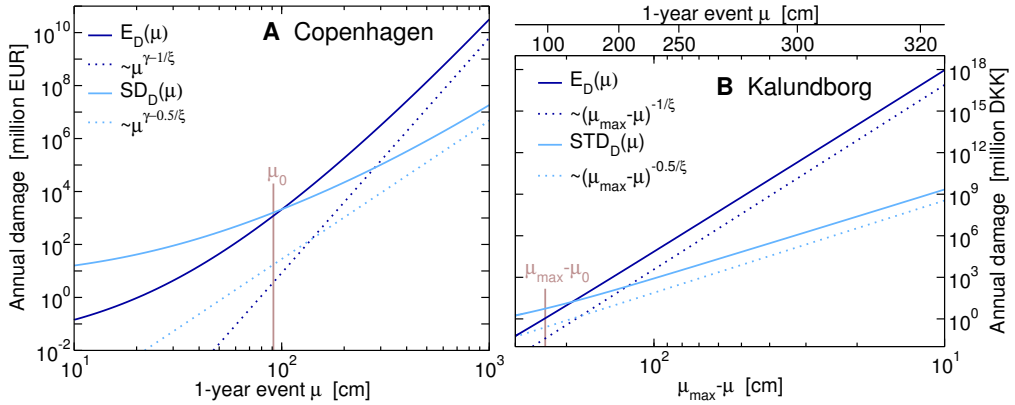

Figure IV.4: Expected annual damage (dark blue) and standard deviations (light blue) in **(A)** Copenhagen and **(B)** Kalundborg as a function of the mean sea level (parametrised by the 1-year flood μ). The dotted lines show the asymptotic relations Eqs. (IV.12), (IV.13) and (IV.14) with $\gamma = 1.6$ and $\xi = -0.14$ (Copenhagen) and $\gamma = 4.1$ and $\xi = 0.08$ (Kalundborg). The values for the current 1-year floods $\mu_0 = 91.21\,\text{cm}$ (Copenhagen) and $\mu_0 = 95.35\,\text{cm}$ (Kalundborg) are indicated by brown vertical lines. The abscissa in the right panel is inverted and shows the difference between the 1-year flood μ and $\mu_{max} = 332.04\,\text{cm}$ (at the top, the corresponding 1-year floods are displayed).

becomes very large and ends in a permanent flooding of the considered region. It is likely that the municipality counteracts this tendency as soon as the occurring damage exceeds a tolerable value. Our projections are therefore explicitly based on a "no adaptation" scenario. We also disregard a modification of the damage function due to precedent damage and e.g. reduction of asset value. It can be seen that rising mean sea levels lead to an increase in expected damage and standard deviation, which is well described by our asymptotic results already for moderate values of μ. This holds particularly for Kalundborg, but also in the case of Copenhagen – a similar shape of the dashed and solid lines can be detected. Overall, the asymptotic behaviours provide good estimates under the current conditions for both case studies. This shows that adequate projections of future flood damage can be obtained based on very few parameters. It needs to be highlighted again that in both cases the damage function exponent γ plays only a minor role. While for Kalundborg the approximation is even independent from it, the asymptotic projection for Copenhagen, $\mu^{\gamma-1/\xi} \approx \mu^{1.6+7.1}$, is clearly dominated by the shape parameter $\xi = -0.14$.

In practice, one is often interested in a temporal development of damage. In order to further elaborate on this issue, our approach requires a projection of mean sea levels. For the city of Copenhagen, such have been extracted from the Dynamical Interactive Vulnerability Assessment (DIVA) tool (Hinkel and Klein, 2003; Vafeidis et al., 2008) and we were thus able to study the damage as a function of time. Again, we suppose that changes in mean sea levels result in a shift of extreme events and add the estimated mean sea level rise to the corresponding events. Figure IV.5A displays the sea level projections for the SRES scenarios B1 (medium climate sensitivity) and A1B (high climate sensitivity) with a total rise of 11 and 26 cm by 2050 respectively. Panel B shows the resulting annual damage, exhibiting a steeper slope than the sea levels with an increase by a factor of roughly 2 (B1) and 4.6 (A1B) by 2050, respectively.

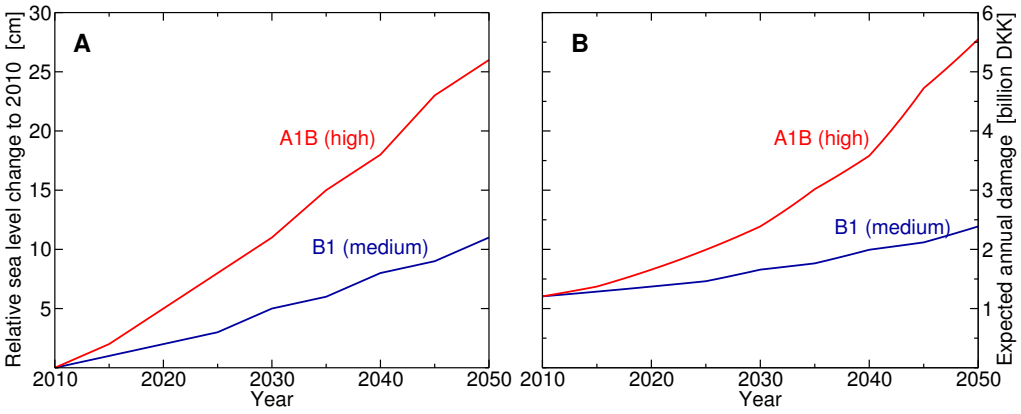

Figure IV.5: **(A)** Mean sea level projections for the SRES scenarios A1B (high climate sensitivity) and B1 (medium climate sensitivity) in Copenhagen provided by the DIVA tool (Hinkel and Klein, 2003; Vafeidis et al., 2008). **(B)** The expected annual damage as a function of time, based on the two scenarios.

IV.5 The Effect of Protection Measures

At this point, it is important to bear in mind that the severity of a flood disaster is not only determined by environmental factors but also to a significant extent by human decisions (Pielke Jr. and Downton, 2000). In particular, the implementation of a flood defence measure can counteract the increasing flood risk (Fig. IV.1C). However, identifying the appropriate height of the protection measure is crucial for choosing a cost-efficient solution, i.e. an investment that pays off within a considered time period. Therefore, we investigate the effect of varying protection heights ω on the residual damage, assuming that inundations from flood levels below ω are completely avoided (as suggested by Hallegatte et al., 2013). Since the distribution of sea levels is bounded in the case $\xi < 0$, the damage vanishes for a protection measure higher than the maximum possible water level x_{max}. This is not the case for $\xi \geqslant 0$. In summary, we find the asymptotic relations

$$E_D(\omega) \sim \begin{cases} \omega^{\gamma} e^{-\omega/\sigma} & \text{if } \xi = 0 \text{ (for large } \omega) \\ (x_{max} - \omega)^{-1/\xi} & \text{if } \xi < 0 \text{ (for } \omega \text{ close to } x_{max}) \\ \omega^{\gamma - 1/\xi} & \text{if } \xi > 0 \text{ (for large } \omega) \end{cases} . \tag{IV.15}$$

As for rising sea levels, the behaviour of the expected damage depends fundamentally on the shape parameter ξ. While we find a decay that is dominated by an exponential component in the case $\xi = 0$, a power law relation independent of the scale parameter σ is found if $\xi > 0$. For $\xi < 0$, the expected damage follows a power law with the proximity of the protection height ω to the maximum water level x_{max}. Remarkably, the expressions differ not only in their functional forms but also in the parameters involved. For instance, the exponent γ of the damage function does not influence the behaviour in the case $\xi < 0$ (as in Copenhagen). This highlights the decisive character of the shape parameter ξ, whose sign is not always unambiguous (Martins and Stedinger, 2000). Although a steep decrease in the damage is found in all cases, full flood safety can only be achieved if $\xi < 0$, and a residual risk needs to be dealt with

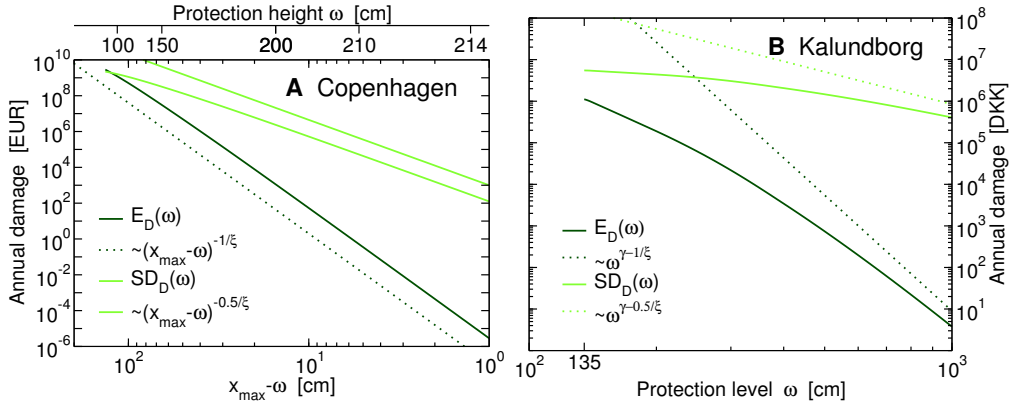

Figure IV.6: Expected annual damage (dark green) and standard deviations (light green) in **(A)** Copenhagen and **(B)** Kalundborg as a function of the protection level ω. The abscissa in the left panel is inverted and shows the difference between the protection level ω and the maximum possible water level $x_{max} = 215.28\,\text{cm}$ (at the top, the corresponding protection heights are displayed). Since no considerable damage occurs in Kalundborg for sea levels below 135 cm, only protection levels above $\omega = 135\,\text{cm}$ are considered. The dotted lines follow the power laws from Eqs. (IV.15) and (IV.16) with the estimated damage function exponents $\gamma = 1.6$ (Copenhagen) and $\gamma = 4.1$ (Kalundborg).

otherwise, even if potential protection failures, such as dyke breaches, are disregarded. Considering the standard deviations, similar expressions are found (again with an additional factor of 0.5 in the exponents):

$$\mathrm{STD}_D(\omega) \sim \begin{cases} \omega^\gamma e^{-0.5\omega/\sigma} & \text{if } \xi = 0 \text{ (for large } \omega) \\ (x_{max} - \omega)^{-0.5/\xi} & \text{if } \xi < 0 \text{ (for } \omega \text{ close to } x_{max}) \\ \omega^{\gamma - 0.5/\xi} & \text{if } \xi > 0 \text{ (for large } \omega) \end{cases} . \tag{IV.16}$$

Hence, in all cases, the relative variation of the damage, STD_D/E_D, grows with increasing protection levels. Consequently, damage in regions with high flood protection standards is subject to a wider range of relative uncertainty, indicating a higher contribution of low-probability high-impact events to the total damage (Merz et al., 2009). This shows that although coastal protection can reduce the average damage significantly, it cannot always avert the threat of very extreme floods.

Regarding the case studies Copenhagen and Kalundborg, Fig. IV.6 shows that the results from the numerical analyses of different protection levels can be very well approximated by our analytical relations from Eqs. (IV.15) and (IV.16). In contrast to the consideration of rising mean sea levels (Fig. IV.4), the Copenhagen case provides a better accordance than Kalundborg. This is due to the fact that in Copenhagen the parameter space of ω is limited by x_{max} and hence the asymptotic range of convergence is closer to the considered value. In any case, our results represent suitable estimations, which might be useful in planning and decision-making processes of coastal protection measures.

IV.6 Comparison with Block Maxima Approach

Beside the Point Process approach, the method of block maxima using the Generalised Extreme Value (GEV) distribution is a common approach in extreme value theory (Coles, 2001). Mathematically speaking, the GEV distribution is the limit distribution of properly normalised maxima of a sequence of independent and identically distributed random variables. In practice, it is used to estimate the distribution of the maximum value within a time window of a certain size (e.g. 1 year). Using the block maxima approach, only one flood event (the most severe) per year is considered, implying that all other events (i.e. the second, third, ... largest) are neglected. However, the Point Process approach and the block maxima approach are strongly interrelated (Coles, 2001; Katz et al., 2005). In particular, the parameters from the one approach can be easily derived from the other.

Complementary to the work in hand, an analogous analysis using the block maxima instead of the Point Process approach has been carried out recently (Boettle et al., 2013b). Considering sea level rise, the asymptotic results of the two approaches differ significantly and a less steep increase in annual damage is found for arbitrary shape parameters ξ, if block maxima are considered. This is due to the fact that the average number of damage-causing floods per year increases and the omission of events in the block maxima approach takes effect. In the case that more than one flooding per year is expected, the Point Process method therefore represents the better choice as it adds significant information.

In contrast, an increasing variability in the sea levels, reflected in a changing scale parameter σ (see Appendix IV.B), leads to the same results for the two approaches. This can be explained by Eq. (IV.3), which indicates that for an increasing scale parameter σ the number of annual flood events converges to 1. That is, on average there is one exceedance of the given threshold per year, which naturally coincides with the annual maximum sea level.

Finally, investigating increasing protection levels, the results of the two approaches again coincide. This is not surprising, since for high protection levels, inundations are very rare and more than one flooding per year is very unlikely. Consequently, the disregard of additional floods becomes negligible and the annual flood damage is typically determined by one – the most severe – flood event.

Both approaches are based on extreme value theory but differ in the extreme sea levels that are taken into account. Since the Point Process approach presented in this work is able to consider *all* relevant flood events, it can be considered as advantageous, particularly for the investigation of sea level rise impacts. However, the choice of the threshold u is crucial and not always evident which makes the method more complex to apply. In general, as we have seen, the shape parameter ξ is very decisive for the damage behaviour. Its determination is therefore of utmost importance and in case of doubt the method with a better data availability should be followed in order to guarantee the best possible estimation of ξ.

IV.7 Discussion

Despite the accurate analytical formulation of the work at hand, some weaknesses need to be noted. For instance, the occurrence probability of a flood event on a specific day is assumed to be independent from the other days. In the short-term there is a strong correlation between sea levels. This becomes apparent when considering the fact that storm surge events typically last for several days. In addition, it has been shown, that sea level records also comprise long-term correlations (Barbosa et al., 2006; Dangendorf et al., 2014). The clustering of extreme events (Eichner et al., 2007) might amplify the uncertainty. On the other hand, this is counteracted by the fact that two or more subsequent flood events (e.g. three sea level exceedances within 1 month) do not provide individual damages. That is, the actual damage is likely to be dominated by the first or highest of these events and will most likely not equal the sum of the damages corresponding to these events (given that they occur in a sufficiently long distance of time). In summary, although the presented approach still has some intrinsic errors, it overcomes the major shortcoming of a block maxima approach and hence can be considered as superior.

Studying the effect of sea level rise, we find that in any case the expected damage increases super-linearly with the mean sea level, when considering typical values of the shape parameter. This means that the losses always increase at a higher rate than the sea levels – a universal result that needs to be explored when the climate change impacts of sea level rise are discussed economically.

Our work also shows that the upcoming losses from sea level rise are mostly determined by the type of sea level extremes (i.e. the sign of the parameter ξ), which crucially dictates the power of $E_D(\mu)$ (assuming constant coastal assets). This finding brings us to the following insights: (i) Since the steepness of the damage function (exponent γ) is mostly irrelevant, potential policies aiming at changing the slope of the damage function via relocation of valuable assets can reduce the expected losses, but a priori have only a marginal mitigation effect on the development of future flood damage. That is, such policies change the proportionality constant but hardly alter the proportionality. (ii) A reliable characterisation of sea level extremes is essential for a systematic assessment of climate change impacts due to sea level rise in the form of coastal floods. Thus, we plead for a high-resolution sea level network (Woodworth, 2010) if the losses from sea level rise are to be assessed on the regional or global scale.

In general, our results show how the complexity of climate change, adaptation, and flood damage can be disentangled by surprisingly simple and general expressions which are applicable to arbitrary regions and case studies. These relations are the basis for understanding the effect of sea level rise on coastal flood damage and are of great importance for the development of broad-scale assessment models in the context of climate change (e.g. Leimbach et al., 2010; Nordhaus and Yang, 1996).

The main text is complemented in two ways. Firstly, an additional analysis of flood damage in Copenhagen and Kalundborg as a function of the scale parameter σ is provided in Appendix IV.A. Finally, all expressions describing the asymptotic behaviours of the damage and its standard deviation are mathematically proven in Appendix IV.B.

Appendix

IV.A Further Results

In addition to varying the parameters μ and ω as discussed in the main text, the alteration of the scale parameter σ represents also a potential impact from climate change. Such an effect could be explained by changing wind patterns leading to a lower or higher variability of water levels. Although alterations of σ can be observed (Mudersbach and Jensen, 2010), the underlying mechanism behind is still unexplained. Nevertheless, for the sake of completeness, we investigate the hypothetical effect of a varying scale parameter σ on the annual damage – analogous to the other parameter shifts. The corresponding asymptotic relations, Eqs. (IV.20) and (IV.21), are derived in the following section. Figure IV.7 illustrates the comparison of numerical calculations with the asymptotic results. It can be seen that in both case studies the increase of damage is less steep than the asymptotic behaviours for σ close to the present value σ_0 and that a convergence is found for considerably larger values of σ.

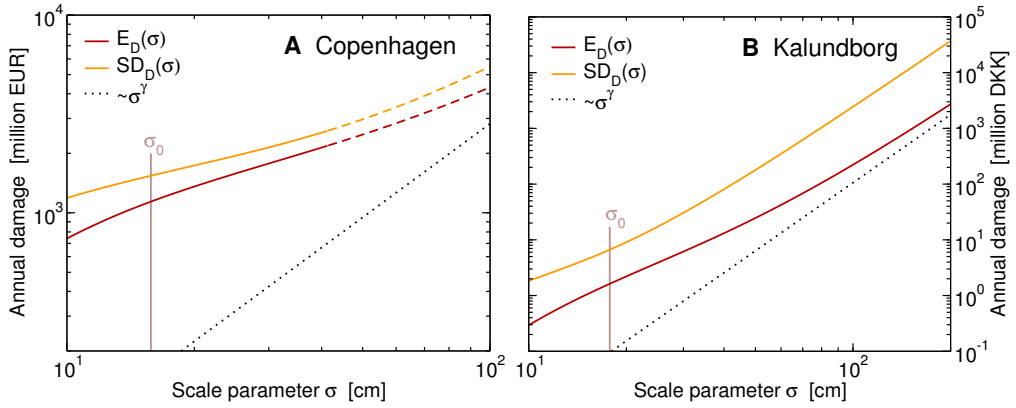

Figure IV.7: Expected annual damage (red) and standard deviations (orange) in **(A)** Copenhagen and **(B)** Kalundborg as a function of the scale parameter σ. The solid lines were numerically calculated with the available damage functions; the dashed continuations use an extrapolation of the damage function as a power law with exponent $\gamma = 1.6$ (Copenhagen) and $\gamma = 4.1$ (Kalundborg). The dotted line shows the asymptotic results from Eqs. (IV.20) and (IV.21) and the current values of the scale parameter $\sigma_0 = 15.79\,\text{cm}$ (Copenhagen) and $\sigma_0 = 17.78\,\text{cm}$ (Kalundborg) are displayed as brown vertical lines.

IV.B Analytical Derivation of Parameter Effects

In this section we derive the asymptotic relations from the main text. The section comprises three parts, each part considering the effects of changing parameters μ, σ, as well as ω on one variable. First, in Sec. IV.B.1, we derive the effects of changing parameter values on the expected number of annual flood events. That is, how many threshold exceedances of the sea level can be expected within one year? Given such an exceedance, the magnitude of the sea level is still random with a certain probability distribution, from which a probability distribution of the corresponding damage can be derived. How

this distribution alters with changing parameters is described in Sec. IV.B.2. Finally, combining the number of flood events and the damage of a single flood event provides the annual damage. The derivation of the relations for the expectation value and the standard deviation of the annual damage is presented in Sec. IV.B.3.

The provided expressions describe the damage for asymptotically large parameter values or, in case they are bounded, for parameters approaching their limit. This means that the numerically calculated values divided by the analytic result obtained converge to a non-zero constant number for increasing parameter values. In the whole section, the Generalised Pareto probability density function with regard to the threshold u, the shape parameter ξ, and the scale parameter σ is denoted by $h_{u,\xi,\sigma}$.

IV.B.1 *Effects on the Occurrence Rate*

The investigation of the occurrence rate Λ is based on Eq. (IV.3). It has to be noted that shifting the parameter μ entails a modification of the scale parameter σ by virtue of Eq. (IV.4). In particular, the denominator in the case $\xi \neq 0$ is constant for varying μ. One can see that for $\xi > 0$ the parameter μ is bounded from above by a value $\mu_{max} = \mu + \sigma/\xi$, at which Λ becomes infinite. Accordingly, we study the asymptotic behaviour for μ approaching μ_{max} in that case. Straightforward calculations provide the asymptotic relations for Λ as a function of μ:

$$\Lambda(\mu) \sim \begin{cases} e^{\mu/\sigma} & \text{if } \xi = 0 \text{ (for large } \mu) \\ \mu^{-1/\xi} & \text{if } \xi < 0 \text{ (for large } \mu) \\ (\mu_{max} - \mu)^{-1/\xi} & \text{if } \xi > 0 \text{ (for } \mu \text{ close to } \mu_{max}) \end{cases} . \tag{IV.17}$$

Considering a variable scale parameter σ, we obtain the relation

$$\Lambda(\sigma) \sim 1 \ \text{(for large } \sigma) ,$$

which holds for arbitrary values of ξ and asymptotically large σ. In the last part of our analysis, we alter the protection height ω, represented by setting the threshold to $u = \omega$, which also leads to a modification of the scale parameter σ. Using Eq. (IV.5), it follows asymptotically:

$$\Lambda(\omega) \sim \begin{cases} e^{-\omega/\sigma} & \text{if } \xi = 0 \text{ (for large } \omega) \\ (x_{max} - \omega)^{-1/\xi} & \text{if } \xi < 0 \text{ (for } \omega \text{ close to } x_{max}) \\ \omega^{-1/\xi} & \text{if } \xi > 0 \text{ (for large } \omega) \end{cases} ,$$

where ω is assumed to be below the maximum possible sea level x_{max} in the case $\xi < 0$. If a protection level above this value is chosen, no inundation can occur and Λ is 0.

With these expressions, the frequency of events is fully described for large parameter values and, in combination with the following section, the behaviour of the annual damage is derived in Sec. IV.B.3. Note that Eq. (IV.17) holds only for small values of Λ and that the results are therefore only valid for the corresponding parameter values (Embrechts et al., 1997). Otherwise, if Λ becomes too large, the GPD is not an adequate estimation for the water levels.

IV.B.2 *Effects on the Event Damage Distribution*

Not only the number of flood events is affected by evolving parameters. As described in Sec. IV.2.2, in the case of a flood, its magnitude follows a GPD, which in turn is modified by changing parameters. In the following, all integrals are integrated over the whole support of the corresponding density function. For reasons of simplicity, we omit all integral limits in the text. Furthermore, we assume the shape parameter ξ to be small enough such that all integrals exist (Katz et al., 2002) – this is ensured for $\xi < 1/\gamma$ (expectation value) and $\xi < 0.5/\gamma$ (standard deviation). A divergence would imply an infinite variance or average value of the annual damage.

Theorem 1 (μ relations). *Let the water levels above a threshold u follow a GPD with parameters ξ and σ and let us suppose a power damage function $F(x) = x^\gamma$ ($\gamma \in \mathbb{R}^+$). For the damage D_i of a single event we obtain asymptotically*

$$E_{D_i}(\mu) \sim \begin{cases} 1 & \text{if } \xi = 0 \text{ (for large } \mu) \\ \mu^\gamma & \text{if } \xi < 0 \text{ (for large } \mu) \\ 1 & \text{if } \xi > 0 \text{ (for } \mu \text{ close to } \mu_{max}) \end{cases} \quad \textit{and}$$

$$STD_{D_i}(\mu) \sim \begin{cases} 1 & \text{if } \xi = 0 \text{ (for large } \mu) \\ \mu^\gamma & \text{if } \xi < 0 \text{ (for large } \mu) \\ \mu_{max} - \mu & \text{if } \xi > 0 \text{ (for } \mu \text{ close to } \mu_{max}) \end{cases}$$

with $\mu_{max} := \mu + \sigma/\xi$.

Proof. The relations for $\xi = 0$ follow immediately from equations provided in Sec. IV.2.6. In the case $\xi < 0$, a varying μ leads to a linear increase in σ according to Eq. (IV.4). Therefore, the relations are equivalent to $E_{D_i}(\sigma) \sim \sigma^\gamma$ and $STD_{D_i}(\sigma) \sim \sigma^\gamma$. The definition of the expectation value now provides

$$E_{D_i}(\sigma)/\sigma^\gamma = \int F(z + u/\sigma) h_{0,\xi,1}(z)\,dz \overset{\sigma\to\infty}{\longrightarrow} \int z^\gamma h_{0,\xi,1}(z)\,dz = \text{const.} \neq 0\,.$$

Furthermore, using the notation $m_k := \int z^k h_{0,\xi,1}(z)\,dz$, we obtain

$$\begin{aligned} \left(STD_{D_i}(\sigma)/\sigma^\gamma\right)^2 &= \int F(z + u/\sigma)^2 h_{0,\xi,1}(z)\,dz \\ &\quad - \left(\int F(z + u/\sigma) h_{0,\xi,1}(z)\,dz\right)^2 \\ &\overset{\sigma\to\infty}{\longrightarrow} m_{2\gamma} - m_\gamma^2 = \text{const.} \neq 0\,, \end{aligned}$$

which shows the asymptotic relations for $\xi < 0$. In both cases we used uniform convergence to swap the integral and the limit.

As mentioned above, μ is bounded by $\mu_{max} = \mu + \sigma/\xi$ in the case $\xi > 0$ and we study the asymptotic behaviour for μ approaching μ_{max}. Considering $\mu \to \mu_{max}$, Eq. (IV.4) implies $\sigma \to 0$ and by using the uniform convergence of the integrand, it follows

$$E_{D_i}(\mu) = \int F(\sigma z + u) h_{0,\xi,1}(z)\,dz \overset{\mu\to\mu_{max}}{\longrightarrow} F(u),$$

which shows $E_{D_i} \sim 1$ for μ approaching μ_{max}. In order to investigate the standard deviation for $\xi > 0$, we make use of the Taylor expansion around $z = 0$:

$$(\sigma z + u)^\gamma = u^\gamma + \gamma\sigma u^{\gamma-1} z + \gamma(\gamma-1)\sigma^2 u^{\gamma-2} z^2 + \mathcal{O}(\sigma^3)\,.$$

We obtain:

$$\begin{aligned}
\mathrm{Var}_{D_i}(\sigma) &= \int (\sigma z + u)^{2\gamma} h_{0,\xi,1}(z))\,dz - \left(\int (\sigma z + u)^\gamma h_{0,\xi,1}(z)\,dz\right)^2 \\
&= \int \left(u^{2\gamma} + 2\gamma u^{2\gamma-1}\sigma z + 2\gamma(2\gamma-1)u^{2\gamma-2}\sigma^2 z^2 + \mathcal{O}(\sigma^3)\right) \\
&\quad h_{0,\xi,1}(z)\,dz - \left(\int \left(u^\gamma + \gamma u^{\gamma-1}\sigma z + \gamma(\gamma-1)u^{\gamma-2}\sigma^2 z^2\right.\right. \\
&\quad \left.\left. + \mathcal{O}(\sigma^3)\right) h_{0,\xi,1}(z)\,dz\right)^2 \\
&= u^{2\gamma} + 2\gamma u^{2\gamma-1}\sigma m_1 + 2\gamma(2\gamma-1)u^{2\gamma-2}\sigma^2 m_2 + \mathcal{O}(\sigma^3) \\
&\quad -\left(u^{2\gamma} + 2\gamma u^{2\gamma-1}\sigma m_1 + \gamma^2 u^{2\gamma-2}\sigma^2 m_1^2\right. \\
&\quad \left. + 2\gamma(\gamma-1)u^{2\gamma-2}\sigma^2 m_2 + \mathcal{O}(\sigma^3)\right) \\
&= \underbrace{\text{const.}}_{\neq 0} \cdot \sigma^2 + \mathcal{O}(\sigma^3)
\end{aligned}$$

with the k-th moments $m_k := \int z^k h_{0,\xi,1}(z)\,dz$. Considering that σ converges linearly to 0 for $\mu \to \mu_{max}$, it follows that $\mathrm{STD}_{D_i}(\sigma)/\sigma \to \text{const.} \neq 0$ for $\sigma \to 0$ and in turn $\mathrm{STD}_{D_i}(\mu) \sim \mu_{max} - \mu$ for $\mu \to \mu_{max}$. □

Theorem 2 (σ relations). *Let the water levels above a threshold u follow a GPD with parameters ξ and σ and let us suppose a power damage function $F(x) = x^\gamma$ ($\gamma \in \mathbb{R}^+$). For the damage D_i of a single flood event we obtain*

$$E_{D_i}(\sigma) \sim \sigma^\gamma \quad \textit{and} \quad \mathrm{STD}_{D_i}(\sigma) \sim \sigma^\gamma$$

for asymptotically large σ.

Proof. The proof corresponds to the case of increasing μ for $\xi < 0$ in Theorem 1. □

Finally, we derive expressions for the dependence on the protection height. As can be found in Coles (2001), a change of the threshold from u to u' affects the scale parameter σ by virtue of Eq. (IV.5), which leaves the annualities of sea levels above the threshold unchanged.

Theorem 3 (ω relations). *Let the water levels above a threshold $u = \omega$ follow a GPD with parameters ξ and σ, and let us suppose a power damage function $F(x) = x^\gamma$ ($\gamma \in \mathbb{R}^+$). For the damage D_i of a single event we obtain asymptotically*

$$E_{D_i}(\omega) \sim \begin{cases} \omega^\gamma & \text{if } \xi = 0 \text{ (for large } \omega) \\ 1 & \text{if } \xi < 0 \text{ (for } \omega \text{ close to } x_{max}) \\ \omega^\gamma & \text{if } \xi > 0 \text{ (for large } \omega) \end{cases} \quad \textit{and}$$

$$\mathrm{STD}_{D_i}(\omega) \sim \begin{cases} \omega^{\gamma-1} & \text{if } \xi = 0 \text{ (for large } \omega) \\ x_{max} - \omega & \text{if } \xi < 0 \text{ (for } \omega \text{ close to } x_{max}) \\ \omega^\gamma & \text{if } \xi > 0 \text{ (for large } \omega) \end{cases},$$

where $x_{\max} := u - \sigma/\xi$ *denotes the maximum possible sea level in the case* $\xi < 0$.

Proof. Let u denote the current value of the threshold and ω the variable protection height corresponding to the new threshold u'. We use Eq. (IV.5) to calculate the scale parameter σ' which describes the excesses above the threshold $\omega = u'$ and obtain

$$\begin{aligned} E_{D_i}(\omega) &= \int F(x) h_{\omega,\xi,\sigma}(x)\,dx \\ &= \int (\sigma' z + \omega)^{\gamma} h_{0,\xi,1}(z)\,dz \\ &= \int \big(\sigma z + \xi z(\omega - u) + \omega\big)^{\gamma} h_{0,\xi,1}(z)\,dz\,. \end{aligned} \tag{IV.18}$$

In the case $\xi \geqslant 0$, the uniform convergence of the integrand provides

$$\begin{aligned} E_{D_i}(\omega)/\omega^{\gamma} &= \int \big(\xi z + 1 + z(\sigma - \xi u)/\omega\big)^{\gamma} h_{0,\xi,1}(z)\,dz \\ &\overset{\omega\to\infty}{\longrightarrow} \int (\xi z + 1)^{\gamma} h_{0,\xi,1}(z)\,dz \\ &= \text{const.} \neq 0\,, \end{aligned}$$

which shows the asymptotic relation $E_{D_i}(\omega) \sim \omega^{\gamma}$ for $\xi \geqslant 0$. For the corresponding standard deviation in the case $\xi = 0$ it follows that

$$\mathrm{Var}_{D_i}(\omega) = \int \big(\sigma z + \omega\big)^{2\gamma} h_{0,0,1}(z)\,dz - \left(\int \big(\sigma z + \omega\big)^{\gamma} h_{0,0,1}(z)\,dz\right)^2.$$

Using the Taylor expansion around $z = 0$,

$$(\sigma z + \omega)^{\gamma} = \omega^{\gamma} + \gamma\omega^{\gamma-1}\sigma z + \gamma(\gamma-1)/2\omega^{\gamma-2}\sigma^2 z^2 + \mathcal{O}(\omega^{\gamma-3})\,,$$

we obtain

$$\begin{aligned} \mathrm{Var}_{D_i}(\omega) = \int &\big(\omega^{2\gamma} + 2\gamma\omega^{2\gamma-1}\sigma z + \gamma(2\gamma-1)\omega^{2\gamma-2}\sigma^2 z^2 + \mathcal{O}(\omega^{2\gamma-3})\big) \\ &h_{0,0,1}(z)\,dz - \left(\int \big(\omega^{\gamma} + \gamma\omega^{\gamma-1}\sigma z + \gamma(\gamma-1)/2\omega^{\gamma-}\sigma^2 z^2 \right. \\ &\left. +\mathcal{O}(\omega^{\gamma-3})\big) h_{0,0,1}(z)\,dz\right)^2 \end{aligned}$$

and straightforward calculations provide

$$\mathrm{Var}_{D_i}(\omega) = (m_2 - m_1^2)\gamma^2\sigma^2\omega^{2\gamma-2} + \int \mathcal{O}(\omega^{2\gamma-3}) h_{0,0,1}(z)\,dz\,,$$

again using $m_k := \int z^k h_{0,0,1}(z)\,dz$. Now,

$$\begin{aligned} \lim_{\omega\to\infty} \mathrm{Var}_{D_i}(\omega)/\omega^{2\gamma-2} &= \lim_{\omega\to\infty} (m_2 - m_1^2)\gamma^2\sigma^2 \\ &\quad + \lim_{\omega\to\infty} \int \mathcal{O}(\omega^{-1}) h_{0,0,1}(z)\,dz \\ &= (m_2 - m_1^2)\gamma^2\sigma^2 \\ &= \text{const.} \neq 0 \end{aligned}$$

proves the expression for STD_{D_i} in the case $\xi = 0$.

For $\xi > 0$ holds

$$\begin{aligned}
\mathrm{Var}_{D_i}(\omega)/\omega^{2\gamma} &= \int \frac{1}{\omega^{2\gamma}} \big(z(\sigma + \xi\omega - \xi u) + \omega\big)^{2\gamma} h_{0,\xi,1}(z)\,dz \\
&\quad - \left(\int \frac{1}{\omega^{\gamma}} \big(z(\sigma + \xi\omega - \xi u) + \omega\big)^{\gamma} h_{0,\xi,1}(z)\,dz \right)^2 \\
&\overset{\omega\to\infty}{\longrightarrow} \int (\xi z + 1)^{2\gamma} h_{0,\xi,1}(z)\,dz - \left(\int (\xi z + 1)^{\gamma} h_{0,\xi,1}(z)\,dz \right)^2 \\
&= \text{const.} \neq 0\,,
\end{aligned}$$

which proves the asymptotic relation $\mathrm{STD}_{D_i}(\omega) \sim \omega^{\gamma}$.

For the case $\xi < 0$, we consider Eq. (IV.18):

$$\begin{aligned}
\mathrm{E}_{D_i}(\omega) &= \int \big(\sigma z + \xi z(\omega - u) + \omega\big)^{\gamma} h_{0,\xi,1}(z)\,dz \\
&= \int \big(\xi z(\omega - x_{\max}) + \omega\big)^{\gamma} h_{0,\xi,1}(z)\,dz \\
&\overset{\omega\to x_{\max}}{\longrightarrow} \int x_{\max}^{\gamma} h_{0,\xi,1}(z)\,dz = x_{\max}^{\gamma}\,,
\end{aligned}$$

where we use the uniform convergence of the integrand to swap the integral and the limit. This proves the relation for E_{D_i}. In order to investigate the standard deviation, we define $\Delta\omega := x_{\max} - \omega$ and examine the limit $\Delta\omega \to 0$. A Taylor expansion of $(\omega - \xi\Delta\omega z)^{\gamma}$ around $z = 0$ provides

$$\begin{aligned}
(\omega - \xi\Delta\omega z)^{\gamma} = \omega^{\gamma} &+ \gamma\omega^{\gamma-1}(-\xi\Delta\omega)z \\
&+ \gamma(\gamma-1)/2\,\omega^{\gamma-2}(-\xi\Delta\omega)^2 z^2 + \mathcal{O}(\Delta\omega^3)
\end{aligned} \tag{IV.19}$$

and for the variance holds

$$\begin{aligned}
\mathrm{Var}_{D_i}(\omega) &= \int (\omega - \xi\Delta\omega z)^{2\gamma} h_{0,\xi,1}(z)\,dz - \left(\int (\omega - \xi\Delta\omega z)^{\gamma} h_{0,\xi,1}(z)\,dz \right)^2 \\
&\overset{\text{Eq. (IV.19)}}{=} \int \big(\omega^{2\gamma} + 2\gamma\omega^{2\gamma-1}(-\xi\Delta\omega)z \\
&\quad + 2\gamma(2\gamma-1)/2\,\omega^{2\gamma-2}(-\xi\Delta\omega)^2 z^2 + \mathcal{O}(\Delta\omega^3)\big) h_0(z;\xi,1)\,dz \\
&\quad - \left(\int \big(\omega^{\gamma} + \gamma\omega^{\gamma-1}(-\xi\Delta\omega)z \right. \\
&\quad \left. + \gamma(\gamma-1)/2\,\omega^{\gamma-2}(-\xi\Delta\omega)^2 z^2 + \mathcal{O}(\Delta\omega^3)\big) h_0(z;\xi,1)\,dz \right)^2 \\
&= \omega^{2\gamma} - 2\gamma\omega^{2\gamma-1}\xi\Delta\omega m_1 + \gamma(2\gamma-1)\omega^{2\gamma-2}\xi^2\Delta\omega^2 m_2 \\
&\quad + \mathcal{O}(\Delta\omega^3) - \big(\omega^{\gamma} - \gamma\omega^{\gamma-1}\xi\Delta\omega m_1 \\
&\quad + \gamma(\gamma-1)/2\,\omega^{\gamma-2}\xi^2\Delta\omega^2 m_2 + \mathcal{O}(\Delta\omega^3)\big)^2 \\
&= \omega^{2\gamma} - 2\gamma\omega^{2\gamma-1}\xi\Delta\omega m_1 + \gamma(2\gamma-1)\omega^{2\gamma-2}\xi^2\Delta\omega^2 m_2 \\
&\quad + \mathcal{O}(\Delta\omega^3) - \omega^{2\gamma} + 2\gamma\omega^{2\gamma-1}\xi\Delta\omega m_1 \\
&\quad - 2\gamma(\gamma-1)/2\,\omega^{2\gamma-2}\xi^2\Delta\omega^2 m_2 - \gamma^2\omega^{2\gamma-2}\xi^2\Delta\omega^2 m_1^2 \\
&\quad + \mathcal{O}(\Delta\omega^3) \\
&= \gamma^2\omega^{2\gamma-2}\xi^2\Delta\omega^2 m_2 - \gamma^2\omega^{2\gamma-2}\xi^2\Delta\omega^2 m_1^2 + \mathcal{O}(\Delta\omega^3)
\end{aligned}$$

and therefore

$$\begin{aligned} \mathrm{STD}_{D_i}(\omega)/\Delta\omega &= \left(\gamma^2\omega^{2\gamma-2}\xi^2 m_2 - \gamma^2\omega^{2\gamma-2}\xi^2 m_1^2 + \mathcal{O}(\Delta\omega)\right)^{1/2} \\ &\xrightarrow{\Delta\omega\to 0} \text{const.} \neq 0\,, \end{aligned}$$

which shows the statement of the theorem. □

IV.B.3 *Effects on the Annual Damage*

As stated in the main text, the total annual damage D is calculated as the sum of all single event damages D_i, i.e. $D = D_1 + \ldots + D_N$, where $N \sim \mathrm{Poi}(\Lambda)$ is the number of flood events in one year. This implies $E_N = \mathrm{Var}_N = \Lambda$ and using Wald's identities (Beichelt, 2006), it follows

$$E_D = \Lambda E_{D_i} \text{ as well as } \mathrm{Var}_D = \Lambda(\mathrm{Var}_{D_i} + E_{D_i}^2)$$

and together with the results from Secs. IV.B.1 and IV.B.2 we obtain

$$E_D(\mu) \sim \begin{cases} e^{\mu/\sigma} & \text{if } \xi = 0 \text{ (for large } \mu) \\ \mu^{\gamma-1/\xi} & \text{if } \xi < 0 \text{ (for large } \mu) \\ (\mu_{\max}-\mu)^{-1/\xi} & \text{if } \xi > 0 \text{ (for } \mu \text{ close to } \mu_{\max}) \end{cases} \quad \text{as well as}$$

$$\mathrm{STD}_D(\mu) \sim \begin{cases} e^{0.5\mu/\sigma} & \text{if } \xi = 0 \text{ (for large } \mu) \\ \mu^{\gamma-0.5/\xi} & \text{if } \xi < 0 \text{ (for large } \mu) \\ (\mu_{\max}-\mu)^{-0.5/\xi} & \text{if } \xi > 0 \text{ (for } \mu \text{ close to } \mu_{\max}) \end{cases}$$

as asymptotic relations for varying mean sea levels. An altering scale parameter σ leads to

$$E_D(\sigma) \sim \sigma^\gamma \quad \text{and} \tag{IV.20}$$

$$\mathrm{STD}_D(\sigma) \sim \sigma^\gamma \tag{IV.21}$$

for asymptotically large values of σ and for changing protection levels ω holds asymptotically

$$E_D(\omega) \sim \begin{cases} \omega^\gamma e^{-\omega/\sigma} & \text{if } \xi = 0 \text{ (for large } \omega) \\ (x_{\max}-\omega)^{-1/\xi} & \text{if } \xi < 0 \text{ (for } \omega \text{ close to } x_{\max}) \\ \omega^{\gamma-1/\xi} & \text{if } \xi > 0 \text{ (for large } \omega) \end{cases} \tag{IV.22}$$

$$\mathrm{STD}_D(\omega) \sim \begin{cases} \omega^\gamma e^{-0.5\omega/\sigma} & \text{if } \xi = 0 \text{ (for large } \omega) \\ (x_{\max}-\omega)^{-0.5/\xi} & \text{if } \xi < 0 \text{ (for } \omega \text{ close to } x_{\max}) \\ \omega^{\gamma-0.5/\xi} & \text{if } \xi > 0 \text{ (for large } \omega) \end{cases} . \tag{IV.23}$$

All results from the previous sections are summarised in Tab. IV.2.

Table IV.2: The asymptotic behaviour of the number of annual flood events Λ, the expected damage from a single event E_{D_i} and the total annual damage E_D as well as the corresponding standard deviations STD_{D_i} and STD_D, as functions of the 1-year event μ (with regard to a shift of all events), the scale parameter σ and the protection level ω. The values $\mu_{max} = u + \sigma/\xi$ and $x_{max} = \mu - \sigma/\xi$ represent upper limits for the parameters μ and ω in the case $\xi > 0$ and $\xi < 0$, respectively.

		varying parameter			
		1-year event μ	scale σ	protection height ω	
Λ	$\xi = 0$:	$\sim$	$e^{\mu/\sigma}$	$\sim$	$e^{-\omega/\sigma}$
	$\xi < 0$:	$\sim$	$\mu^{-1/\xi}$	$\underset{\omega\to x_{max}}{\sim}$	$(x_{max} - \omega)^{-1/\xi}$
	$\xi > 0$:	$\underset{\mu\to\mu_{max}}{\sim}$	$(\mu_{max} - \mu)^{-1/\xi}$	$\sim$	$\omega^{-1/\xi}$
E_{D_i}	$\xi = 0$:	$\sim$	1	$\sim$	ω^{γ}
	$\xi < 0$:	$\sim$	μ^{γ}	$\underset{\omega\to x_{max}}{\sim}$	1
	$\xi > 0$:	$\underset{\mu\to\mu_{max}}{\sim}$	1	$\sim$	ω^{γ}
E_D	$\xi = 0$:	$\sim$	$e^{\mu/\sigma}$	$\sim$	$\omega^{\gamma} e^{-\omega/\sigma}$
	$\xi < 0$:	$\sim$	$\mu^{\gamma-1/\xi}$	$\underset{\omega\to x_{max}}{\sim}$	$(x_{max} - \omega)^{-1/\xi}$
	$\xi > 0$:	$\underset{\mu\to\mu_{max}}{\sim}$	$(\mu_{max} - \mu)^{-1/\xi}$	$\sim$	$\omega^{\gamma-1/\xi}$
STD_{D_i}	$\xi = 0$:	$\sim$	1	$\sim$	$\omega^{\gamma-1}$
	$\xi < 0$:	$\sim$	μ^{γ}	$\underset{\omega\to x_{max}}{\sim}$	$x_{max} - \omega$
	$\xi > 0$:	$\underset{\mu\to\mu_{max}}{\sim}$	$\mu_{max} - \mu$	$\sim$	ω^{γ}
STD_D	$\xi = 0$:	$\sim$	$e^{0.5\mu/\sigma}$	$\sim$	$\omega^{\gamma} e^{-0.5\omega/\sigma}$
	$\xi < 0$:	$\sim$	$\mu^{\gamma-0.5/\xi}$	$\underset{\omega\to x_{max}}{\sim}$	$(x_{max} - \omega)^{-0.5/\xi}$
	$\xi > 0$:	$\underset{\mu\to\mu_{max}}{\sim}$	$(\mu_{max} - \mu)^{-0.5/\xi}$	$\sim$	$\omega^{\gamma-0.5/\xi}$

Acknowledgements. We would like to thank Stéphane Hallegatte, Carlo S. Sørensen, and Jacob Arpe for the provision of data, as well as Luís Costa, Boris F. Prahl, and Dominik E. Reusser for fruitful discussions and comments. The research leading to these results has received funding from the European Community's Seventh Framework Programme under Grant Agreement No. 308497 (Project RAMSES). We also express our thanks to the Potsdam Research Cluster for Georisk Analysis, Environmental Change and Sustainability (PROGRESS) for their financial support.

V

Adaptation to Sea Level Rise: Calculating Costs and Benefits for the Case Study Kalundborg, Denmark

Markus Böttle[*], *Diego Rybski*[*], *and Jürgen P. Kropp*[*,†]

[*]Potsdam Institute for Climate Impact Research (PIK), Potsdam, Germany
[†]University of Potsdam, Institute of Earth and Environmental Science, Potsdam, Germany

This chapter is published as:
Boettle, M., Rybski, D., and Kropp, J. P. (2013). Adaptation to sea level rise: Calculating costs and benefits for the case study Kalundborg, Denmark. In Schmidt-Thomé, P. and Klein, J., editors, *Climate Change Adaptation in Practice*, pages 25–34. Wiley-Blackwell.

v.1 Introduction

While global warming is still the focus of climate research, severe impacts need to be anticipated and appropriate adaptation strategies to mitigate adverse effects are required. In particular, coastal regions are facing serious consequences. Due to the complex nature of impacts from sea level rise (and climate change in general), decisions on adaptation are difficult to take. Cost-Benefit Analysis (CBA) is one possible tool to support such decisions and to estimate the economic efficiency of adaptation investments. Unlike, for example, multi-criteria decision analysis (see Chapter 4 in this book[1] or Triantaphyllou, 2000), where the input of subjective preferences is necessary, CBA is a purely rational and monetary approach which is probably one of the reasons for its wide acceptance.

Although the sea level rise is a steadily ongoing process, the consequences are not in general likely to be from a progressing, permanent inundation of areas, but from single floodings, which are likely to become more frequent and severe in the future (IPCC, 2012). Therefore, the assessment of impacts should be based on extreme events, such as extreme sea levels due to storm surges.

This chapter is organised as follows. In the second section we introduce a stochastic framework for the assessment of annual flood damages and describe its application in the case study of Kalundborg. The third section investigates possible factors influencing flood risk and the fourth section describes the resulting cost-benefit analysis, again exemplifying the case study of Kalundborg in order to demonstrate the applicability of the approach. The final section summarises and draws conclusions.

v.2 Risk Assessment

v.2.1 *Risk*

Many definitions of the term risk can be found in literature. Commonly, risk is vaguely defined as probability times consequence, where the probability refers to a certain flood event and consequence stands for the corresponding monetary damage. Since we are not only interested in one specific event (e.g. a 100-year flood) but in all possible floods (i.e. events of arbitrary return level), the flood risk is obtained by summing the risks of all flood magnitudes (Merz et al., 2010a; Poussin et al., 2012). In our context, flood risk describes the average annual flood damage in a specific region. Thus, the term is associated with a single year and estimating the risk of a longer time period necessitates a summation of the annual risks. However, the calculation of risk requires knowledge about the frequencies of flood events on the one hand and information about the corresponding consequences on the other hand.

1 Boettle et al. (2013c)

v.2.2 *Extreme Value Theory*

Extreme events such as floods are typically characterised by their exceedance probability or their recurrence time (annuality). Extreme value theory is commonly used to describe such frequencies in a mathematical framework (Leadbetter et al., 1983; Coles, 2001; Hawkes et al., 2008). In particular, the Generalised Extreme Value (GEV) distribution is employed to describe the maximum annual water level at a certain gauge, using three parameters: the location μ, the scale σ, and the shape ξ. In order to estimate these parameters from historical gauge data, several algorithms are available (e.g. via L-moments Hosking 1990; Wang 1990 or maximum likelihood Phien and Fang 1989; Hosking 1990). However, μ, σ, ξ contain all the necessary information about the stochastic occurrence of extreme water levels in the current state, that is, for the present environmental conditions. In view of rising mean sea levels and changing storm intensities, these parameters should be considered as altering (Woth et al., 2006; Mudersbach and Jensen, 2010). Consequently, it needs to be assumed that the risk will alter over time.

v.2.3 *Damage Functions*

Apart from the stochastic description of flood events, their interrelation with the associated damages needs to be assessed comprising two steps. Firstly, the affected assets need to be determined. For this purpose hydrodynamic models or simplified flood algorithms (Poulter and Halpin, 2008) provide characteristics on how each asset is affected (e.g. the inundation height of each building). Secondly, the economic damage needs to be elaborated, typically by a damage function. Although the damage is influenced by several factors (such as inundation duration, contamination load, warning time, or flow velocity (Wind et al., 1999; Kreibich et al., 2005; Thieken et al., 2005; Middelmann-Fernandes, 2010) the inundation depth is usually considered as the main factor and so called stage-damage functions are commonly used on the building level (Smith, 1994; Dutta et al., 2002; Apel et al., 2009). Such functions relate the inundation level of a certain asset with the corresponding damage and different types of functions can be applied to take account of the variety of assets or buildings (Blong, 2003; Kang et al., 2005; Penning-Rowsell et al., 2005). The integration of all building damages within the considered area for flood events of variable magnitude then leads to a *macroscopic damage function* providing the total damage for the case study as a function of the sea level (Hallegatte et al., 2011; Boettle et al., 2011).

v.2.4 *Integration*

Since one does not know when a certain flood event occurs, the damage function is linked with the stochastic properties of the above mentioned extreme water levels, namely with the GEV distribution. The flood risk can then be calculated by means of these two components. Considering the maximum annual water level as a random variable with probability density p and the damage

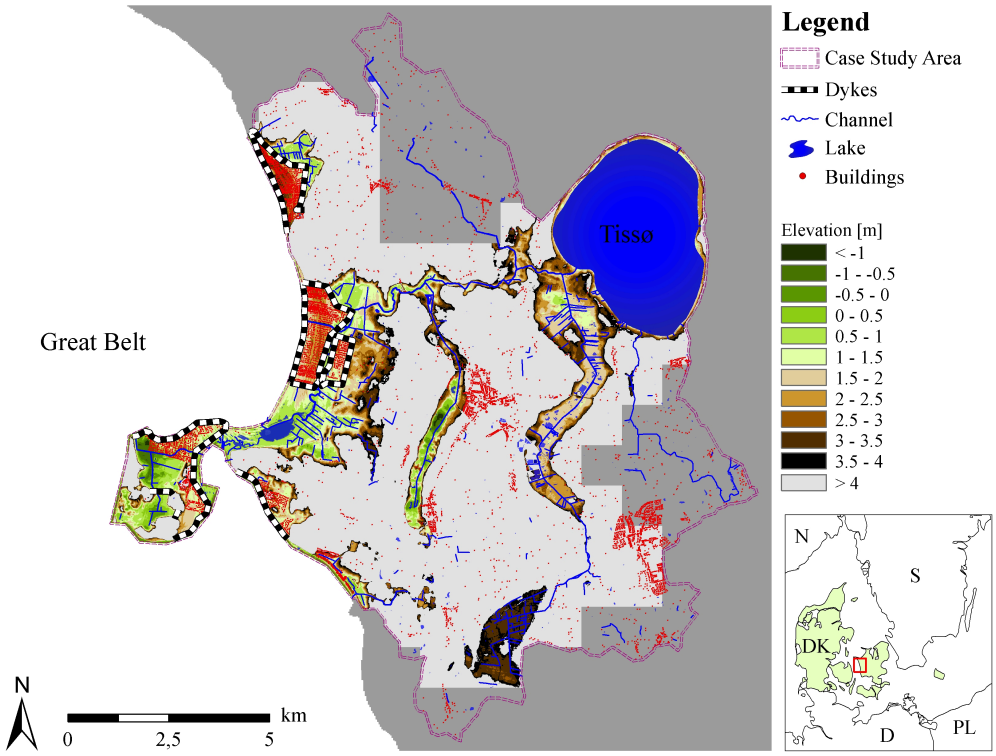

Figure v.1: Case study area south of the City of Kalundborg with locations of the proposed protection measures (bold black and white line). The elevation data is colour coded (light grey indicates elevations above 4 m, dark grey stands for no data). The white area represents the sea and buildings are indicated by red dots. *Source*: Digital Elevation Model (DEM) owned by Niras BlomInfo A/S Denmark.

function D as a transformation, basic stochastics provide the following formula for the risk R:

$$R = \int D(x)p(x)dx, \tag{v.1}$$

where x takes all possible water levels. In fact, this term accounts only for one flood event per year (considering the heaviest flood) and neglects any additional floods. Still, this represents just a small shortcoming, since more than one flood event per year is rare in most areas.

v.2.5 *Example*

We want to show how this procedure is performed for a case study region south of the city of Kalundborg in Denmark (Fig. v.1), which comprises mostly summer cottages, located in low-lying areas near the coast. So far, no flood defences are implemented in the area but in view of rising sea levels a debate on how assets can be protected from future storm surges is ongoing. One specific protection measure is described in Sec. v.3.

Basically, the whole risk assessment procedure involves three steps: (i) the estimation of GEV parameters from historical gauge data, (ii) the elaboration of a macroscopic damage function, and (iii) the actual calculation of the risk according to Eq. (v.1).

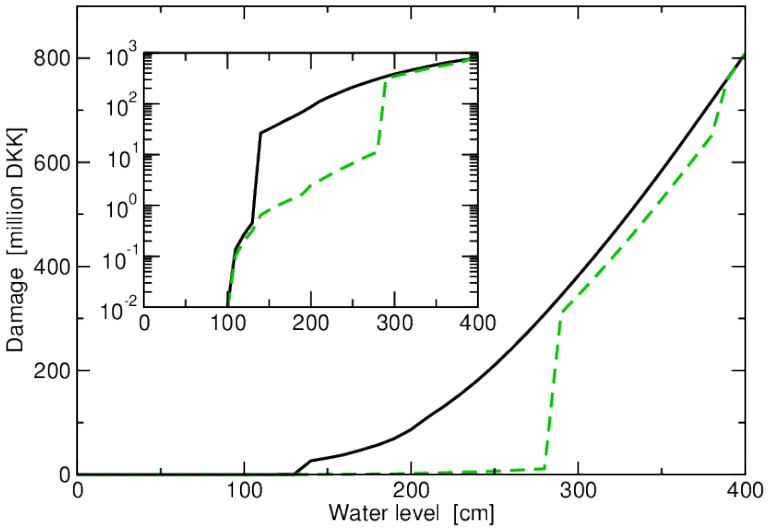

Figure v.2: Damage function for the case study Kalundborg without flood defence (black) and with proposed dyke protection (dashed green) obtained as linear interpolation of damages at water levels with 10 cm distance. The inset shows the same curves in semi-logarithmic scale.

For the Kalundborg case study, a macroscopic damage curve is presented in Boettle et al. (2011) on the basis of a high resolution elevation model and detailed cadastral information using a flood-fill algorithm (4 nearest neighbours). The function, shown in Fig. v.2, provides monetary building damages for sea levels between zero and four meters and is based on a linear building damage function. For further details we refer to Boettle et al. (2011).

Regarding the distribution of maximum annual water levels, 32 maximum annual water level measurements at the gauge in Kalundborg between 1971 and 2006 were used[2]. Although this dataset barely allows reliable estimates for the GEV parameters to be derived, we perform the analysis with this information since more extensive data were not available. In addition to the maximum sea levels, mean sea level data from a gauge close to Kalundborg (Korsør) is publicly available[3] and was used to deduce a linear upward trend in the corresponding period of approximately 0.16 cm per year. After subtracting this trend from the time series the GEV parameters $\mu \approx 91.3$, $\sigma \approx 16.96$, and $\xi \approx 0.00$ were obtained using maximum likelihood estimation for censored sample data (Phien and Fang, 1989). The parameters imply that flood events of arbitrary height are possible within the model and no upper bound for water levels exists (Coles, 2001). However, with regard to computational aspects, it is only possible to consider water levels up to a certain limit. In our case a limit of four meters above mean sea level has been chosen, which means a consideration of extreme events up to a recurrence time of approximately five billion years (given the present parameters). In practice, the integral in Eq. (v.1) is approximated by the following sum

$$R \approx \Delta x \sum_{i=1}^{N} D(x_i) p(x_i) \,, \tag{v.2}$$

2 We want to thank Jacob Arpe for the provision of data.

3 http://www.psmsl.org/

where x_i takes values between zero and four meters with equal distances Δx and $N := 4m/\Delta x$ being the number of discretisation steps. Performing this summation, a total flood risk of approximately 2.8 million Danish Crowns (DKK) is obtained for the case study Kalundborg in 2010. This figure represents an average value and not a prediction of damages in 2010. In contrast, it is very likely that the real damage is far away from the expected value and it needs a much longer observation period to find a settling of the average close to the expected damage. For instance, considering a period of 100 years a total damage of around 280 million DKK is estimated (assuming constant conditions), but no information on the composition of this damage is provided. Possibly, the whole damage stems from one single event and no other damages occur.

v.3 Risk Influencing Factors

The calculations above refer to one specific year and several factors, for example, environmental or anthropogenic effects, can change the underlying conditions. On the one hand, sea level rise or changing wind patterns can affect the occurrence probabilities of extreme water levels and therefore impact the expected damages via the GEV parameters (Mudersbach and Jensen, 2010). This interrelation is little understood so far, but adverse effects on the flood risk can be expected at least from a rise in sea level (IPCC, 2012). On the other hand, socio-economic development and land use changes affect the distribution of assets and therefore the damage function and the expected damages. In particular, the implementation of flood defence systems or no further settlement in flood-prone areas can effectively mitigate flood damages (Pielke Jr. and Downton, 2000).

In the following we investigate the influence of two factors on the flood risk in the Kalundborg case study: (i) sea level rise and (ii) the implementation of a flood protection measure. A more general perspective on these effects can be found in Boettle et al. (2013b).

v.3.1 *Sea Level Rise*

Since in general, the impact of rising mean sea levels on extremes is not clear (Woodworth, 2010), we follow Hallegatte et al. (2011) and use the very intuitive approach of adding mean sea level rise to today's extremes. However, future mean sea levels depend on several unpredictable factors, such as global CO_2 emissions. We therefore employ SRES emissions scenarios (IPCC, 2000) in order to see how the flood risk could evolve. The corresponding local sea level projections for the region of Vestsjælland have been provided by the Dynamical Interactive Vulnerability Assessment (DIVA) tool (Hinkel and Klein, 2003; Vafeidis et al., 2008), considering medium and high climate sensitivity. Assuming all other factors (such as storm intensities, economic values, location of assets) to be constant, we consider the expected damage in the case study as a function of time. As Fig. v.3 illustrates, an increase of the flood risk by a factor between four (B1, medium) and 28 (A1FI, high) by 2100 can be found. The developments of the corresponding mean sea levels are shown in the inset. Consequently, the average annual damages in the case study will be

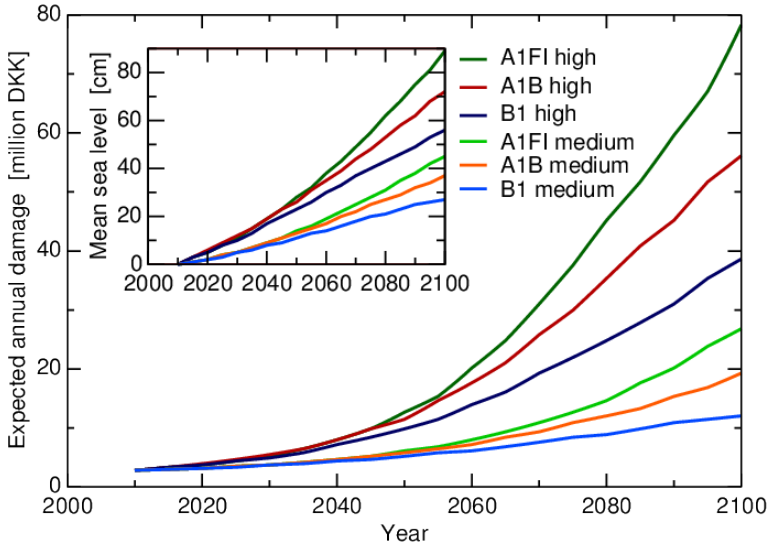

Figure v.3: Development of the expected annual damages (undiscounted) in the case study Kalundborg for several SRES scenarios. Corresponding sea level projections relative to the current sea level for the region of Vestsjælland are obtained from the DIVA tool (Hinkel and Klein, 2003; Vafeidis et al., 2008) and are shown in the inset. All lines represent a linear interpolation of annual values.

many times higher than today, which represents an increasing threat to house owners. Additionally, the results show that the ranges between medium and high climate sensitivity are approximately of the same order as the differences between the scenarios. Hence, the uncertainties due to the unknown socio-economic future and due to a vague understanding of the climate sensitivity are of similar relevance.

v.3.2 *Flood Protection*

Currently, several possibilities of protecting the most flood-prone areas in the case study from future storm surges are being discussed. The construction of dykes and the removal or a retrofitting of threatened structures with stilts is among the suggestions. In our context, such protection measures would affect the shape of the macroscopic damage function since smaller damages from certain sea levels can be expected. We want to examine the effectivity of one of these adaptation options provided by the municipality of Kalundborg, namely the construction of several dykes around low-lying areas. The suggested dykes, illustrated in Fig. v.1, have a total length of approximately 18 km and a height of 2.8 m above mean sea level, whereas the dykes at the coastline have an additional metre of height to protect from wave overtopping. Regarding the costs, the total construction would entail expenses of approximately 265 million DKK[4]. However, an analogous procedure as for the no-protection scenario provides a damage function for the adaptation scenario (depicted as a dashed green line in Fig. v.2). Based on this damage function, an expected annual damage of approximately 127,000 DKK for the year 2010 was calculated, which means a flood reduction of more than 95 % compared to

4 Estimated costs provided by the Municipality.

the current situation. Despite this impressive number, the efficiency evaluation of the described project needs to consider further aspects, such as the related implementation costs and the avoided damages over a longer time period. A detailed analysis is described in Sec. v.4.

In view of this example, the question about the appropriate height of the dykes arises. In practice, this issue is not always open to discussion due to legal regulations prescribing the protection height (see e.g. Chapter 4 in this book[5]). Nevertheless, we want to investigate the general effect of varying protection levels on the expected annual damage in Kalundborg. Therefore, we calculate the flood risk assuming different protection heights. Instead of performing a flood simulation and deriving a damage function for each height as in the example described above, we approximate the new damage functions by setting the original damage function to zero for all water levels below the given protection height, that is,

$$D_\omega(x) := \begin{cases} 0 & \text{if } x \leqslant \omega \\ D(x) & \text{if } x > \omega \end{cases}, \tag{v.3}$$

where D denotes the original damage function (Fig. v.2, black line), x the sea level, and ω the posed protection height. Now we are able to derive the flood risk for arbitrary protection levels according to Eq. (v.2). The resulting risks are displayed as a function of ω in Fig. v.4. It can be seen that the expected damage does not change visibly for protection levels below 100 cm. This is mainly due to the fact that it can avoid flooding only from very small extreme events, which contribute in only a minor way to the flood risk (as suggested by the damage function in Fig. v.2). This behaviour is followed by a slow reduction between 110 cm and 140 cm. For higher protection levels the expected damage decreases roughly exponentially and finally almost vanishes. For instance, protection levels above 270 cm mitigate the residual risk to an almost negligible amount of less than 10,000 DKK per year. These values differ considerably from the more specific example above, where a protection height of 280 cm at several locations was supposed and a residual risk of approximately 127,000 DKK was found. The reason for this deviation is that the suggested dykes in the example do not protect all assets and some buildings would still suffer from regular flooding. This explanation is supported by the inset of Fig. v.2, where the dashed green line exhibits damages of more than one million DKK for flood levels around 160 cm – in contrast, Eq. (v.3) provides no damages for a protection height of 280 cm.

v.4 Cost-Benefit Analysis

In order to evaluate the economic efficiency of an investment, all related costs and benefits need to be taken into account. In our context, benefits emerge exclusively in terms of avoided damages and we consider the benefits only implicitly by discussing the costs. However, regarding a specific adaptation measure, the avoided damages correspond to the difference between the residual damage and the damages in the no-adaptation case. Hence, we compare

5 Boettle et al. (2013c)

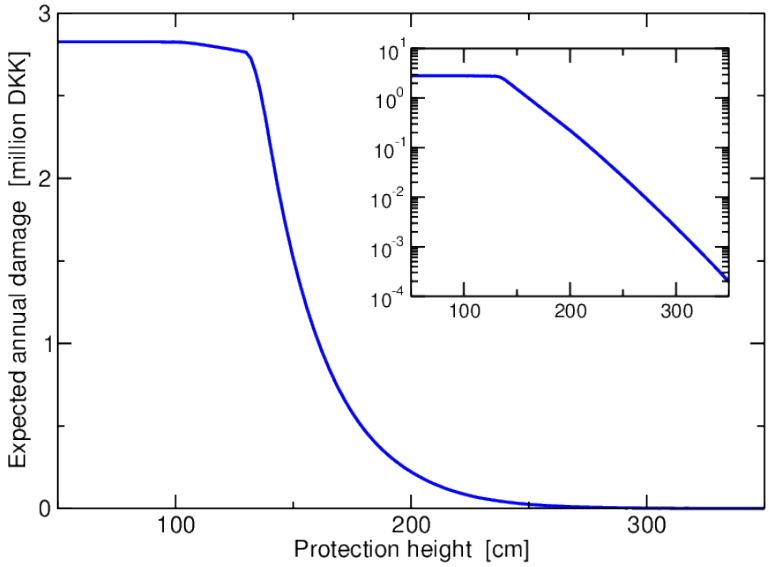

Figure v.4: Expected annual damage in the case study Kalundborg as a function of the protection height, presuming no damages occur up to the corresponding water level. The inset shows the same curve in semi-logarithmic scale.

all costs occurring in the adaptation scenario with those related to the no-adaptation policy. In order to take the preference of present to future consumption into account, future costs are commonly *discounted* to their present value by a certain *discount rate* (Halsnæs et al., 2007). return rate of private-sector investments, low rates (e.g. 1%) have a social aspect representing the interests of future generations (Portney and Weyant, 1999). The discount rate plays a crucial role for the valuation of future damages. For example, a damage of 100,000 € in 50 years has a present value of 60,804 € considering a 1 % discount rate but only 8720 € at a 5 % discount rate. Thus, high discount rates depreciate upcoming damages and therefore make adaptation measures less profitable since the costs for implementation typically emerge in the near future and are therefore not discounted. Especially for long-term decisions this exponential depreciation of future costs becomes dominant. To mitigate this effect, declining rates have been proposed (e.g. Weitzman, 2001, 2010). However, since discount rates are discussed very controversially, we will not choose one specific but will consider several constant rates.

Making an investment one wants to know, if and when it amortises, that is, when the (discounted) avoided damages exceed the expenditures and the investment becomes profitable. Hence, we need to cumulate the costs for the lifetime of the project. Figure v.5 shows the development of costs for several SRES scenarios with (solid lines) and without (dashed lines) considering the described protection measure and disregarding discounting. In the adaptation scenarios the costs start at the construction costs of 265 million DKK followed by a less steep increase, representing lower annual damages. One can see that the point of amortisation (intersection of solid with dashed lines) depends strongly on the underlying sea level rise scenarios (inset of Fig. v.3). Table v.1 summarises the years, when the investment is amortised considering several sea level scenarios and discount rates. The importance of the discount rate becomes apparent: While the investment amortises until 2070 in all sea level scenarios disregarding discounting, it does not become profitable until 2100 in

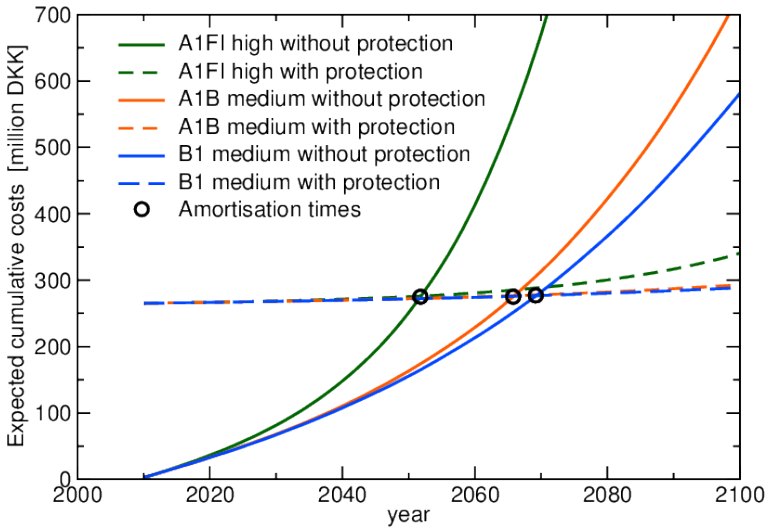

Figure v.5: Comparison of the expected cumulative costs supposing the proposed protection measure (dashes lines) with the no-protection option (solid lines) considering several sea level scenarios and disregarding discounting. Corresponding scenario projections for the region of Vestsjælland are obtained from the DIVA tool (Hinkel and Klein, 2003; Vafeidis et al., 2008) and are shown in the inset of Fig. v.3. All lines represent linear interpolations of annual values.

any case for discount rates higher than 4 %. The results also suggest that the uncertainty due to unknown climate sensitivity is of a similar magnitude as for the choice of the discount rate. Surprisingly, the underlying SRES scenario plays only a minor role for the amortisation time, which is already indicated by the developments of the corresponding mean sea levels (inset of Fig. v.3).

It is worth mentioning that these results are based on purely monetary values and exclude any nonmonetary aspects (e.g. social or ecological). Therefore, it might be reasonable to implement an option, although it is not efficient in a CBA sense.

Table v.1: Amortisation years for the described protection measure and several SRES scenarios, climate sensitivities and discount rates.

	B1		A1B		A1FI	
	High	Medium	High	Medium	High	Medium
0 %	2055	2070	2053	2066	2052	2065
1 %	2063	2088	2059	2081	2059	2078
2 %	2076	–	2069	–	2068	2099
3 %	–	–	2087	–	2082	–
4 %	–	–	–	–	–	–

Note: A dash '–' indicates that the investment will not be amortised until 2100. The corresponding sea level scenarios are obtained from the DIVA tool (Hinkel and Klein, 2003; Vafeidis et al., 2008) and are illustrated in the inset of Fig. v.3.

v.5 Conclusions

A method to perform CBA for adaptation measures in the context of sea level rise has been described and the analysis for a specific protection system in Kalundborg was presented. It was found that in general the results depend fundamentally on assumptions regarding future mean sea levels and on the choice of the discount rate. For a time horizon until 2100, it was found that the proposed dyke system is a profitable investment in all sea level scenarios (with an earliest amortisation time of 2052) only for discount rates less than 2 %. For rates above 4 % no sea level scenario led to an amortisation before 2100, which shows the crucial character of the discount rate in a cost-benefit analysis. Due to this fundamental effect, the discount rates need to be discussed in detail and agreed upon by the decision makers and stakeholders.

Our approach also comprises the estimation of annual damages and thus allows a further investigation of the effects of sea level rise and protection measures on the flood risk. For instance, we have shown that the expected annual damage strongly depends on the rate of sea level rise and an increase by a factor between four and 28 by 2100 was estimated (disregarding discounting), which implies great uncertainty due to the unknown development of future mean sea levels. It can be concluded that in any case adaptation to projected future conditions can considerably reduce expected damages in the region.

With regard to different protection levels in the Kalundborg case study, it is found that the residual annual damage decreases approximately exponentially with the height, assuming that all assets are protected up to a certain water level. Since the implementation costs for protection measures typically increase monotonically with the height, the optimal protection level can be derived. This optimum describes the minimum of the sum of all costs related to the protection measure and the residual damages.

Our results could be of particular importance for local authorities responsible for the decision making process regarding adaptation to sea level rise, because they include the dynamics of sea levels as well as possible adaptation plans. In general, we obtained insights into the interplay of protection height, sea level rise and the corresponding residual damage.

Acknowledgements. The authors would like to thank Anika Nockert, Lena Reiber and Olivia Roithmeier for creating the map. We appreciate financial support by the BaltCICA Project (part-financed by the EU Baltic Sea Region Programme 2007–13).

VI

Systematic Derivation of Macroscopic Damage Functions and Protection Needs for European Cities[1]

VI.1 The Need for Systematic Assessments

Coastal floods are local events. Accordingly, their consequences as well as sea level rise impacts on them need to be assessed on corresponding scales from the first principles. Here, we consider coastal cities as the objects of our examinations. First, because they are self-contained entities of limited spatial extent which are simultaneously exposed to the same flood hazard and second, because they comprise the most relevant areas in terms of (economic) damage potential (Jongman et al., 2012; Hunt and Watkiss, 2011). Large-scale impacts (e.g. on a country or continental level) are then derived by aggregating these consequences. However, the meaningfulness of such aggregations is not always clear. For instance, if the city-scale impacts are assessed by means of different methodologies which require individual interpretations and hence lead to distorted results when simply aggregated. A similar problem arises when impacts shall be compared between cities, e.g. for a priorisation of adaptation measures at different locations. On a large scale, these issues can be only solved by a systematic methodology that is applied to all considered regions. One particular requirement for the assessment of sea level rise impacts on the flood damage in a given city is the availability of a macroscopic damage function. Accordingly, a systematic and transferable methodology to dervie such functions is desired.

In our view, two basic requirements are indispensable for a systematic assessment of macroscopic flood damage curves, namely (i) a moderate complexity and (ii) data consistency. The first aspect involves a manageable amount of work load which can be equally accomplished for all cities. For instance, it is hardly feasible to perform a detailed modelling of flood routing or a stock-taking of individual buildings (as done in Chapter II for *one* caste study) for a large set of cities. We therefore propose a methodology of an intermediate level of complexity, which, albeit not implying the best possible assessment on a regional scale, represents an optimal trade-off for our purpose. The second requirement shall ensure the comparability of results, which can not be presumed if the data is obtained from different sources and possibly based on divergent acquisition methods. The most common approach for such assessments is based on population and GDP data for the estimation of exposed asset values and the subsequent application of a flood-damage function (see e.g. the DIVA model, or Hallegatte et al., 2013; Ward et al., 2013). We want to contribute a different methodology and base our estimations on land cover information and country-specific damage functions for a variety of land uses.

1 The content of this chapter will be part of an article which is currently under preparation in collaboration with Luís Costa, Diego Rybski, and Jürgen P. Kropp.

The second aspect of this chapter is the assessment of protection needs, i.e. the required flood defence measures that are necessary to protect a case study city against damage from certain floods. We are not aware of a general methodology for this purpose. From our perspective, the DIVA procedure (Hinkel and Klein, 2009) falls short in this respect as it simply suggests a dyke construction along the entire coastline (see also the discussion in Sec. 1.2). We will therefore introduce a more elaborated approach in the following section.

The goal of this chapter is to show how assessments of macroscopic damage functions as well as protection needs can be systematically designed and that appropriate results for further analyses can be obtained on the European scale. After providing a brief sketch of the applied methodology in Sec. VI.2, the results are presented and discussed in Sec. VI.3.

VI.2 Methodology

Following the previously used terminology, a macroscopic flood damage function provides the direct monetary damage that is caused by a hypothetical flood event of a certain magnitude in a delineated region (e.g. a city). Our elaboration of macroscopic damage functions involves five steps, which we briefly describe in the following. For further details, we refer to Boettle et al. (2014) and Jongman et al. (2012), where comprehensive explanations on the methods and the employed data can be found. The steps include:

(i) *Identification of urban areas*
First, the areas in which the damage shall be estimated need to be defined. For this purpose, we apply the City Cluster Algorithm (CCA) (Rozenfeld et al., 2008; Zhou et al., 2013) for entire Europe and identify all urban clusters in proximity to the ocean. From the obtained clusters, the 140 largest have been chosen as objects of further investigations (see Fig. VI.4). It needs to be mentioned, that these clusters do not correspond to administrative cities but represent connected areas of urban land cover. In some cases, even a unification of adjacent cities has been observed. For instance, our analysis provides a joint cluster for the cities of Antwerp and Brussels.

(ii) *Flood route modelling*
Based on the EU-DEM elevation data with a horizontal resolution of 25 m (EEA, 2013) and a flood fill algorithm using 8 nearest neighbours (Boettle et al., 2011) the flooded grid cells at a presumed flood height are determined. In addition to the information, whether a grid cell is flooded or not, also the corresponding inundation heights are recorded.

(iii) *Inferring land use of flooded areas*
The flooded areas are further investigated. Starting with Corine Land Cover (CLC) information (EEA, 2006b), we use the Land Use/Cover Area frame Statistical Survey (LUCAS) report in order to infer the corresponding land *uses*. The LUCAS report provides the empirical composition of land uses for all CLC classes in Europe (EEA, 2006a). At this point, we have all physical information needed: the inundation height of each grid cell for a given flood level as well as its land use.

(iv) *Application of land use damage functions*
The physical information from the previous steps is then converted to monetary damage by employing damage functions for the corresponding land uses. Adequate damage functions are provided by the Joint Research Centre (JRC, Huizinga, 2007), who developed country-specific stage-damage relations for various land use classes in Europe considering damages to buildings as well as their inventory. Using the land cover/use relation from the LUCAS report, we infer damage functions for CLC classes as a composition of corresponding land use damage functions. Eventually, their application provides the damage in each individual grid cell at a given flood level.

(v) *Aggregation to cluster-scale*
Within each urban cluster, all damages caused by a specific flood height are summarised. I.e.

$$D(x) = \sum_i D_i(x)\,,$$

where D is the total damage in the considered cluster at flood level x. The index i runs through all grid cells in the cluster and D_i is the damage function for the corresponding land class.

As an additional step, the protection needs in terms of a *required protection course* are estimated. Here, the protection course is interpreted as the entirety of all flood defence measures, whether they are dykes, sea walls or any other artificial construction. That is, we identify all grid cells, in which the construction of a flood defence structure is required in order to avert any of the previously determined damage. A grid cell is attributed to require a defence structure, if and only if it is adjacent to a grid cell that would suffer damage otherwise. Straightforwardly, the required height of the structure in a given grid cell is defined by the difference between its elevation and the considered flood level. Figure VI.1 illustrates the procedure for a flood level of 1.5 m in the urban cluster of Copenhagen. Please note that potential damage to non-urban cells is disregarded by design and is accordingly not averted by the proposed measure. This is intended since damage in non-urban areas is expected to be very moderate and thus hardly justifies costly flood defence investments.

The whole procedure described beforehand is carried out for each urban cluster and all flood levels between 0 m and 10 m in steps of 0.5 m. Accordingly, we obtain the flood damage as well as the required protection courses for all 140 urban clusters and each flood height $x = 0\,\text{m}, 0.5\,\text{m}, 1\,\text{m}, \ldots, 10\,\text{m}$.

At this point, it is important to note that existing protection structures are only considered in our estimations if they are represented in the employed Digital Elevation Model (DEM). To be precise, our curves estimate the *potential* damage and considerable deviations from the actually occurring damage in some cases cannot be ruled out.

VI.3 Results and Discussion

The derived damage functions of all 140 urban clusters are depicted in Fig. VI.2. As the clusters differ widely in their size, also the damage estimates vary by

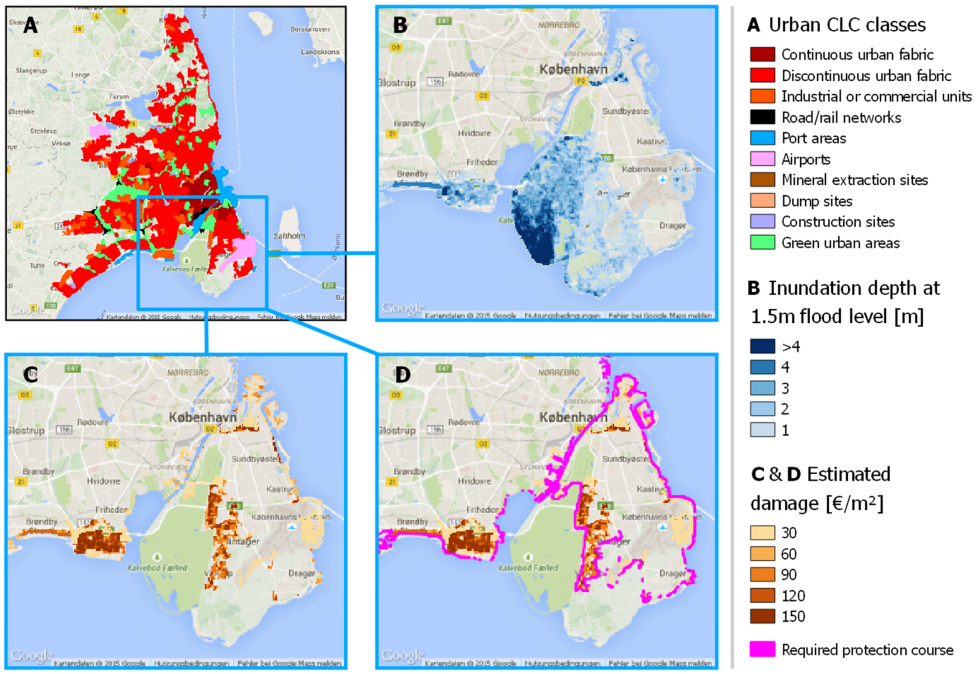

Figure VI.1: Procedure for the estimation of flood damage and protection needs for the urban cluster of Copenhagen at a 1.5 m flood height. (**A**) Identification of the urban cluster and its composition of CLC classes. (**B**) Inundation heights according to the applied flood fill algorithm. (**C**) Spatial distribution of the damage within the urban cluster. (**D**) Required course of flood defence structures to avoid any damage (purple).

several orders of magnitude. The illustrated curves are therefore normalised by dividing each curve by the corresponding damage at a 10 m flood level and they all end up at a normalised damage value of 1, accordingly. Several characteristics become visible. Probably most eye-catching is, that some curves exhibit a considerable damage at a 0 m flood level, which is obviously not realistic. This is the case for some low-lying cities, such as in the Netherlands, and can be attributed to the missing information about existing protection measures. Apart from that, it can be seen that almost all curves expose a convex increase for low and moderate flood levels. At higher flood levels, the damage saturates for roughly half of the curves, i.e. they become concave above a certain flood height. This behaviour appears plausible. Namely when most parts of the city are already inundated and no additional urban area gets flooded. However, the flood level at which this occurs remains a priori unclear.

In order to gain more detailed insights, we characterise the curves by means of an appropriate functional form. For this purpose, we propose the following functional model, that covers all of the obtained damage curves:

$$D(x) := \frac{a_1}{1 + \left(\frac{x - L_0}{a_2}\right)^{-a_3}}, \quad \text{for } x > L_0. \tag{VI.1}$$

Here, the parameter L_0 denotes the urban fabric land cover cell with the lowest elevation in the considered cluster and is directly derived from the available land cover and elevation data. It characterises the 'starting point' of the function, that is, there is no damage for $x \leqslant L_0$. The remaining parameters a_1, a_2, a_3 describe the vertical scaling, the horizontal stretching and the curvature of the

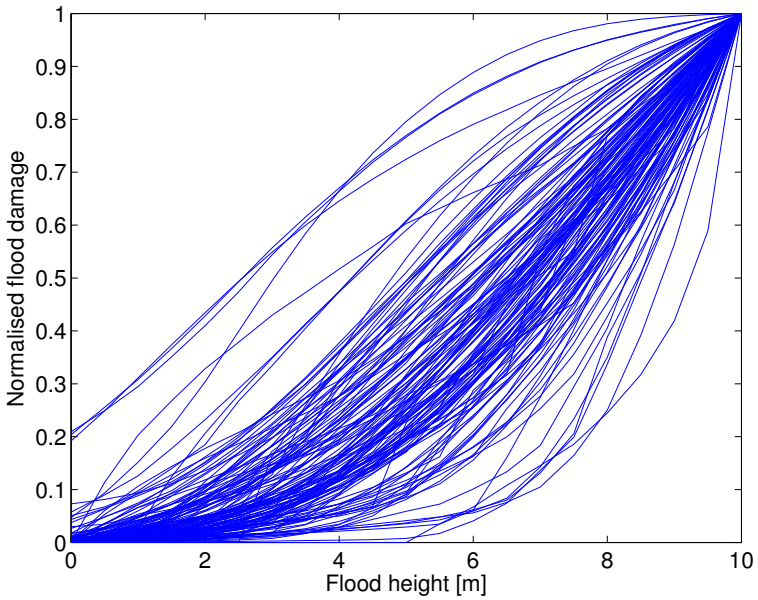

Figure VI.2: Damage functions of the 140 urban clusters, normalised by their maximum damage. I.e. each original function is divided by its damage at a 10 m flood level.

function, respectively. In general, the function D has a sigmoidal shape. It increases convexly for flood levels below an inflection point x_I and saturates for $x > x_I$ with a limiting damage of a_1. Please note that x_I lies in many cases far above 10 m and a flattening of these damage curves is therefore not visible in Fig. VI.2. For $x < x_I$ and particularly for x close to L_0, the following approximation can be inferred from Eq. (VI.1):

$$D(x) \approx \text{const.} \cdot (x - L_0)^{a_3}, \text{ for } x \in [L_0, x_I]. \tag{VI.2}$$

Accordingly, D follows roughly a power law in the range $[L_0, x_I]$ and a_3 corresponds to the exponent γ in the previous chapters, Eqs. (III.2) and (IV.6). The proposed model Eq. (VI.1) can therefore be considered as a generalisation of the power law model.

The parameters a_1, a_2, a_3 have been fitted to each of the 140 damage curves by minimising the mean squared error and visually good fits have been obtained. In order to further elaborate on the power law assumption from Chapters III and IV, we additionally estimate the power law exponents for flood levels $x \in [L_0, x_I]$, as suggested by the approximation Eq. (VI.2). By doing so, we are able to compare the exponents a_3 from Eq. (VI.1) with the exponents from a power law model on an appropriate range. We find that the two exponents are strongly correlated (with a correlation coefficient of $\rho = 0.97$). However, as can be seen from the cross-plot in Fig. VI.3A, the exponents a_3 are systematically larger than the estimated power law exponents. This is due to the fact, that the chosen range for the power law fit, $[L_0, x_I]$, already reaches a region where the damage increase weakens and hence reduces the exponent. This effect disappears completely, when the range is slightly limited, e.g. when the curve is fitted on $[L_0, 0.9x_I]$.

The inflection points x_I indicate the flood levels, at which the saturation of the damage takes visibly effect and above which the power law assumption becomes invalid. Considering their return periods, it turns out that they represent

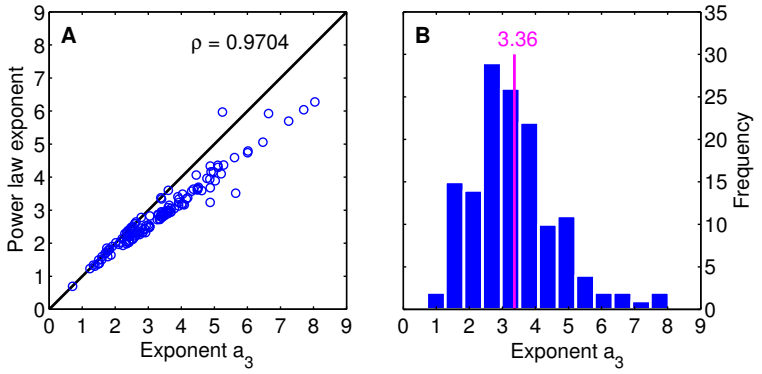

Figure VI.3: Fitted damage function exponents for the 140 urban clusters. (**A**) Cross-plot of estimated exponents α_3 according to Eq. (VI.1) with power law exponents when fitted to the curve up to the inflection point x_I, as in the approximation Eq. (VI.2). (**B**) Histogram of the 140 exponents α_3 across Europe with a mean exponent of 3.36 (purple line).

very rare events in almost all cases. For only seven urban clusters the return period of x_I falls below 10,000 years (based on extreme value information from Vousdoukas et al., 2015). Accordingly, we can conclude that the power law assumption from the previous chapters is well justified for the most relevant sea levels, even though the behaviour is expected to change above a certain flood level.

As we consider the exponent as a major characterisation of macroscopic damage functions, the estimated exponents provide valuable information about the typical shape of damage curves. Figure VI.3B shows a histogram of the estimated exponents, ranging from 0.7 to 8.0. Since only one of the exponents lies below 1 (for the city of Helsinki), the damage functions expose a super-linear behaviour in all other cases and increase on average steeper than cubically (with a mean exponent of 3.36). This allows us to put the previously determined exponents into context. While Kalundborg, whose damage function was derived on a high level of detail in Chapter II, exhibits a relatively high exponent of 4.1, the exponent of 1.6 for Copenhagen (Hallegatte et al., 2013) can be located at a very low quantile of the distribution. Considering the spatial distribution of the exponents, Fig. VI.4 depicts the estimated exponents of all 140 urban clusters within Europe. The exponent values can be interpreted as follows: high exponent values indicate a heavy damage increase for very extreme flood levels but at the same time imply a moderate slope for low flood levels. In contrast, low exponents imply a relatively high damage already for low/moderate flood levels but a less steep increase at high flood levels. Hence, the exponent α_3 provides a significant characterisation of the damage curve, even though it does not comprise information about the flood risk in the considered city.

At this point, we want to contrast our approach with the methodology followed by DIVA and Hallegatte et al. (2013) and pinpoint the two fundamental differences. These are (i) the estimation of exposed asset values and (ii) the relative damage functions. While our assessment is based on the land cover/use of a considered grid cell, the other approach uses the population density as an indicator for the present asset values and subsequently applies *one* relative damage function to the entire city/region. Although both approaches can

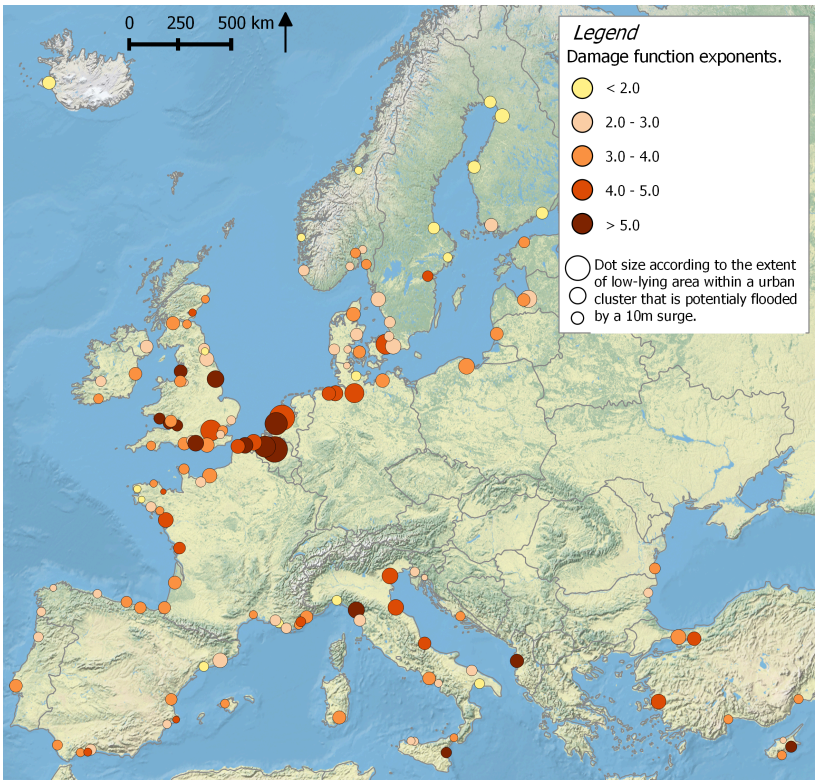

Figure VI.4: Cluster locations within Europe and the estimated exponent a_3 of their damage curve, indicated by the colour. The size of the balls corresponds to the size of the urban cluster.

hardly be validated and are justified only by plausibility arguments, a land use based assessment appears more adequate from the first principles. However, a reason for choosing the population based approach might be a better availability of homogeneous data beyond the European scale. A comparison of the two methodologies is pending and a matter of future research. Still, this cannot compensate for a efforts towards a validation by means of damage records, at least on a sample basis.

Regarding the protection needs of an urban cluster, we estimated the course of a required flood defence measure for protection levels between 0 m and 10 m. The results are exemplified by the urban cluster of Trondheim (Norway) in Fig. VI.5A–C, where the required protection courses are illustrated for protection levels of 1 m, 2 m and 4 m. Finally, Fig. VI.5D shows the length of the required measure as a function of the protection level. As our algorithm provides a defence structure that averts *any* damage, the proposed course is not necessarily efficient in the sense that it potentially supposes costly protection segments to avoid only little, tolerable damage. By visually inspecting Fig. VI.5, such can be suspected for a 1 m protection level in Trondheim. A risk-based optimisation of this method could therefore involve a significant improvement.

In addition to the protection course, the heights of the individual protection segments (i.e. the height of the defence measure at each location) have been deduced from the DEM. Hence, presupposing an intended flood defence level, we are able to estimate the associated constructional efforts. In a final step, this information can be used to estimate the monetary expenses of these strategies by employing unit cost estimates (Hoozemans et al., 1993; Jonkman et al.,

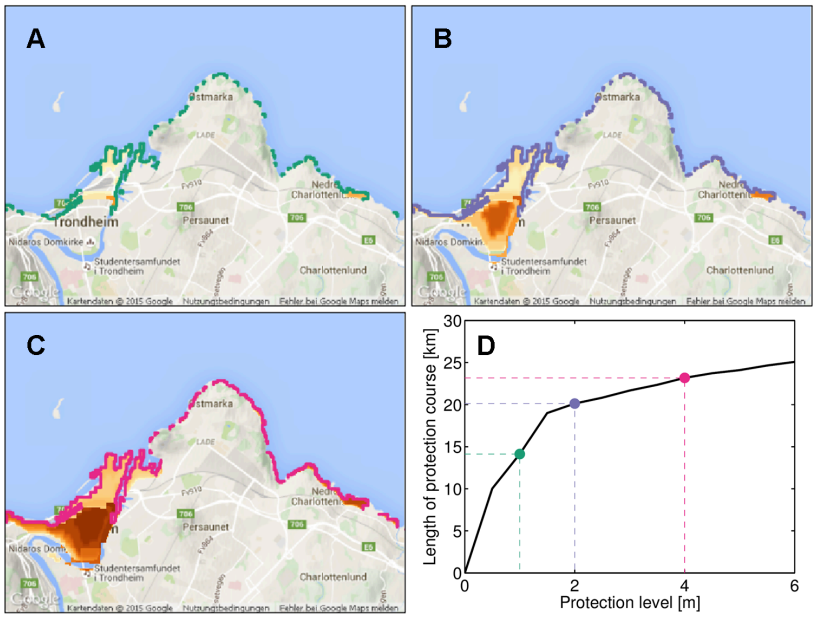

Figure VI.5: (**A**)–(**C**) Required protection courses in the urban cluster of Trondheim (Norway) for flood levels 1 m (green), 2 m (purple) and 4 m (magenta), respectively. The brownish shades indicate the estimated damage in the corresponding grid cell. (**D**) Length of the required protection course as a function of protection levels.

2013). We thus pave the way towards transferable cost assessments of sea level rise adaptation. Having also extreme sea level data with a high spatial coverage (Vousdoukas et al., 2015) and information about existing protection levels available, all prerequisites for a Europe-wide evaluation of flood protection measures (by means of a Cost-Benefit Analysis) are on hand. A crucial aspect in this context is the acquisition of currently installed flood defence levels in the considered regions. To our knowledge, Hallegatte et al. (2013) provide the only available database for this purpose. However, it is very incomplete with regard to our investigated cities and in large part relies on personal estimations. More effort towards such a collection of data is therefore urgently needed (de Moel et al., 2015).

VII

Discussion and Conclusions

VII.1 General Achievements

The thesis at hand has been devoted to the assessment of coastal flood damage in view of sea level rise and the economic evaluation of potential flood defence measures – particularly in the most vulnerable areas, namely cities. The overarching objective of gaining fundamental insights into the interplay between the involved processes has been met by keeping all considerations as general as possible. In this way, we were able to unravel the basic interrelations of quantities and results of universal validity have been obtained. Furthermore, the developed approaches are useful for two purposes: (i) decision making with regard to sea level rise adaptation on a local level and (ii) flood impact assessments on larger scales (e.g. European or global) which allow for a comparison across different regions. Accordingly, our work is governed by systematic methodologies with an intermediate level of complexity.

The presented derivations incorporate concepts from various disciplines. Whilst the elaboration of macroscopic damage functions is primarily a *geographic* task, the characterisation of flood events is performed by *stochastic* means. The combination of these two aspects then provides a framework from which the asymptotic behaviour of the flood damage for varying parameter values was studied based on *physical* and *mathematical* methods. Finally, specific damage estimations were integrated into a Cost-Benefit Analysis (CBA) which can be located in the *economic* domain. This makes the presented work truly multi-disciplinary and distinguishes it from many studies in this field.

While each of the presented research articles already comprises an individual discussion, the achievements with regard to the posed Research Questions RQ 1 through RQ 4 are summarised in the following sections. The Research Questions will be revisited and the corresponding contributions from Chapters II–VI are reviewed and interlinked. Furthermore, we elaborate on the scientific relevance of our findings, set them into a broader context, and discuss existing limitations.

Finally, the chapter concludes with a brief outlook of remaining research issues and provides a general conclusion in Sec. VII.6.

VII.2 Macroscopic Damage Functions

Macroscopic flood damage functions, i.e. functions providing the total damage within a spatially delineated region at a given flood level, are a prerequisite to assess coastal flood damage on a case study level. Nevertheless, we are not aware of scientific contributions elaborating on their main influencing factors nor on their typical shape. This gave rise to our first Research Question, RQ 1: *What are the major determinants of macroscopic flood damage functions and what is their typical shape?*

Our work revealed that two regimes of a macroscopic damage function need to be considered with regard to the most influencing factors: (i) For low and moderate flood levels, the macroscopic damage primarily depends on the employed Digital Elevation Model (DEM) and (ii) for very extreme events, the building damage function becomes more decisive (Figs. II.5 and II.6).

This main finding implies that for the damage assessment of low and moderate flood levels, accurate elevation data is indispensable and in practice, the acquisition of a high quality DEM should be endeavoured. In such a case, the individual building damage is relatively moderate and the total damage is predominantly determined by the number of affected assets. Hence, small errors in the DEM can have a large impact on the total estimated damage. Surprisingly, this effect has been observed equally for all applied microscopic (i.e. building-scale) damage functions (Fig. II.6). Although the absolute damage of such events is rather low, this can have a crucial effect on the flood risk in the considered region because of their high frequency. In contrast, for high flood levels, the number of additional affected buildings becomes less important and the estimated damage is more strongly affected by the microscopic damage function for individual buildings (Fig. II.6). The elaboration of well adapted microscopic damage functions is therefore recommended when focusing on high flood levels (Fig. II.5).

Regarding the flood route determination, the comparison of two different methods exhibited only little influence on the resulting damage curves for all considered flood levels. This indicates in general that the DEM and the microscopic damage functions are the dominant factors in the assessment of macroscopic damage functions.

The gained knowledge supports the development of macroscopic damage functions and hence also contributes to RQ 2 (Sec. VII.3) since an accurate damage function is a prerequisite for the estimation of the expected flood damage in a considered region. Furthermore, the set of damage curves for Kalundborg obtained from the various determination modes provides an indication about the uncertainty arising from inaccuracies in the utilised data and microscopic damage functions. Whereas a huge range with several orders of magnitude has been detected for low flood levels, a variation of roughly one order of magnitude was found for high flood levels (Fig. II.6). In general, a considerable sensitivity of the estimated damage to errors in the input data has been detected and a cautious treatment with such estimates needs to be recommended, equally for all flood levels.

Presupposing a quadratic building damage function as defined in Eq. (II.4), Fig. III.3 illustrates that the increase in macroscopic damage in Kalundborg can be described by a power law as a function of the flood level. More general insights into the shape of macroscopic damage functions could be gained by investigating the curves of 140 coastal cities in Europe (Fig. VI.2) which have been developed in an automatised manner in Chapter VI. We have shown that the initial damage increase of these curves can be characterised well by a power law, which supports our assumption on their functional form in Chapters III and IV. The corresponding exponents are estimated to lie in the range of 0.7–8 with a mean value of 3.4 (Fig. VI.3) implying an average increase that is steeper than cubic. It is noteworthy that the lowest exponent represents an outlier and

the second smallest value is already above 1.2. Accordingly, our results suggest an unambiguously super-linear behaviour in general.

However, a flattening of the curve has been observed in many cases for very extreme flood levels (typically at flood levels above 5 m). Such a saturation appears plausible, namely when large parts of the considered region are flooded and only little marginal damage is caused by additionally affected assets. Still, it remains unclear in which cases and at which water level this occurs. Nevertheless, we were able to infer a three-parametric functional model, Eq. (VI.1), which integrates all considered cases. The provided functional form generally describes a sigmoidal shape but exposes a power law increase up to a certain flood level. Since the turning point at which the curve becomes concave is variable, the model integrates purely convex as well as sigmoidal damage curves for the investigated flood levels of up to 10 m. As discussed in Sec. VI.3, a saturation could be detected only for very extreme flood levels with return periods beyond 10,000 years in almost all cases (133 out of 140). Hence, the assumption of a power law behaviour for the relevant range of flood levels is well justified. This finding represents an essential prerequisite for answering RQ 3, where we aim for a functional description of damage estimates (Sec. VII.4).

As we do not have information about existing flood defences (as long as they are not represented in the DEM), some of the functions are expected to be distorted in reality for low and medium flood heights. The ability to predict the damage from such flood levels is therefore limited in some cases and the development of a database consisting of present flood defence levels in coastal regions needs to be pursued (de Moel et al., 2015). Our results are still well suited to estimate the potential damage for the case that the flood protection fails or is simply insufficient.

While our findings about typical damage function shapes are substantiated by a large set of functions, the investigation of their determining factors could be based on only a single case study. Although we suppose the main conclusions to be transferable to other regions, it remains unclear to what extent this is actually the case. In order to solve this issue, the consideration of a larger set of regions using a common, highly detailed methodology is unavoidable. This, however, would involve an amount of work that is out of the scope of this thesis and is left as a matter of future research. Nevertheless, our analysis provides a useful indication that is to our knowledge the first of its kind.

In general, it must be noted that any investigation of macroscopic damage functions is hampered by the deficient availability of damage records on the corresponding scale, which makes validation or calibration impossible. The main reason for this is the rare occurrence of meaningful flood events (at a given location). But also the acquisition of actual damage (on a case study level) in the aftermath of a flood poses a big challenge (de Moel et al., 2015). *Synthetic* approaches, such as presented in Chapters II and VI, are therefore the one and only alternative. As our land cover based approach fundamentally contrasts with the population based methodology followed by DIVA and Hallegatte et al. (2013), a comparison of the two represents a worthwhile task which is subject to future work (see also discussion in Sec. VI.3).

Our findings can be well integrated into a generalised damage assessment, where a functional form of the macroscopic damage needs to be presupposed (as addressed by RQ 3). Furthermore, they clear the way for adjusting damage

functions to regions with deficient data availability. For instance, we can derive a damage function from only few damage records by estimating the provided parameters.

In summary, the presented results make a considerable contribution for answering RQ 1. First, by identifying two basic regimes of macroscopic damage functions where the estimated damage is dominated by different influencing factors and second, by characterising the functional form of a macroscopic damage function from which a typical shape could be deduced.

VII.3 Assessment of Sea Level Rise Impacts and Protection Measures

The evaluation of potential adaptation measures requires a framework which is capable of estimating both coastal flood damage as well as the effect of sea level rise and the considered adaptation on them. This need is verbalised in the second Research Question, RQ 2: *How can the assessment of sea level rise impacts and the economic efficiency of adaptation measures be designed in a systematic and flexible way?*

This issue is a direct follow-up of RQ 1 since such an assessment is necessarily based on information about the damage emerging from single flood events, i.e. a macroscopic damage function. We propose a framework that essentially combines extreme value statistics with macroscopic damage functions in order to estimate direct monetary flood damage within a specified region and a given time period (illustrated in Fig. I.3). Two complementary methods from extreme value theory have been pursued: (i) a Block Maxima approach, considering only the most severe flood event per year (Chapter III), and (ii) a Peak Over Threshold (POT) approach, characterising all sea levels above a certain magnitude in combination with a Point Process (PP) to model the occurrence of such events (Chapter IV). The framework is flexible in the sense that it can be easily applied to specific case studies as well as arbitrary climate and protection scenarios by assuming non-stationarity of the corresponding parameters. Accordingly, the framework is capable of evaluating the economic efficiency of potential protection measures taking arbitrary sea level scenarios into account.

When applied to the city of Copenhagen, we were able to quantify the sea level rise impact on the annual flood damage for several sea level pathways. In particular, we found roughly a doubling of annual damage, presupposing an optimistic sea level increase of 11 cm between 2010 and 2050 (Fig. IV.5). Furthermore, the economic evaluation of a concrete protection measure has been illustrated for the case study of Kalundborg (Fig. V.5). The performed analysis particularly highlighted the crucial character of the chosen discount rate as well as the considered time horizon in a CBA (Tab. V.1). For instance, while an amortisation of the protection investment has been estimated for the year 2063, supposing a 1 % discount rate, no amortisation before 2100 is expected when choosing a rate of 3 % (both estimates based on SRES scenario B1). The presented estimations demonstrate the usability of our framework and can be generally performed for arbitrary case study regions, given the availability of a damage function and sea level data.

As the economic assessment of protection investments is often found to be impeded by the absence of sufficient information about the costs of such measures, a generalised method for the cost estimation is desired. Yet only

very vague information about the typical costs of dyke protections is available (Hoozemans et al., 1993; Jonkman et al., 2013) and it is questionable whether this provides appropriate estimates for specific cases at all – particularly when more complex constructions, such as sea walls or flood barriers, shall be investigated. Nonetheless, this kind of estimations represent the only realistic option for assessments beyond case study level.

The proposed approaches can be well employed for damage assessments in urban areas considering sea level rise. Furthermore, due to its easy applicability, the presented framework paves the way for a systematised application to a large set of regions in the context of supra-regional or even global considerations. Potential data sources for such an undertaking are systematically derived damage functions (as provided in Chapter VI or Hallegatte et al., 2013), knowledge about the required protection efforts (see Chapter VI), and information about extreme sea levels (e.g. Vousdoukas et al., 2015). Still, there is great need for improving such information with broad spatial coverage.

The principal approach of calculating the expected annual damage is very common and is also followed by the DIVA model (Hinkel et al., 2014) and Hallegatte et al. (2013). Therefore, the advantages of our methodology need to be pinpointed here. This is, in the first place, the use of state-of-the-art extreme value theory including the non-stationarity of all involved parameters. We thus obtain full flexibility and can assess the effect of arbitrary parameter changes by considering the entire probability distribution of extreme sea levels. In contrast, Hallegatte et al. (2013) base their estimations on only several flood levels, namely the 1-, 10-, 100-, and 1000-year event (obtained from the DIVA tool). Beside the imprecise approximation of the integral in Eq. (III.3), this impedes the investigation of altering storm conditions by means of a changing scale parameter (Sec. IV.A) and is hence insufficient for our purpose. Moreover, the moderate complexity of our approach provides a transparency which facilitates the revision of our results by improving individual components.

The generality of the framework also allows for the transfer of its basic idea to other natural hazards. Prerequisites for this are the availability of occurrence probabilities for certain magnitudes of the considered hazard as well as an *impact function*, relating the hazard magnitude with the impact (e.g. monetary damage). Potential fields of application include storms and associated (monetary) damage, droughts and resultant crop failures, or heat waves and related mortalities (Prahl et al., 2016).

To conclude, we can state that the presented methodologies present a systematic and flexible way for the assessment of sea level rise impacts as well as adaptation effects due to coastal protection and hence meet all requirements mentioned in RQ 2.

VII.4 General Effects of Sea Level Rise and Adaptation

The previous section discussed the assessment of flood damage at a given location. From a more general perspective one would like to know whether the development of damage with rising mean sea levels can be universally described. This motivates our third Research Question, RQ 3: *What are the functional relationships of the mean sea level and the implemented protection height with coastal flood damage?*

As justified in the discussion of RQ 1, the functional form of a macroscopic damage function F can be characterised by a power law, i.e. $F(x) \sim x^\gamma$ (with γ denoting the *damage function exponent* for the considered region). By presupposing this type of damage function for a given region, we find that the development of the expected annual damage can be approximated well by surprisingly simple functional expressions. These approximations have been deduced from asymptotic considerations and are furthermore mathematically proven to hold for asymptotic large parameter values. As summarised in Tabs. III.1 and IV.2, functional relations could be obtained for a varying mean sea level, altering storm intensities as well as the introduction of a certain protection level for both the Block Maxima and the POT/PP approach.

Regarding the effect of sea level rise, we find in general a super-linear increase in the expected damage with the mean sea level. However, the results differ for the two stochastic approaches: whereas the annual damage increases like a power law with exponent γ in the Block Maxima approach, a more complex picture was found when employing a Point Process (Sec. IV.6). In that case, the sign of the shape parameter ξ decides on the fundamental behaviour of the damage increase and three possible developments are detected. Remarkably, the parameter ξ can be regarded as a characterisation of the considered region and is invariant under shifts and scaling operations as performed for the modelling of climatic changes. In other words, the functional shape of damage development with rising sea levels is independent from the current mean sea level and the prevailing storm climate. A very astonishing result from the POT/PP approach regarding sea level rise is the weak influence of the damage function exponent γ, which does not appear for $\xi \geqslant 0$ and has only a minor influence for $\xi < 0$ (Sec. IV.3). The discrepancy between the results of the two approaches pinpoints the major differences of the underlying methodologies, namely the consideration of a different set of flood events (see discussion in Sec. IV.6). Accordingly, the question of which approach is more adequate for a considered region cannot be answered in its generality and depends on the focus of the investigation.

Scrutinising the damage behaviour for varying protection levels ω or altering wind patterns (modelled by varying the scale parameter σ), the results of both stochastic approaches coincide. These are, firstly, a decrease with rising protection heights of various types (again, dependent on ξ) and secondly, a power law increase of expected damage with exponent γ (i.e. σ^γ). Overall, the results explain how individually varying parameters amplify the damage or counteract each other.

In addition to the fundamental insights provided by these mathematically proven results, we have shown that the provided expressions represent good damage approximations for small variations under current conditions (see Figs. III.4, III.6, III.7, III.8, III.9, III.10, IV.4, IV.6, and IV.7). In particular for varying mean sea levels, a good convergence of our expressions with numerically calculated estimations was confirmed. This allows a projection of the future flood damage solely based on the discussed parameters and hence underpins the general usability of our results.

The damage function exponent γ is a fundamental ingredient of our investigations. Our assumption about the functional form of macroscopic damage functions, and thus about the mere existence of such an exponent, is therefore

crucial. As the 140 derived damage functions in Europe show, this assumption was justified even though the damage curves saturate in many cases (see discussion in Sec. VI.3). Considering our findings on the damage function exponent γ, we can state that the expected annual flood damage will rise superlinearly with the mean sea level (in 139 out of 140 cases) and on average even faster than cubically (Fig. VI.3B). However, exploring the effect of very large rates of sea level rise, the introduction of a saturation effect in the damage functions could be worthwhile. This remains subject to future research though. Less simple functional relations and potentially several regimes of behaviour can be expected.

In order to study the climate change effects on the expected flood damage, a link between environmental changes and extreme value parameters needs to be established. Whereas there seems to be a consensus that rising mean sea levels roughly lead to a likewise upward shift of extreme floods (Sec. I.1), it is not clear how changing meteorological patterns take effect (Mudersbach and Jensen, 2010). Further research on these effects is therefore desirable in order to provide damage estimates for given climate projections. Another starting point for further research could be the investigation of factors that determine the rate of asymptotic convergence. I.e. whether we can make an a priori judgement about the quality of our asymptotic approximation. Finally, it appears worthwhile to study the effect of an altering damage function. Such changes could have several reasons: First, the implementation of soft protection measures such as early warning systems or land use management. Second, city growth as well as socio-economic development (Hinkel et al., 2014), and third, the occurrence of several flood events in quick succession. For instance, a damaged building will lower the estimated damage as long as it is not restored between the events.

Our findings significantly improve the general understanding of the interplay between coastal flood damage, the mean sea level, and implemented protection levels. All considered interrelations could be disentangled by means of simple functional expressions for both stochastic perspectives and a profound answer to RQ 3 has been obtained. The provided relations are of particular relevance for integrated assessment models, such as REMIND (Luderer et al., 2013) or FUND (Tol, 2002b), which model the economic development along a given emission/climate pathway.

VII.5 Aleatory Uncertainty of Flood Damage Estimations

As we perceive a flood as a stochastic event, the estimation of damage inevitably involves an inherent uncertainty stemming from this randomness. By means of the presented framework, we are able to quantify this uncertainty and can thus address the final Research Question of this thesis, RQ 4: *How large is the aleatory uncertainty in flood damage estimations?*

The issue of uncertainty is a prevailing aspect of flood damage estimations and is directly linked to RQ 2. After deriving the probability distribution of the annual flood damage (Sec. VII.3), we measure the (aleatory) uncertainty of the actual damage by means of the corresponding standard deviation. Based on this, our analyses show that the standard deviation of our estimates is of the same order of magnitude as the expected damage itself (Figs. III.4, III.6 and

IV.4). Moreover, since the flood levels and hence also the damages are skewly-distributed, it is very likely that the occurring damage in a specific year exceeds the expected damage by many times. This is of high relevance for the general perception of and the dealing with damage projections.

At this point, we want to highlight once more that this uncertainty does not comprise any *epistemic* sources (e.g. from vaguely determined extreme value parameters or the flood-damage relation). Therefore, the total error of our estimations is expected to be significantly higher. This huge degree of unpredictability accentuates the need for an adequate conveyance of results to stakeholders, who should be aware of the possible fluctuations around the expected damage.

Postulating a rise of mean sea levels, the uncertainty of damage estimations will further increase (Figs. III.4, III.6 and IV.4). However, considering the relative uncertainty (i.e. the standard deviation divided by the expected damage), a decrease has been detected. For instance, the relative error of our estimates for the city of Copenhagen, which currently amounts to 34 % would decrease to approximately 26 % supposing 20 cm of sea level rise (Sec. III.6). This surprising finding implies, in a sense, a better predictability of future flood damage. In contrast, a growth of the relative uncertainty has been found for increasing protection levels despite a decline in absolute values. Although enhanced protection standards help to avoid flood damage, there always remains a chance of being insufficient, which entails a high variance in relation to the low average damage.

The presented investigations, which to our knowledge are the only available quantification of aleatory uncertainty, could be further expedited by considering the entire probability distribution of the damage instead of taking only the standard deviation as a measure. Especially in view of the skewness of the damage distribution, this could potentially improve the information content. For instance, certain quantiles of the damage distribution could be inferred. On the downside, this would make the results more complex and hence less comprehensible.

In summary, our findings provide fundamental insights into the aleatory uncertainty that is generally involved in flood risk assessments and thus answer RQ 4.

VII.6 Concluding Remarks and Outlook

With the presented work, we have shown how sea level rise impacts on coastal flood damage can be assessed in a systematic and flexible manner. We thus facilitate the comparability of regional assessments and lay the foundation for meaningful large scale estimations. To be more specific, we contributed to several aspects: (i) macroscopic damage functions, (ii) the estimation of expected flood damage as well as the economic assessment of protection measures, and finally, (iii) the quantification of the aleatory uncertainty involved in damage estimation. Accordingly, our contributions are particularly useful for decision making in the context of sea level rise on any scale. Moreover, by means of our generalised investigations we made considerable progress in the understanding of the flood damage process.

With regard to the presented methodological approaches, we are confident that they will fertilise future research in this or an adjacent research field. Several starting points for further investigations have already been mentioned. Here, we want to highlight the projection of sea level rise impacts and the evaluation of potential adaptation strategies on a European scale, towards which the first steps have already been undertaken (Chapter VI). Having such results at hand provides the basis for an impact comparison with, for instance, the DIVA model. Finally, the additional consideration of indirect flood impacts (by adjusting the damage function) could be an ultimate goal of this track. Lastly, it appears worthwhile to include further sources of (epistemic) uncertainty in our framework in order to shed light on the actual uncertainty of flood damage estimations and to relate their magnitude to the aleatory one discussed in this work.

Bibliography

Abeysirigunawardena, D. S. and Walker, I. J. (2008). Sea level responses to climatic variability and change in northern British Columbia. *Atmos. Ocean*, 46(3):277–296.

Adler, C. E. and Hirsch Hadorn, G. (2014). The IPCC and treatment of uncertainties: topics and sources of dissensus. *WIREs Clim. Change*, 5:663–676.

Aerts, J. C. J. H., Botzen, W. J. W., Emanuel, K., Lin, N., de Moel, H., and Michel-Kerjan, E. O. (2014). Evaluating flood resilience strategies for coastal megacities. *Science*, 344:472–474.

Anthoff, D., Nicholls, R. J., and Tol, R. S. J. (2010). The economic impact of substantial sea-level rise. *Mitig. Adapt. Strateg. Glob. Change*, 15(4):321–335.

Anthoff, D. and Tol, R. S. J. (2013). The uncertainty about the social cost of carbon: A decomposition analysis using FUND. *Clim. Change*, 117(3, SI):515–530.

Apel, H., Aronica, G. T., Kreibich, H., and Thieken, A. H. (2009). Flood risk analyses – how detailed do we need to be? *Nat. Hazards*, 49(1):79–98.

Apel, H., Merz, B., and Thieken, A. H. (2008). Quantification of uncertainties in flood risk assessments. *J. River Basin*, 6(2):149–162.

Apel, H., Thieken, A. H., Merz, B., and Blöschl, G. (2004). Flood risk assessment and associated uncertainty. *Nat. Hazards Earth Syst. Sci.*, 4(2):295–308.

Arfken, G. B. and Weber, H. J. (2005). *Mathematical Methods for Physicists*. Elsevier, 6th edition.

Balica, S. F., Wright, N. G., and van der Meulen, F. (2012). A flood vulnerability index for coastal cities and its use in assessing climate change impacts. *Nat. Hazards*, 64:73–105.

Barbosa, S. M., Fernandes, M. J., and Silva, M. E. (2006). Long-range dependence in North Atlantic sea level. *Physica A: Statistical Mechanics and its Applications*, 371(2):725–731.

Beichelt, F. (2006). *Stochastic processes in science, engineering, and finance*. Chapman & Hall/CRC, Boca Raton, FL, USA.

Bender, J., Wahl, T., and Jensen, J. (2014). Multivariate design in the presence of non-stationarity. *J. Hydrol.*, 514:123–130.

Blong, R. (2003). A new damage index. *Nat. Hazards*, 30(1):1–23.

Boettle, M., Costa, L., Kriewald, S., Kropp, J. P., Prahl, B. F., and Rybski, D. (2014). Development of a library of impact functions and general uncertainty measures. http://www.ramses-cities.eu/resources. Accessed 16 September 2015.

Boettle, M., Kropp, J. P., Reiber, L., Roithmeier, O., Rybski, D., and Walther, C. (2011). About the influence of elevation model quality and small-scale damage functions on flood damage estimation. *Nat. Hazards Earth Syst. Sci.*, 11(12):3327–3334.

Boettle, M., Rybski, D., and Kropp, J. P. (2013a). Adaptation to sea level rise: Calculating costs and benefits for the case study Kalundborg, Denmark. In Schmidt-Thomé, P. and Klein, J., editors, *Climate Change Adaptation in Practice*, chapter 3, pages 25–34. Wiley-Blackwell, Chichester, UK.

Boettle, M., Rybski, D., and Kropp, J. P. (2013b). How changing sea level extremes and protection measures alter coastal flood damages. *Water Resour. Res.*, 49(3):1199–1210.

Boettle, M., Schmidt-Thomé, P., and Rybski, D. (2013c). Coastal protection and multi-criteria decision analysis: Didactically processed examples. In Schmidt-Thomé, P. and Klein, J., editors, *Climate Change Adaptation in Practice*, chapter 4, pages 35–49. Wiley-Blackwell, Chichester, UK.

Bubeck, P., de Moel, H., Bouwer, L. M., and Aerts, J. C. J. H. (2011). How reliable are projections of future flood damage? *Nat. Hazards Earth Syst. Sci.*, 11:3293–3306.

Büchele, B., Kreibich, H., Kron, A., Thieken, A., Ihringer, J., Oberle, P., Merz, B., and Nestmann, F. (2006). Flood-risk mapping: Contributions towards an enhanced assessment of extreme events and associated risks. *Nat. Hazards Earth Syst. Sci.*, 6(4):485–503.

Carbognin, L., Teatini, P., Tomasin, A., and Tosi, L. (2010). Global change and relative sea level rise at Venice: what impact in term of flooding. *Clim. Dynam.*, 35(6):1055–1063.

Cazenave, A. and Le Cozannet, G. (2013). Sea level rise and its coastal impacts. *Earth's Future*, 2:15–34.

Church, J. A., Clark, P. U., Cazenave, A., Gregory, J. M., Jevrejeva, S., Levermann, A., Merrifield, M. A., Milne, G. A., Nerem, R. S., Nunn, P. D., Payne, A. J., Pfeffer, W. T., Stammer, D., and Unnikrishnan, A. S. (2013). Sea level change. In Stocker, T. F., Qin, D., Plattner, G.-K., Tignor, M., Allen, S. K., Boschung, J., Nauels, A., Xia, Y., Bex, V., and Midgley, P. M., editors, *Climate Change 2013: The Physical Science Basis. Contribution of Working Group I to the Fifth Assessment Report of the Intergovernmental Panel on Climate Change*. Cambridge University Press, Cambridge, UK and New York, NY, USA.

Church, J. A. and White, N. J. (2011). Sea-level rise from the late 19th to the early 21st century. *Surv. Geophys.*, 32(4–5):585–602.

Coles, S. (2001). *An Introduction to Statistical Modeling of Extreme Values*. Springer Series in Statistics. Springer, London, UK.

Costa, L., Tekken, V., and Kropp, J. P. (2009). Threat of sea level rise: Costs and benefits of adaptation in European union coastal countries. *J. Coastal Res.*, SI 56:223–227.

CPSL (2010). *CPSL Third Report. The role of spatial planning and sediment in coastal risk management*. Wadden Sea Ecosystem No. 28. Common Wadden Sea Secretariat, Trilateral Working Group on Coastal Protection and Sea Level Rise (CPSL), Wilhelmshaven, Germany.

Dangendorf, S., Rybski, D., Mudersbach, C., Müller, A., Kaufmann, E., Zorita, E., and Jensen, J. (2014). Evidence for long-term memory in sea level. *Geophys. Res. Lett.*, 41(15):5530–5537.

Dasgupta, S., Laplante, B., Meisner, C., Wheeler, D., and Yan, J. (2008). The impact of sea level rise on developing countries: a comparative analysis. *Climatic Change*, 93(3–4):379–388.

Dawson, R. J., Ball, T., Werritty, J., Werritty, A., Hall, J. W., and Roche, N. (2011). Assessing the effectiveness of non-structural flood management measures in the Thames estuary under conditions of socio-economic and environmental change. *Global Environ. Chang.*, 21(2, SI):628–646.

de Moel, H., Asselman, N. E. M., and Aerts, J. C. J. H. (2012). Uncertainty and sensitivity analysis of coastal flood damage estimates in the west of the Netherlands. *Nat. Hazards Earth Syst. Sci.*, 12:1045–1058.

de Moel, H., Jongman, B., Kreibich, H., Merz, B., Penning-Rowsell, E., and Ward, P. J. (2015). Flood risk assessments at different spatial scales. *Mitig. Adapt. Strateg. Glob. Change*, 20:865–890.

Delcan Corporation (2012). Cost of adaptation, sea dikes & alternative strategies: final report. Technical report, British Columbia. Ministry of Forests, Lands and Natural Resource Operations.

Devoy, R. J. N. (2008). Coastal vulnerability and the implications of sea-level rise for Ireland. *J. Coastal Res.*, 24(2):325–341.

Dossou, K. M. R. and Glehouenou-Dossou, B. (2007). The vulnerability to climate change of Cotonou (Benin): the rise in sea level. *Environ. Urban.*, 19(1):65–79.

Dutta, D., Herath, S., and Musiake, K. (2002). Direct flood damage modelling towards urban flood risk management. *Proceedings of the Joint Workshop on Urban Safety Engineering 2001*, ICUS Report:127–143.

Dutta, D., Herath, S., and Musiake, K. (2003). A mathematical model for flood loss estimation. *J. Hydrol.*, 277(1–2):24–49.

EEA (2006a). The thematic accuracy of CORINE land cover 2000. assessment using LUCAS (land use/cover area frame statistical survey). Technical Report no7/2006, European Environment Agency.

EEA (2006b). Urban morphological zones. http://www.eea.europa.eu/data-and-maps/data/ds_resolveuid/R4XDW7ODPC. Accessed 16 September 2015.

EEA (2013). DEM over Europe from the GMES RDA project (EU-DEM, resolution 25m) – version 1. http://www.eea.europa.eu/data-and-maps/data/ds_resolveuid/ca503256de1b4231b029e4145d0a8b7b. Accessed 16 September 2015.

Eichner, J. F., Kantelhardt, J. W., Bunde, A., and Havlin, S. (2007). Statistics of return intervals in long-term correlated records. *Phys. Rev. E*, 75(1).

El Adlouni, S., Ouarda, T. B. M. J., Zhang, X., Roy, R., and Bobee, B. (2007). Generalized maximum likelihood estimators for the nonstationary generalized extreme value model. *Water Resour. Res.*, 43.

Elmer, F., Hoymann, J., Duethmann, D., Vorogushyn, S., and Kreibich, H. (2012). Drivers of flood risk change in residential areas. *Nat. Hazards Earth Syst. Sci.*, 12:1641–1657.

Embrechts, P., Klüppelberg, C., and Mikosch, T. (1997). *Modelling Extremal Events for Insurance and Finance*. Applications of Mathematics. Springer, Berlin, Heidelberg, New York.

FEMA (2006). *HAZUS-MH MR5, Multi-hazard Loss Estimation Methodology – Flood model, Technical Manual*. Federal Emergency Management Agency, Washington, DC, USA.

Fernando, A.-D., Corfee-Morlot, J., Kiunsi, R. B. R., Pelling, M., Roberts, D., and Solecki, W. (2014). Urban areas. In Field, C. B., Barros, V. R., Dokken, D. J., Mach, K. J., Mastrandrea, M. D., Bilir, T. E., Chatterjee, M., Ebi, K. L., Estrada, Y. O., Genova, R. C., Girma, B., Kissel, E. S., Levy, A. N., MacCracken, S., Mastrandrea, R. R., and White, L. L., editors, *Climate Change 2014: Impacts, Adaptation, and Vulnerability. Contribution of Working Group II to the Fifth Assessment Report of the Intergovernmental Panel on Climate Change*. Cambridge University Press, Cambridge, UK and New York, NY, USA.

Fleming, K., Johnston, P., Zwartz, D., Yokoyama, Y., Lambeck, K., and Chappell, J. (1998). Refining the eustatic sea-level curve since the Last Glacial Maximum using far- and intermediate-field sites. *Earth Planet. Sci. Lett.*, 163(1-4):327–342.

Gattuso, J.-P., Hinkel, J., Khattabi, A., McInnes, K., Saito, Y., and Sallenger, A. (2014). Coastal systems and low-lying areas. In Field, C. B., Barros, V. R., Dokken, D. J., Mach, K. J., Mastrandrea, M. D., Bilir, T. E., Chatterjee, M., Ebi, K. L., Estrada, Y. O., Genova, R. C., Girma, B., Kissel, E. S., Levy, A. N., MacCracken, S., Mastrandrea, R. R., and White, L. L., editors, *Climate Change 2014: Impacts, Adaptation, and Vulnerability. Contribution of Working Group II to the Fifth Assessment Report of the Intergovernmental Panel on Climate Change*. Cambridge University Press, Cambridge, UK and New York, NY, USA.

Gesch, D. B. (2009). Analysis of lidar elevation data for improved identification and delineation of lands vulnerable to sea-level rise. *J. Coastal Res.*, 53(SI):49–58.

Grünthal, G., Thieken, A. H., Schwarz, J., Radtke, K. S., Smolka, A., and Merz, B. (2006). Comparative risk assessments for the city of Cologne – storms, floods, earthquakes. *Nat. Hazards*, 38(1-2):21–44.

Haigh, I. D., Nicholls, R., and Wells, N. (2010). Assessing changes in extreme sea levels: Application to the English channel, 1900-2006. *Cont. Shelf Res.*, 30(9):1042–1055.

Haigh, I. D., Wahl, T., Rohling, E. J., Price, R. M., Pattiaratchi, C. B., Calafat, F. M., and Dangendorf, S. (2014). Timescales for detecting a significant acceleration in sea level rise. *Nat. Commun.*, 5.

Hallegatte, S., Green, C., Nicholls, R. J., and Corfee-Morlot, J. (2013). Future flood losses in major coastal cities. *Nature Clim. Change*, 3:802–806.

Hallegatte, S., Ranger, N., Mestre, O., Dumas, P., Corfee-Morlot, J., Herweijer, C., and Muir Wood, R. (2011). Assessing climate change impacts, sea level rise and storm surge risk in port cities: A case study on Copenhagen. *Climatic Change*, 104(1):113–137.

Halsnæs, K., Shukla, P., Ahuja, D., Akumu, G., Beale, R., Edmonds, J., Gollier, C., Grübler, A., Ha Duong, M., Markandya, A., McFarland, M., Nikitina, E., Sugiyama, T., Villavicencio, A., and Zou, J. (2007). Framing issues. In Metz, B., Davidson, O. R., Bosch, P. R., Dave, R., and Meyer, L. A., editors, *Climate Change 2007: Impacts, Mitigation. Contribution of Working Group III to the Fourth Assessment Report of the Intergovernmental Panel on Climate Change*, pages 117–167. Cambridge University Press, Cambridge, UK and New York, NY, USA.

Hanson, S., Nicholls, R., Ranger, N., Hallegatte, S., Corfee-Morlot, J., Herweijer, C., and Chateau, J. (2011). A global ranking of port cities with high exposure to climate extremes. *Climatic Change*, 104(1):89–111.

Hawkes, P. J., Gonzalez-Marco, D., Sanchez-Arcilla, A., and Prinos, P. (2008). Best practice for the estimation of extremes: A review. *J. Hydraul. Res.*, 46(Extra Issue 2):323–332.

Hay, C. C., Morrow, E., Kopp, R. E., and Mitrovica, J. X. (2015). Probabilistic reanalysis of twentieth-century sea-level rise. *Nature*, 517:481–484.

Hinkel, J., Jaeger, C., Nicholls, R. J., Lowe, J., Renn, O., and Peijun, S. (2015). Sea-level rise scenarios and coastal risk management. *Nature Clim. Change*, 5:188–190.

Hinkel, J. and Klein, R. J. T. (2003). DINAS-COAST: developing a method and a tool for dynamic and interactive vulnerability assessment. *LOICZ Newsletter*, 27:1–4.

Hinkel, J. and Klein, R. J. T. (2009). Integrating knowledge to assess coastal vulnerability to sea-level rise: The development of the DIVA tool. *Global Environ. Chang.*, 19(3):384–395.

Hinkel, J., Lincke, D., Vafeidis, A. T., Perrette, M., Nicholls, R. J., Tol, R. S. J., Marzeion, B., Fettweis, X., Ionescu, C., and Levermann, A. (2014). Coastal flood damage and adaptation costs under 21st century sea-level rise. *Proc. Natl. Acad. Sci. USA*, 111(9):3292–3297.

Hinkel, J., van Vuuren, D. P., Nicholls, R. J., and Klein, R. J. T. (2013). The effects of adaptation and mitigation on coastal flood impacts during the 21st century. An application of the DIVA and IMAGE models. *Clim. Change*, 117(4):783–794.

Hoozemans, F. M. J., Marchand, M., and Pennekamp, H. A. (1993). *A Global Vulnerability Analysis: Vulnerability Assessment for Population, Coastal Wetlands and Rice Production on a Global Scale*. Delft Hydraulics, Delft, the Netherlands, 2nd edition.

Horritt, M. S. and Bates, P. D. (2002). Evaluation of 1d and 2d numerical models for predicting river flood inundation. *J. Hydrol.*, 268:87–99.

Horton, B. P., Rahmstorf, S., Engelhart, S. E., and Kemp, A. C. (2014). Expert assessment of sea-level rise by AD 2100 and AD 2300. *Quat. Sci. Rev.*, 84:1–6.

Hosking, J. R. M. (1990). L-moments: Analysis and estimation of distributions using linear combinations of order statistics. *J. R. Stat. Soc.*, 52(1):105–124.

Hosking, J. R. M. and Wallis, J. F. (1987). Parameter and quantile estimation for the generalized pareto distribution. *Technometrics*, 29(3):339–349.

Houston, J. R. and Dean, R. G. (2011). Sea-level acceleration based on U.S. tide gauges and extensions of previous global-gauge analyses. *J. Coastal Res.*, 27(3):409–417.

Huizinga, H. J. (2007). Flood damage functions for EU member states. Implemented in the framework of the contract #382442-F1SC awarded by the European Commission – Joint Research Centre.

Hunt, A. and Watkiss, P. (2011). Climate change impacts and adaptation in cities: a review of the literature. *Clim. Change*, 104:13–49.

Hunter, J. (2010). Estimating sea-level extremes under conditions of uncertain sea-level rise. *Clim. Change*, 99:331–350.

Hunter, N. M., Bates, P. D., Neelz, S., Pender, G., Villanueva, I., Wright, N. G., Liang, D., Falconer, R. A., Lin, B., Waller, S., Crossley, A. J., and Mason, D. C. (2008). Benchmarking 2d hydraulic models for urban flooding. *Proc. Inst. Civil Eng. – Water Manag.*, 161:13–30.

Hurlimann, A., Barnett, J., Fincher, R., Osbaldiston, N., Mortreux, C., and Graham, S. (2014). Urban planning and sustainable adaptation to sea-level rise. *Landscape Urb. Plan.*, 126:84–93.

Ibáñez, C., Day, J. W., and Reyes, E. (2014). The response of deltas to sea-level rise: Natural mechanisms and management options to adapt to high-end scenarios. *Ecol. Eng.*, 65:122–130.

IPCC (2000). Special report on emissions scenarios (SRES): A special report of working group III of the intergovernmental panel on climate change. In Nakićenović, N. and Swart, R., editors, *Emissions Scenarios*. Cambridge University Press, Cambridge, UK, and New York, NY, USA.

IPCC (2007). Climate change 2007: Impacts, adaptation and vulnerability. In Parry, M. L., Canziani, O. F., Palutikof, J. P., van der Linden, P. J., and Hanson, C. E., editors, *Contribution of Working Group II to the Fourth Assessment Report of the Intergovernmental Panel on Climate Change*. Cambridge University Press, Cambridge, UK and New York, NY, USA.

IPCC (2012). Managing the risks of extreme events and disasters to advance climate change adaptation. In Field, C. B., Barros, V., Stocker, T. F., Qin, D., Dokken, D. J., Ebi, K. L., Mastrandrea, M. D., Mach, K. J., Plattner, G.-K., Allen, S. K., Tignor, M., and Midgley, P. M., editors, *A Special Report of Working Groups I and II of the Intergovernmental Panel on Climate Change*. Cambridge University Press, Cambridge, UK, and New York, NY, USA.

IPCC (2014). Summary for policymakers. In Field, C. B., Barros, V. R., Dokken, D. J., Mach, K. J., Mastrandrea, M. D., Bilir, T. E., Chatterjee, M., Ebi, K. L., Estrada, Y. O., Genova, R. C., Girma, B., Kissel, E. S., Levy, A. N., MacCracken, S., Mastrandrea, R. R., and White, L. L., editors, *Climate Change 2014: Impacts, Adaptation, and Vulnerability. Contribution of Working Group II to the Fifth Assessment Report of the Intergovernmental Panel on Climate Change*. Cambridge University Press, Cambridge, UK and New York, NY, USA.

Jevrejeva, S., Grinsted, A., and Moore, J. C. (2014a). Upper limit for sea level projections by 2100. *Environ. Res. Lett.*, 9(10).

Jevrejeva, S., Moore, J. C., and Grinsted, A. (2012). Sea level projections to AD2500 with a new generation of climate change scenarios. *Global Planet. Change*, 80–81:14–20.

Jevrejeva, S., Moore, J. C., Grinsted, A., Matthews, A. P., and Spada, G. (2014b). Trends and acceleration in global and regional sea levels since 1807. *Global Planet. Change*, 113:11–22.

Jongman, B., Kreibich, H., Apel, H., Barredo, J. I., Bates, P. D., Feyen, L., Gericke, A., Neal, J., Aerts, J. C. J. H., and Ward, P. J. (2012). Comparative flood damage model assessment: towards a European approach. *Nat. Hazards Earth System Sci.*, 12:3733–3752.

Jonkman, S. N., Hillen, M. M., Nicholls, R. J., Kanning, W., and van Ledden, M. (2013). Costs of adapting coastal defences to sea-level rise – new estimates and their implications. *J. Coastal Res.*, 29(5):1212–1226.

Kang, J. L., Su, M. D., and Chang, L. F. (2005). Loss functions and framework for regional flood damage estimation in residential area. *J. Mar. Sci. Technol.*, 13(3):193–199.

Katsman, C. A., Sterl, A., Beersma, J. J., van den Brink, H. W., Church, J. A., Hazeleger, W., Kopp, R. E., Kroon, D., Kwadijk, J., Lammersen, R., Lowe, J., Oppenheimer, M., Plag, H.-P., Ridley, J., von Storch, H., Vaughan, D. G., Vellinga, P., Vermeersen, L. L. A., van de Wal, R. S. W., and Weisse, R. (2011). Exploring high-end scenarios for local sea level rise to develop flood protection strategies for a low-lying delta-the Netherlands as an example. *Clim.Change*, 109(3–4):617–645.

Katz, R. W. (2010). Statistics of extremes in climate change. *Clim. Change*, 100(1):71–76.

Katz, R. W., Brush, G. S., and Parlange, M. B. (2005). Statistics of extremes: Modeling ecological disturbances. *Ecology*, 86(5):1124–1134.

Katz, R. W., Parlange, M. B., and Naveau, P. (2002). Statistics of extremes in hydrology. *Adv. Water Resour.*, 25:1287–1304.

Kauker, F. and Langenberg, H. (2000). Two models for the climate change related development of sea levels in the North Sea – a comparison. *Clim. Res.*, 15:61–67.

Kreibich, H., Thieken, A., Petrow, T., Müller, M., and Merz, B. (2005). Flood loss reduction of private households due to building precautionary measures - lessons learned from the Elbe flood in August 2002. *Nat. Hazards Earth Syst. Sci.*, 5:117–126.

Kriebel, D. L., Geiman, J. D., and Henderson, G. R. (2015). Future flood frequency under sea-level rise scenarios. *J. Coastal Res.*, 0(0):0.

Leadbetter, M. R., Lindgren, G., and Rootzen, H. (1983). *Extremes and Related Properties of Random Sequences and Processes*. Springer Series in Statistics. Springer, New York, NY, USA.

Leimbach, M., Bauer, N., Baumstark, L., and Edenhofer, O. (2010). Mitigation costs in a globalized world: climate policy analysis with REMIND-R. *Environ. Model. Assess.*, 15(3):155–173.

Levermann, A., Clark, P. U., Marzeion, B., Milne, G. A., Pollard, D., Radic, V., and Robinson, A. (2013). The multimillennial sea-level commitment of global warming. *Proc. Natl. Acad. Sci. USA*, 110(34):13745–13750.

Liu, J. P. and Milliman, J. D. (2004). Reconsidering melt-water pulses 1A and 1B: Global impacts of rapid sea-level rise. *J. Ocean U. China*, 3(2):183–190.

Lowe, J. A., Woodworth, P. L., Knutson, T., McDonald, R. E., McInnes, K. L., Woth, K., von Storch, H., Wolf, J., Swail, V., Bernier, N. B., Gulev, S., Horsburgh, K. J., Unnikrishnan, A. S., Hunter, J. R., and Weisse, R. (2010). Past and future changes in extreme sea levels and waves. In Church, J. A., Woodworth, P. L., Aarup, T., and Wilson, W. S., editors, *Understanding Sea-Level Rise and Variability*, pages 326–375. Wiley-Blackwell, Chichester, UK.

Luderer, G., Leimbach, M., Bauer, N., Kriegler, E., Aboumahboub, T., Arroyo-Currás, T., Baumstark, L., Bertram, C., Giannousakis, A., Hilaire, J., Klein, D., Mouratiadou, I., Pietzcker, R., Piontek, F., Roming, N., Schultes, A., Schwanitz, V. J., and Strefler, J. (2013). Description of the REMIND model (version 1.5). https://www.pik-potsdam.de/research/sustainable-solutions/models/remind/description-of-remind-v1.5. Accessed 16 September 2015.

Martins, E. S. and Stedinger, J. R. (2000). Generalized maximum-likelihood generalized extreme-value quantile estimators for hydrologic data. *Water Resour. Res.*, 36(3):737–744.

Mazria, E. and Kershner, K. (2007). *Nation Under Siege: Sea Level Rise at Our Doorstep*. 2030 Research Center.

McGranahan, G., Balk, D., and Anderson, B. (2007). The rising tide: assessing the risks of climate change and human settlements in low elevation coastal zones. *Environ. Urban.*, 19(1):17–37.

McInnes, K. L., Macadam, I., Hubbert, G., and O'Grady, J. (2013). An assessment of current and future vulnerability to coastal inundation due to sea-level extremes in Victoria, southeast Australia. *Int. J. Climatol.*, 33(1):33–47.

Mcleod, E., Poulter, B., Hinkel, J., Reyes, E., and Salm, R. (2010). Sea-level rise impact models and environmental conservation: A review of models and their applications. *Ocean Coastal Manage.*, 53(9):507–517.

Meehl, G. A., Hu, A., Tebaldi, C., Arblaster, J. M., Washington, W. M., Teng, H., Sanderson, B. M., Ault, T., Strand, W. G., and White, J. B. (2012). Relative outcomes of climate change mitigation related to global temperature versus sea-level rise. *Nature Clim. Change*, 2:576–580.

Menéndez, M. and Woodworth, P. L. (2010). Changes in extreme high water levels based on a quasi-global tide-gauge data set. *J. Geophys. Res.*, 115.

Merz, B., Elmer, F., and Thieken, A. H. (2009). Significance of 'high probability/low damage' versus 'low probability/high damage' flood events. *Nat. Hazards Earth Syst. Sci.*, 9(3):1033–1046.

Merz, B., Hall, J., Disse, M., and Schumann, A. (2010a). Fluvial flood risk management in a changing world. *Nat. Hazards Earth Syst. Sci.*, 10(3):509–527.

Merz, B., Kreibich, H., Schwarze, R., and Thieken, A. H. (2010b). Review article "assessment of economic flood damage". *Nat. Hazards Earth Syst. Sci.*, 10(8):1697–1724.

Merz, B., Kreibich, H., Thieken, A. H., and Schmidtke, R. (2004). Estimation uncertainty of direct monetary flood damage to buildings. *Nat. Hazards Earth Syst. Sci.*, 4(1):153–163.

Merz, B., Thieken, A. H., , and Blöschl, G. (2002). Uncertainty analysis for flood risk estimation. In Spreafico, M. and Weingartner, R., editors, *International Conference on Flood Estimation*, CHR Report II-17, pages 577–585.

Merz, B. and Thieken, A. H. (2004). Separating natural and epistemic uncertainty in flood frequency analysis. *J. Hydrol.*, 309(1–4):114–132.

Merz, B. and Thieken, A. H. (2009). Flood risk curves and uncertainty bounds. *Nat. Hazards*, 51(3):437–458.

Michael, J. A. (2007). Episodic flooding and the cost of sea-level rise. *Ecological Economics*, 63(1):149–159.

Middelmann-Fernandes, M. H. (2010). Flood damage estimation beyond stage-damage functions: an Australian example. *J. Flood Risk Manag.*, 3(1):88–96.

Milne, G. A., Long, A. J., and Bassett, S. E. (2005). Modelling Holocene relative sea-level observations from the Caribbean and South America. *Quaternary Sci. Rev.*, 24(10-11):1183–1202.

Mudersbach, C. and Jensen, J. (2010). Nonstationary extreme value analysis of annual maximum water levels for designing coastal structures on the German North Sea coastline. *J. Flood Risk Manag.*, 3(1):52–62.

Mudersbach, C., Wahl, T., Haigh, I. D., and Jensen, J. (2013). Trends in high sea levels of German North Sea gauges compared to regional mean sea level changes. *Cont. Shelf Res.*, 65:111–120.

Munich Re (2014). Topics Geo. Natural catastrophes 2013. Analyses, assessments, positions. http://www.munichre.com/site/corporate/get/documents_E1854204088/mr/assetpool.shared/Documents/5_Touch/_Publications/302-08121_en.pdf. Accessed 16 September 2015.

Nascimento, N., Machado, M. L., Baptista, M., and Silva, A. D. P. E. (2007). The assessment of damage caused by floods in the Brazilian context. *Urban Water J.*, 4(3):195–210.

Nicholls, R., Brown, S., Hanson, S., and Hinkel, J. (2010). *Economics of Coastal Zone Adaptation to Climate Change*. World Bank. Discussion paper number 10.

Nicholls, R. J. (2004). Coastal flooding and wetland loss in the 21st century: changes under the SRES climate and socio-economic scenarios. *Global Environ. Chang.*, 14(1):69–86.

Nicholls, R. J. (2007). *Adaptation Options for Coastal Areas and Infrastructure: An Analysis for 2030*. UNFCC, Bonn, Germany.

Nicholls, R. J. and Cazenave, A. (2010). Sea-level rise and its impact on coastal zones. *Science*, 328:1517–1520.

Nicholls, R. J., Hanson, S. E., Lowe, J. A., Warrick, R. A., Lu, X., and Long, A. J. (2014). Sea-level scenarios for evaluating coastal impacts. *WIREs Clim. Change*, 5(1):129–150.

Nicholls, R. J. and Tol, R. S. J. (2006). Impacts and responses to sea-level rise: a global analysis of the SRES scenarios over the twenty-first century. *Phil. Trans. R. Soc. A*, 364(1841):1073–1095.

Nicholls, R. J., Wong, P. P., Burkett, V. R., Codignotto, J. O., Hay, J. E., McLean, R. F., Ragoonaden, S., and Woodroffe, C. D. (2007). Coastal systems and low-lying areas. In Parry, M. L., Canziani, O. F., Palutikof, J. P., van der Linden, P. J., and Hanson, C. E., editors, *Climate Change 2007: Impacts, Adaptation and Vulnerability. Contribution of Working Group II to the Fourth Assessment Report of the Intergovernmental Panel on Climate Change*, pages 315–356. Cambridge University Press, Cambridge, UK and New York, NY, USA.

Nordhaus, W. D. and Yang, Z. (1996). A regional dynamic general-equilibrium model of alternative climate-change strategies. *Am. Econ. Rev.*, 86:741–765.

Obeysekera, J. and Park, J. (2013). Scenario-based projection of extreme sea levels. *J. Coastal Res.*, 29(1):1–7.

Orlić, M. and Pasarić, Z. (2013). Semi-empirical versus process-based sea-level projections for the twenty-first century. *Nature Clim. Change*, 3:735–738.

Penning-Rowsell, E., Johnson, C., Tunstall, S., Tapsell, S., Morris, J., Chatterton, J., and Green, C. (2005). *The Benefits of Flood and Coastal Risk Management: A Manual of Assessment Techniques*. Middlesex University Press, London, UK.

Petherick, A. (2012). Enumerating adaptation. *Nature Clim. Change*, 2(4):228–229.

Phien, H. N. and Fang, T.-S. E. (1989). Maximum likelihood estimation of the parameters and quantiles of the general extreme-value distribution from censored samples. *J. Hydrol.*, 105(1-2):139–155.

Pielke Jr., R. A. and Downton, M. W. (2000). Precipitation and damaging floods: Trends in the United States, 1932-97. *J. Climate*, 13(20):3625–3637.

Portney, P. R. and Weyant, J. P. (1999). *Discounting and Intergenerational Equity*. Resources for the future. RFF Press, Washington DC, USA.

Poulter, B. and Halpin, P. N. (2008). Raster modelling of coastal flooding from sea-level rise. *Int. J. Geogr. Inf. Sci.*, 22(2):167–182.

Poussin, J. K., Ward, P. J., Bubeck, P., Gaslikova, L., Schwerzmann, A., and Raible, C. C. (2012). *Flood Risk Modelling*, chapter 6, pages 93–121. Earthscan, London, UK, and New York, NY, USA.

Prahl, B. F., Rybski, D., Boettle, M., and Kropp, J. P. (2016). Damage functions for climate-related hazards: Unification and uncertainty analysis. *Nat. Hazards Earth Syst. Sci*, 16:1189–1203.

Rahmstorf, S. and Coumou, D. (2011). Increase of extreme events in a warming world. *Proc. Natl. Acad. Sci. USA*, 108(44):17905–17909.

Rahmstorf, S., Perrette, M., and Vermeer, M. (2012). Testing the robustness of semi-empirical sea level projections. *Clim. Dyn.*, 39(3-4):861–875.

Rahmstorf, S. and Vermeer, M. (2011). Discussion of: Houston, J.R. and Dean, R.G., 2011. Sea-level acceleration based on U.S. tide gauges and extensions of previous global-gauge analyses. Journal of Coastal Research, 27(3), 409-417. *J. Coastal Res.*, 27(4):784–787.

Reiss, R.-D. and Thomas, M. (2007). *Statistical Analysis of Extreme Values*. Birkhäuser, Basel, Switzerland, 3rd edition.

Rozenfeld, H. D., Rybski, D., Andrade Jr., J. S., Batty, M., Stanley, H. E., and Makse, H. A. (2008). Laws of population growth. *Proc. Natl. Acad. Sci. USA*, 105(48):18702–18707.

Rowley, R. J., Kostelnick, J. C., Braaten, D., Li, X., and Meisel, J. (2007). Risk of rising sea level to population and land area. *Eos Trans. AGU*, 88(9):105–116.

Sachs, J. D., Mellinger, A. D., and Gallup, J. L. (2001). The geography of poverty and wealth. *Sci. Am.*, 284(3):70–75.

Seneviratne, S. I., Nicholls, N., Easterling, D., Goodess, C. M., Kanae, S., Kossin, J., Luo, Y., Marengo, J., McInnes, K., Rahimi, M., Reichstein, M.and Sorteberg, A., Vera, C., and Zhang, X. (2012). Changes in climate extremes and their impacts on the natural physical environment. In Field, C. B., Barros, V., Stocker, T. F., Qin, D., Dokken, D. J., Ebi, K. L., Mastrandrea, M. D., Mach, K. J., Plattner, G.-K., Allen, S. K., Tignor, M., and Midgley, P. M., editors, *Managing the Risks of Extreme Events and Disaster to Advance Climate Change Adaptation*, A Special Report of Working Groups I and II of the Intergovernmental Panel on Climate Change (IPCC), pages 109–230. Cambridge University Press, Cambridge, UK, and New York, NY, USA.

Smith, D. I. (1994). Flood damage estimation – a review of urban stage-damage curves and loss functions. *Water SA*, 20(3):231–238.

Solomon, S., Plattner, G. K., Knutti, R., and Friedlingstein, P. (2009). Irreversible climate change due to carbon dioxide emissions. *Proc. Natl. Acad. Sci. USA*, 106(6):1704–1709.

Steinhäuser, J. M., Rybski, D., and Kropp, J. P. (2015). Indirect identification of damage functions from damage records. arXiv:1509.01786.

Stive, M. J. F., Aarninkhof, S. G. J., Hamm, L., Hanson, H., Larson, M., Wijnberg, K. M., Nicholls, R. J., and Capobianco, M. (2002). Variability of shore and shoreline evolution. *Coast. Eng.*, 47(2):211–235.

Thieken, A. H., Müller, M., Kreibich, H., and Merz, B. (2005). Flood damage and influencing factors: new insights from the august 2002 flood in Germany. *Water Resour. Res.*, 41(12).

Thieken, A. H., Olschewski, A., Kreibich, H., Kobsch, S., and Merz, B. (2008). Development and evaluation of FLEMOps – a new Flood Loss Estimation MOdel for the private sector. *WIT Trans. Ecol. Envir.*, 118.

Tol, R. S. J. (2002a). Estimates of the damage costs of climate change - part II. dynamic estimates. *Environ. Resour. Econ.*, 21(2):135–160.

Tol, R. S. J. (2002b). Estimates of the damage costs of climate change. part 1: Benchmark estimates. *Environ. Resour. Econ.*, 21(1):47–73.

Triantaphyllou, E. (2000). *Multi-Criteria Decision Making Methodologies: A Comparative Study*, volume 44 of *Applied Optimization*. Kluwer Academic, Dordrecht, Netherlands.

Vafeidis, A. T., Nicholls, R. J., McFadden, L., Tol, R. S. J., Hinkel, J., Spencer, T., Grashoff, P. S., Boot, G., and Klein, R. J. T. (2008). A new global coastal database for impact and vulnerability analysis to sea-level rise. *J. Coastal Res.*, 24(4):917–924.

Vellinga, P., Katsman, C., Sterl, A., Beersma, J., Hazeleger, W., Church, J., Kopp, R., Kroon, D., Oppenheimer, M., Plag, H.-P., Rahmstorf, S., Lowe, J., Ridley, J., von Storch, H., Vaughan, D., van de Wal, R., Weisse, R., Kwadijk, J., Lammersen, R., and Marinova, N. (2009). Exploring high-end climate change scenarios for flood protection of the Netherlands. http://www.knmi.nl/bibliotheek/knmipubWR/WR2009-05.pdf. Accessed 16 September 2015.

Vermeer, M. and Rahmstorf, S. (2009). Global sea level linked to global temperature. *Proc. Natl. Acad. Sci. USA*, 106(51):21527–21532.

Vousdoukas, M. I., Voukouvalas, E., Annunziato, A., Giardino, A., and Feyen, L. (2015). Projections of extreme storm surge levels along europe. *submitted to Clim. Dynam.*

Wang, Q. J. (1990). Estimation of the GEV distribution from censored samples by method of partial probability weighted moments. *J. Hydrol.*, 120(1-4):103–114.

Ward, P. J., Jongman, B., Sperna Weiland, F., Bouwman, A., van Beek, R., Bierkens, M. F. P., Ligtvoet, W., and Winsemius, H. C. (2013). Assessing flood risk at the global scale: model setup, results, and sensitivity. *Environ. Res. Lett.*, 8(4).

Warrick, R. (2009). From CLIMPACTS to SimCLIM: The development of an integrated assessment model. In Knight, C. G. and Jaeger, J., editors, *Integrated Regional Assessment: Challenges and Case Studies*. Cambridge University Press, Cambridge, UK.

Weitzman, M. L. (2001). Gamma discounting. *Am. Econ. Rev.*, 91(1):260–271.

Weitzman, M. L. (2010). Risk-adjusted gamma discounting. *J. Environ. Econ. Manag.*, 60(1):1–13.

Wind, H. G., Nierop, T. M., de Blois, C. J., and de Kok, J. L. (1999). Analysis of flood damages from the 1993 and 1995 Meuse floods. *Water Resour. Res.*, 35(11):3459–3465.

Woodworth, P. L. (2010). A survey of recent changes in the main components of the ocean tide. *Cont. Shelf Res.*, 30(15):1680–1691.

Woodworth, P. L., Menendez, M., and Gehrels, W. R. (2011). Evidence for century-timescale acceleration in mean sea levels and for recent changes in extreme sea levels. *Surv. Geophys.*, 32(4-5, SI):603–618.

World Bank (2014). Gross deomestic product 2013. http://databank.worldbank.org/data/download/GDP.pdf. Accessed 16 September 2015.

Woth, K., Weisse, R., and von Storch, H. (2006). Climate change and North Sea storm surge extremes: an ensemble study of storm surge extremes expected in a changed climate projected by four different regional climate models. *Ocean Dynam.*, 56(1):3–15.

Zhou, B., Rybski, D., and Kropp, J. P. (2013). On the statistics of urban heat island intensity. *Geophys. Res. Lett.*, 40(20):5486–5491.

Declaration

I prepared this dissertation without illegal assistance. The work is original except where indicated by reference in the text and no part of the dissertation has been submitted for any other degree. This dissertation has not been presented to any other University for examination, neither in Germany nor in another country.

Potsdam, 22 September 2015

Markus Böttle

Colophon

This document was typeset using a customised version of the typographical look-and-feel `classicthesis` developed by André Miede. The style was inspired by Robert Bringhurst's seminal book on typography *"The Elements of Typographic Style"*. `classicthesis` is available for both LaTeX and LyX:

http://code.google.com/p/classicthesis/

Happy users of `classicthesis` usually send a real postcard to the author, a collection of postcards received so far is featured here:

http://postcards.miede.de/